Cellular and molecular aspects of the anti-inflammatory effects of low-dose radiation therapy

Doktorarbeit

Martin Large

Biologie

Vom Fachbereich Biologie der Technischen Universität Darmstadt

Zur Erlangung des akademischen Grades

eines Doctor rerum naturalium

genehmigte Dissertation von

Dipl. Biologe Martin Large

aus Heidelberg, Deutschland

1. Gutachter: Prof. Dr. Franz Rödel

2. Gutachter: Prof. Dr. Markus Löbrich

3. Gutachter: Prof. Dr. Bodo Laube

Tag der Einreichung: 19.06.2015

Tag der mündlichen Prüfung: 21.09.2015

Darmstadt 2015

D17

The present dissertation was performed within the scope of the EU project: Low-dose Research towards Multidisciplinary Integration (DoReMi). Project grant agreement number: 249689.

Results were in part published in:

Large M, Reichert S, Hehlgans S, Fournier C, Rödel C, Rödel F (2014).
A non-linear detection of phospho-histone H2AX in EA.hy926 endothelial cells following low-dose X-irradiation is modulated by reactive oxygen species.
Radiation Oncology 9(1), 80.

Large M, Hehlgans S, Reichert S, Gaipl US, Fournier C, Rödel C, Weiss C, Rödel F (2015).
Study of the anti-inflammatory effects of low-dose radiation: The contribution of biphasic regulation of the antioxidative system in endothelial cells.
Strahlenther Onkol. Epub ahead of print.

So eine Arbeit wird eigentlich nie fertig, man muss sie für fertig erklären, wenn man nach Zeit und Umständen das möglichste getan hat.

Johann Wolfgang von Goethe

Word of honour

I assure herewith on my word of honour, that I wrote this thesis by myself. All quotes, whether word by word, or in my own words, have been put in quotation marks or otherwise identified as such. The thesis has not been published anywhere else or has been presented to any other examination board.

_____

Martin Large

Darmstadt, 25. September 2015

Contents

List of Figures

List of Tables

Summary/Zusammenfassung

For decades an anti-inflammatory and analgesic effect of low-dose X-irradiation (LD-RT) has clinically been well established in the treatment of a plethora of benign diseases and chronic degenerative disorders with empirically identified single doses < 1 Gy to be most effective. Although considerable progress has been achieved in the understanding of immune modulatory effects of ionising radiation, especially in the low-dose range, the underlying molecular mechanisms are currently not fully resolved. Nevertheless, a modulation of endothelial cell (EC) activity has already been proven to comprise a key element in the therapeutic effects of LD-RT. In line with that, a putative interrelationship between DNA damage repair and a discontinuous dose-response relationship following low-dose irradiation was recently suggested. Moreover, a mechanistic involvement of reactive oxygen species (ROS) production and the cellular antioxidative response to give rise or contribute to these phenomena in endothelial cells remain elusive. Thus, in the present study, radiation effects with a particular focus on low-dose irradiation of ECs were investigated.

To analyse DNA repair capacity, phospho-histone H2AX foci were assayed at 1 h, 4 h and 24 h after irradiation. ROS production, superoxide dismutase (SOD), catalase (CAT), glutathione peroxidase (GPx) and transcription factor nuclear factor E2-related factor 2 (Nrf2) expression and activity were analysed by western immunoblotting, fluorometric 2',7'-dichlorodihydrofluorescein-diacetate (H_2DCFDA), colorimetric assays, flow-cytometry and real-time PCR, respectively. A functional impact of ROS on γH2AX foci numbers and on peripheral blood mononuclear cell (PBMC) adhesion to ECs was assayed in the presence of the ROS scavenger N-acetyl-L-cysteine (NAC) and the Nrf2 activator AI-1.

Irrespective of inflammatory stimulation by tumour necrosis factor-α (TNF-α), immortalised EA.hy926 ECs cells revealed a linear dose-response characteristic of γH2AX foci levels at 1 h and 4 h after irradiation. By contrast, at 24 h after irradiation a discontinuity in residual γH2AX foci levels with locally elevated values following a 0.5 Gy exposure were observed. This effect was unlikely caused by modulation of DNA damage repair, as proven by small molecule inhibitors targeting either the repair pathways homologous recombination (HR) or non-homologous end joining (NHEJ). However, the discontinuity in γH2AX foci levels was abolished by treatment with N-acetyl-L-cysteine (NAC), indicating an involvement of ROS. In line with that, in EA.hy926 ECs a discontinuous expression and enzymatic activity of SOD, CAT and GPx concomitant with a lowered expression and DNA-binding activity of the redox sensitive transcription factor Nrf2 most pronounced after a dose of 0.5 Gy was

observed. Finally, scavenging of ROS by NAC or activation of Nrf2 by AI-1 significantly diminished a lowered adhesion of PBMC to EC, typically detectable following irradiation with a dose of 0.5 Gy

In conclusion, these results indicate a non-linear regulation of ROS production, major compounds of the antioxidative system including SOD, CAT, GPx and Nrf2 expression and activity in EA.hy926 EC following irradiation with doses < 1 Gy. This functionally contributes to a discontinuous level of residual γH2AX foci and a hampered leukocyte/EC adhesion. These data may thus contribute a further component to the plethora of mechanisms implicated in the anti-inflammatory effects of low-dose X-ray exposure.

Bereits seit Jahrzehnten ist eine niedrig dosierte Röntgenbestrahlung (LD-RT) in der Therapie einer Vielzahl von gutartigen und chronisch degenerativen Erkrankungen etabliert. Dabei wurden Einzeldosen < 1 Gy empirisch als die am wirksamsten identifiziert. Obwohl erhebliche Fortschritte in der Aufklärung der immunmodulierenden Effekte ionisierender Strahlung - insbesondere im Bereich niedriger Dosen - erzielt wurden, sind die zugrunde liegenden molekularen Mechanismen derzeit nur unzureichend verstanden. Nichtsdestotrotz konnte bereits eine Modulation der Aktivität von Endothelzellen als entscheidendes Element der therapeutischen Effekte einer LD-RT verifiziert werden. Zusätzlich wurde kürzlich ein möglicher Zusammenhang zwischen der DNA-Schadensreparatur und einer diskontinuierlichen Dosis-Wirkungsbeziehung nach Bestrahlung mit niedrigen Dosen entdeckt. Darüber hinaus ist ein Einfluss der Produktion reaktiver Sauerstoffmetaboliten (ROS) und der zellulären anti-oxidativen Antwort als mögliche Ursache oder Beitrag zu diesen Phänomenen in Endothelzellen bisher ungeklärt. Entsprechend wurden in der vorliegenden Arbeit Bestrahlungseffekte in Endothelzellen mit Fokus auf eine Niedrigdosis-Bestrahlung untersucht.

Für die Analyse der DNA-Reparaturkapazität wurden Phospho-Histon H2AX Foci eine, vier und 24 Stunden nach Bestrahlung analysiert. Die Produktion von ROS, die Expression und Aktivität der Enzyme Superoxid Dismutase (SOD), Katalase (CAT), Gluthation-Peroxidase (GPx) und des Transkriptionsfaktors *Nuclear Factor E2-related Factor 2* (Nrf2) wurden mittels Western Blot, fluorometrischer 2',7'-Dichlorodi-hydrofluorescein-diacetat (H_2DCFDA) Messung, kolorimetrischen Assays, Durchfluss-zytometrie und quantitativer PCR analysiert. Ein funktioneller Einfluss von ROS auf das Level der γH2AX Foci und die Adhäsion mononukleärer Zellen des peripheren Blutes (PBMC) an EC wurde durch den Einsatz des ROS-Fängers N-Acetyl-L-Cysteins (NAC) und des Nrf2-Aktivators AI-1 untersucht.

Dabei wies die immortalisierte Endothelzelllinie EA.hy926, unabhängig von einer pro-inflammatorischen Aktivierung durch Tumornekrosefaktor-α (TNF-α), einen lineare Dosis-Wirkungs-Beziehung an γH2AX Foci eine und vier Stunden nach Bestrahlung auf. Im Gegensatz dazu konnte 24 Stunden nach einer Bestrahlung, ein diskontinuierliches Level an γH2AX Foci mit erhöhten Werten nach einer Bestrahlung mit 0,5 Gy beobachtet werden. Dieser Effekt wird vermutlich nicht durch eine Modulation der DNA-Schadens-Reparatur hervorgerufen, wie Versuche mit niedermolekularen Inhibitoren für die Reparaturmechanismem homologe Rekombination (HR) und nicht-homologe Endverknüpfung (NHEJ) nahelegen. Im Gegensatz dazu konnte die Diskontinuität in der Ausprägung der γH2AX Foci nach Behandlung mit dem ROS-Fänger NAC aufgehoben werden, welches auf eine Beteiligung von ROS an diesem Phänomen hindeutet.

Übereinstimmend mit diesen Ergebnissen gelang es, in EA.hy926 Zellen eine nicht-lineare Expression und enzymatische Aktivität von SOD, CAT und GPx zusammen mit einer verringerten Expression und DNA-Bindungsaktivität des redox-sensitiven Transkriptionsfaktors Nrf2 mit der höchsten Ausprägung nach einer Bestrahlung mit 0,5 Gy nachzuweisen. Schließlich führte eine NAC-vermittelte Hemmung von ROS oder die Aktivierung von Nrf2 durch AI-1 zu einer signifikanten Aufhebung der typischerweise nach Bestrahlung mit einer Dosis von 0,5 Gy beobachteten PBMC/EC-Adhäsions-minderung.

Zusammenfassend belegen die Ergebnisse eine nicht-lineare Regulation der ROS-Produktion und der Expression und Aktivität von Schlüsselelementen des anti-oxidativen Systems (SOD, CAT, GPx und Nrf2) in EA.hy926 EC nach Bestrahlungen im Dosisbereich < 1 Gy. Auf funktionaler Ebene tragen die erwähnten Effekte zu einem diskontinuierlichen Level von γH2AX Foci und einer verminderten Leukozytenadhäsion bei. Diese Daten tragen somit weitere Komponenten in der Vielzahl der Mechanismen bei, die an den anti-inflammatorischen Effekten einer niedrig dosierten Röntgenbestrahlung beteiligt sind.

1. Introduction

1.1 Low-dose radiation therapy

Radiotherapy is recognised as one of the major modalities in the treatment of malignant diseases. However, for decades low-dose radiation therapy (LD-RT) of benign disorders has been clinically documented to be a valuable treatment option for a multitude of degenerative and inflammatory diseases. The first documented clinical application of LD-RT was as early as 1898 when Sokolow and Stenbek reported on beneficial effects of irradiation of polyarthritis resulting in a reduction in pain and swelling of affected joints [1, 2].

High radiation doses, commonly used in cancer treatment (single dose > 1 Gy, total dose > 30 Gy) are well known to exert pro-inflammatory effects [3], by contrast, low-dose exposure (single dose ≤ 1 Gy, total dose ≤ 12 Gy) has been shown to result in anti-inflammatory efficacy such as inflammatory pain relief, reduced swelling and an improvement of angular function [4, 5]. At present, more than 40,000 patients are treated with LD-RT per year in Germany which reflects approximately 20% of patients treated with radiation therapy [6]. Characteristic clinical indications comprise degenerative or inflammatory disorders such as hidradenitis axillaris [7], epicondylitis humeri [8] and morbus dupuytren [9]. The doses of radiation and schedules of fractionation mainly derive from clinically-empirically investigations by von Pannewitz in the late 1930s [10]. In clinical practice, single doses of 0.3–1 Gy distributed in 4–5 fractions for acute or 1–3 fractions for chronic inflammatory disorders resulting in total doses of 3–5 Gy (acute disease) or 12 Gy (chronic disease) were applied according to current S2 guidelines [11].

Several recent clinical investigations evaluating the impact of fractionated treatment with either single doses of 0.5 Gy or 1 Gy (total doses 3 Gy or 6 Gy) in three weeks reported on iso-effectiveness concerning comprehensive pain score (CPS) and clinical response rates in a variety of benign diseases [12, 13]. These trials thus support the hypothesis that radiotherapy with a decreased single dose of 0.5 Gy might be equally effective to single doses of 1 Gy but markedly decreases total dose and may thus be superior in terms of cancerous risk and radiation protection. However, due to very early reports on late harmful side effects and an increased mortality from aplastic anaemia and leukaemia in 1965 [14, 15], LD-RT is considered obsolete in some (Anglo-American) countries. The avoidance from LD-RT was further enhanced by the advent and increased availability of effective non-steroidal or steroidal drugs displaying lower toxicity. Nevertheless, these alternative

treatment options also show considerable numbers of patients with adverse side effects and a substantial number of patients do not display sufficient treatment response if at all [16].

1.2 Inflammation

Inflammation is a uniform response of the immune system to exogenous pathogens, endogen noxae, damaged cells or irritants with the aim to eliminate the initial cause of cell injury, remove necrotic cells/tissue and initiate the process of tissue repair. Inflammation can occur in different forms and modalities which are regulated by diverse mechanisms of induction and resolution [17]. Due to a multitude of components and mechanisms involved, the inflammatory reaction is a complex process which is regulated on numerous levels. A characteristic inflammatory response is divided into four major determinants: inflammatory inducers, detecting sensors, mediators and the target tissues which results in characteristic clinical symptoms already described in the 1st century AD by Celsus: *rubor et tumour cum calore et dolore* (redness and swelling with heat and pain) [17]. Later on, the loss of function was added as the fifth cardinal symptom of inflammation [18]. Moreover, inflammation is a stereotyped response and therefore considered as a mechanism of innate immunity, in contrast to a pathogen specific adaptive immune response [19].

A pivotal molecular mechanism in the inflammatory process is the secretion of regulatory mediators called cytokines by dendritic cells or monocytes/macrophages after sensing an infection by pathogens and/or tissue damage. Examples for inflammation promoting (proinflammatory) cytokines that activate cellular elements are interferons, interleukin (IL) 1, 6, 8, 12 and the major key player tumour necrosis factor-α (TNF-α) [20]. By contrast, anti-inflammatory cytokines like the isoforms of transforming growth factor β (TGF-β $_{1–3}$) or IL-10 down-regulate and thus terminate the inflammatory cascade [21]. Furthermore, proinflammatory cytokines induce a subsequent liberation of chemokines. A broad variety of these signal molecules like monocyte chemoattractant protein-1 (MCP1)/chemokine (C-C motif) ligand 2 (CCL2) or chemotactic cytokine chemokine (C-C motif) ligand 20 (CCL20) recruit phagocytic leukocytes (macrophages, monocytes and granulocytes) to the place of inflammation [22].

The local effects of TNF-α at the site of inflammation comprise a dilatation of blood vessels (vasodilation) in line with an increased blood flow (redness and heat) and increased vascular permeability with a leakage of plasma into the infected tissue (pain

and swelling) [23]. In endothelial cells, TNF-α binding to its surface receptors results in an increased expression of adhesion molecules like intercellular adhesion molecule 1/2 (ICAM-1, ICAM-2) and vascular cell adhesion molecule (VCAM-1). This surface marker expression is mainly mediated by cytokine-mediated activation of the transcription factor nuclear factor kappa-light-chain-enhancer of activated B cells (NF-κB) [24, 25]. With the support of additional adhesion molecules like integrins and selectins (E-selectin, P-selectin) on endothelial cells and their corresponding ligands (e.g. Sialyl-Lewis^X) mononuclear (PBMC) and polymorph nuclear (PMN: granulocytes) leukocytes from peripheral blood adhere to the endothelium layer and next extravasate into the tissue [26, 27]. In more detail, the beginning of this chemotaxis-driven multiphase process is a reversible binding of the leukocytes to selectins. While this binding is too weak to persist the blood flow, leukocytes and the blood vessels establish and lose the connections for several times (rolling adhesion) [28]. This process is followed by a tight binding via ICAM-1, ICAM-2 and VCAM-1 to integrins expressed in the endothelial cell layer [29] and a subsequent spreading, finally resulting in a movement of the PBMC through the endothelium and the basement membrane (diapedesis) into the site of inflammation (Figure 1) [30].

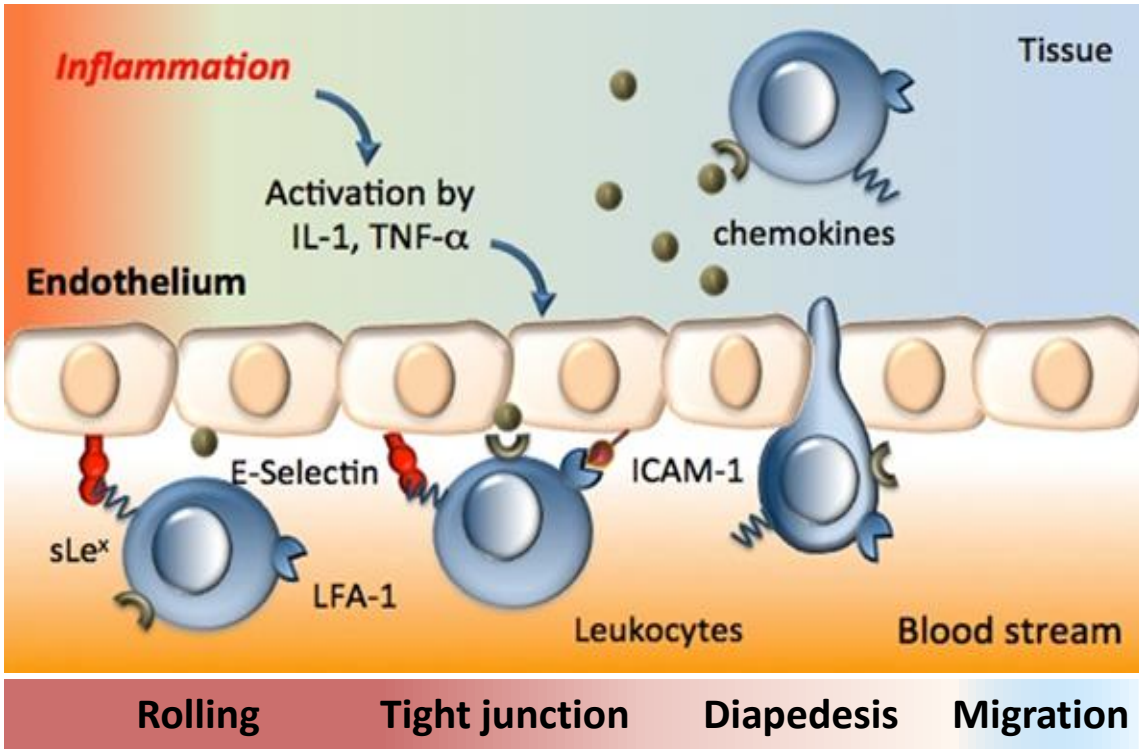

Figure 1. Scheme of leukocyte adhesion to endothelial cells, an initial step in the inflammatory cascade

Guided by cytokines, the initial step of the leukocyte adhesion to endothelial cells is a binding to the endothelial cell layer via selectins (capture). This reversible process occurs several times (rolling) until the leukocytes adhere, mediated by integrins, in a firm way (tight junction). Finally, leukocytes pass through permeable junctions between endothelial cells (diapedesis) into the local site of inflammation.

Whereas an acute inflammation provides a helpful protection against harmful stimuli, it can also turn into a chronic inflammation, if not terminated once the triggering insult is eliminated [17]. Chronic inflammation is related to numerous diseases such as diabetes mellitus type II, atherosclerosis, neurodegenerative diseases, cancer and cancer metastases [17, 28, 31, 32]. Reasons for chronic inflammations may comprise persistent injuries, extended exposure to toxic agents or autoimmune diseases. A prolonged inflammation is characterised by an orchestrated progressive shift in the type of cells present at the site of inflammation (neutrophil to monocyte recruitment) and by simultaneous clearance of dead cells along with a tissue repair that results in fibrosis and new vessel formation (angiogenesis) [33, 34].

1.3 Molecular mechanisms of low-dose radiation therapy

Although considerable progress has been achieved in the understanding of immune modulatory effects of ionising radiation, the underlying mechanisms are not fully resolved at present. During the last decades, however, multiple efforts have been made to unravel the molecular events following radiation exposure and subsequent irradiation-triggered pathways, especially following low doses. In line with that, previous studies revealed a kaleidoscopic variation of pathways involved in the anti-inflammatory effects of doses < 1 Gy, exhibiting a non-linear dose-response relationship most pronounced after a 0.5 Gy exposure [35, 36].

As stated before, an initial event in the inflammatory cascades is the recruitment of PBMC and PMN to the site of local damaged tissue mediated by endothelial cells (EC). Consequently, experiments were performed on the role of EC in the anti-inflammatory efficacy of LD-RT. Among the first mechanisms reported to contribute to the immune modulatory effects was a significant reduction of leukocyte adhesion to inflammatory (TNF-α) stimulated ECs. The most pronounced effect was observed following a 0.5 Gy exposure [37-39]. This characteristic functionally coincides with a non-linear dose and time kinetics for the expression of the anti-inflammatory cytokine TGF-β_1 from EC both *in vitro* and in a murine model. Likewise, neutralization of TGF-β_1 restored leukocyte/EC adhesion indicating a key role of the protein in these effects [38, 40]. On the molecular level, a biphasic characteristic of DNA-binding and transcriptional activity of the transcription factors nuclear factor-κB/p65 (NF-κB) and activator protein 1 (AP-1) with local maxima at 0.5 Gy and 0.3 Gy (AP-1) at 8 hours and 24-30 hours after irradiation (NF-κB) have been reported [41, 42].

Apoptosis, a physiological cellular suicide program, induced by a variety of endogenous and exogenous stimuli including ionising irradiation [43], significantly impacts on immune regulation and radiation response. In line with that, irradiation of PBMC and PMN revealed a discontinuous increase of apoptosis with a plateau or peak following a 0.3 Gy to 0.7 Gy exposure [44, 45]. This may further contribute to a hampered recruitment of inflammatory cells by reducing cell numbers that is further supported by a decreased surface expression of the adhesion molecule E-selectin on ECs [38, 39] or an enhanced proteolytic cleavage of L-selectin from apoptotic PBMC [37]. In addition, a modulation of the pro-survival enzymes mitogen-activated protein (MAP) kinases, protein kinase B (AKT) and a reduced release of CCL20 from PMN following irradiation with doses below 1 Gy have been reported to further contribute to the anti-inflammatory effects of LD-RT [46].

Major cellular elements of the immune system further cover different subtypes of mononuclear leukocytes as main components of the innate host defence. According to this, a characteristic of the effector phase of inflammation comprises differentiation of monocytes into dendritic cells and inflammatory macrophages [47, 48]. The latter support inflammation by a plethora of functions such as phagocytosis followed by antigen presentation, secretion of cytokines and release of reactive oxygen intermediates/species (ROS) or nitric oxide (NO) [49, 50]. NO, mainly processed by the enzyme inducible nitric oxide synthase (iNOS) regulates vascular permeability, promotes oedema formation and is involved in the pathogenesis of inflammatory pain [51]. Following low-dose irradiation of activated macrophages, a decreased expression of the iNOS protein [52] as well as a hampered release of ROS and superoxide production [53] have been reported. More recent data further indicate a hampered nuclear translocation of NF-κB/p65, a lowered secretion of the cytokine Interleukin 1 (IL-1) and an increased expression of TGF-β_1 from stimulated macrophages [54] concomitant with a significantly reduced migration capability [55]. In conclusion, low-dose X-ray irradiation, most pronounced at a dose of 0.5 Gy, induces an anti-inflammatory cytokine microenvironment for macrophages that might be accompanied by resolution of inflammation.

A common characteristic of the effects as reported so far is a discontinuous dose-response relationship shared with non (DNA)-targeted bystander, abscopal or adaptive effects [56]. These recent findings challenged the classical paradigm in radiation biology that deposition of energy to the nucleus and resulting DNA damage is responsible for the biological consequences of radiation exposure [57] and take into consideration a complex intercellular communication. Molecular mechanisms contributing or originating these non-linear dose-response relationships, however, remain vague and most likely originate from an overlap of several processes that may be initiated at various threshold doses and display different time- and dose kinetics [36]. These effects became further evident by a biphasic regulation of inflammatory transcription factor NF-κB [58] and a non-linear expression of X-chromosome linked Inhibitor of Apoptosis Protein (XIAP) in stimulated ECs [42]. In addition to its anti-apoptotic properties, the latter protein regulates the translocation and activity of NF-κB and is therefore involved in the anti-adhesive properties of LD-RT (Figure 2).

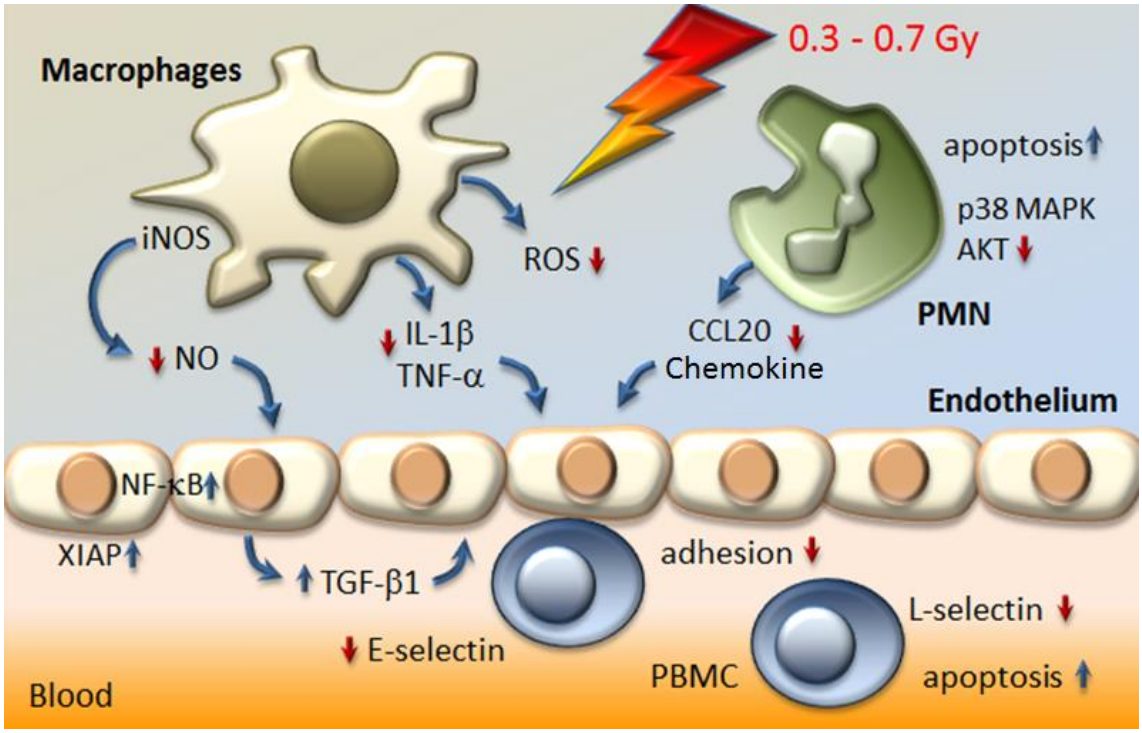

Figure 2. Current model of immunomodulatory effects of low-dose radiation (< 1 Gy) on cells of the immune system

Polymorphonuclear cells (PMN) respond to low-dose exposure with a locally increased rate of apoptosis, a hampered secretion of chemokine (C-C motif) ligand 20 (CCL20) chemokine and alterations in signal transduction pathways p38 mitogen activated protein kinase (MAPK) and protein kinase B (AKT). Furthermore, irradiation results in a hampered adhesion of peripheral blood mononuclear cells (PBMC) to the endothelium, mediated by the secretion of the anti-inflammatory cytokine transforming growth factor β_1 (TGF-β_1), a diminished expression of E-selectin on the surfaces of endothelial cells, a higher rate of apoptosis, and the proteolytic shedding of L-selectin from the surface. Moreover, in stimulated macrophages a reduced activity of the inducible nitric oxide synthase (iNOS) along with reduced levels of nitric oxide (NO), a lowered production of reactive oxygen species (ROS) and a diminished secretion of either interleukin-1β (IL-1β) and/or TNF-α may contribute to local anti-inflammatory effects. Figure modified according to [36].

In addition to an increasing knowledge of underlying cellular and molecular mechanisms, a multitude of animal models of arthritis have been established to study clinical inflammatory parameters and to confirm anti-inflammatory effects of low-dose irradiation. In 1933, von Pannewitz was the first to report on an improvement of symptoms, joint swelling and pain, following irradiation with single doses of 1 Gy in a model of mechanical destruction of cartilage and bone in rabbits [59]. In subsequent years, these characteristics were proven true in a variety of inducible inflammatory models in rabbit, rats and more recently in human tumour necrosis factor α (hTNF-α) transgenic mice [60]. These mice expressed the human cytokine TNF-α and developed a chronic polyarthritis at

an age of 4–6 weeks [61]. In summary, these models uniformly indicate that irradiation with low doses inhibits the proliferation of synovial cells and the synthesis of synovial fluid, reduces the destruction of cartilage and bone, hampers the expression of iNOS and IL-1β, increases expression of heat shock protein 70 (Hsp70) and heme oxygenase-1 (HO-1) [62] and secretion of the anti-inflammatory cytokine TGF-β_1, confirming a hampered leukocyte adhesion and extravasation. Beyond that, the best treatment effects were evident after daily fractions of 0.5 Gy and 1 Gy and an early onset of irradiation [63]. Notably, recent clinical investigations further support the preclinical observation that single doses of 0.5 Gy are isoeffective to a 1 Gy exposure, thus allowing total dose reduction and an improvement in patients` radiation protection [12, 63, 64].

1.4 DNA damage response in eukaryotic cells

Eukaryotic cells have acquired complex molecular mechanisms to preserve chromosomal integrity in their genomes due to damages induced by ionising radiation, by-products of cellular metabolism (e.g. ROS) and environmental mutagens [65, 66] (Figure 3). Maintaining genomic stability is essential for prevention of chromosomal rearrangements that may otherwise result in malignant transformation and altered gene expression [67]. There is a wide range of different types of DNA damage that can arise within the cell, including base damages, single strand breaks, DNA-Protein- and DNA-DNA-crosslinks and most important DNA double-strand breaks (DSBs) [68]. Ionising radiation is able to give rise to all of these types of lesion and due to their substantially importance, DSBs are mainly repaired by two distinct repair mechanisms namely homologous recombination (HR) and non-homologous end joining (NHEJ) [66]. For damage repair by HR, an intact sister chromatid is required and therefore HR is restricted to the S and G2 phases of the cell cycle. By contrast, NHEJ rejoins the two broken DNA ends without the need of a sister chromatid. A fact that renders NHEJ functional in all phases of the cell cycle and thus the major DSB repair mechanism in mammalian cells [69].

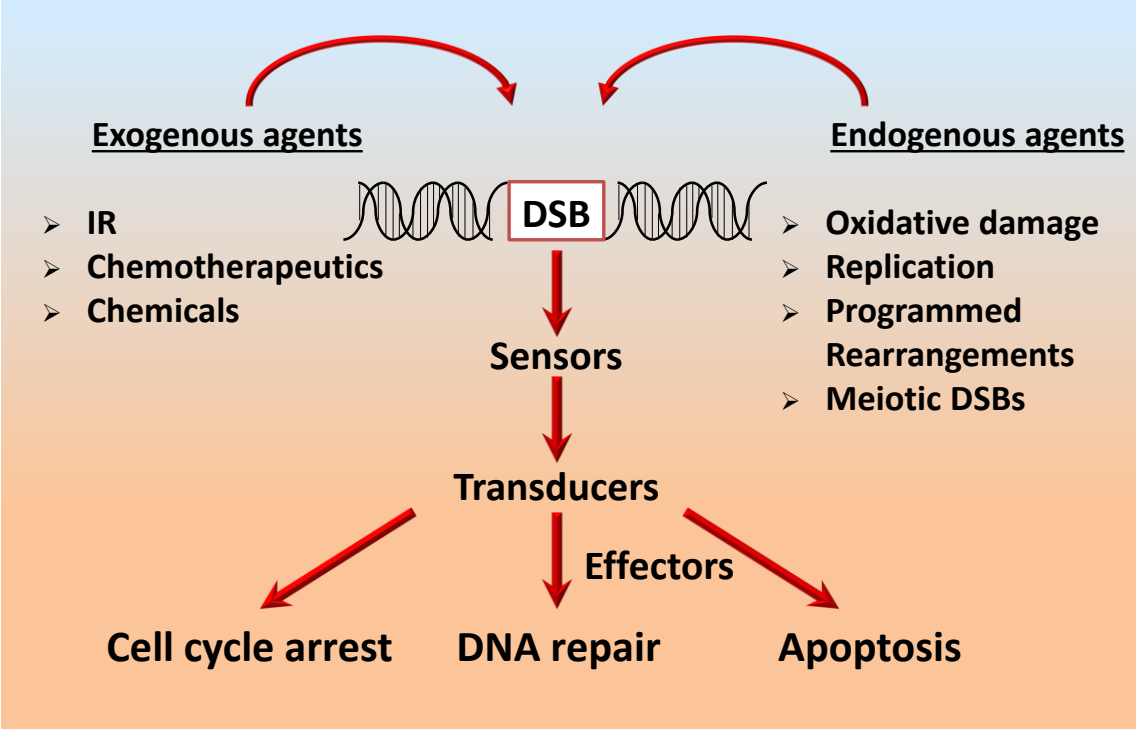

Figure 3. DNA double-strand break signalling pathways and cellular radiation response

DNA double-strand breaks (DSBs) caused by either exo- or endogenous inducers are recognised by sensors which send and intensify their signal via transducers to the effectors, resulting in cell cycle arrest, DNA repair and/or apoptosis. Figure modified according to [70].

1.4.1 Primary damage recognition and signal transduction

The phosphatidylinositol 3-kinase-related (PIK3K) kinase ataxia telangiectasia mutated (ATM) is a protein kinase central to the damage recognition and signal transduction. It is recruited to DSB lesions via the meiotic recombination 11 homolog (MRE11)-RAD50-Nijmegen Breakage Syndrome (NBS1) (MRN) complex [71]. Following activation by auto-phosphorylation [72] and dimer dissociation, ATM phosphorylates a histone H2AX variant at serin139 thus, generating γH2AX which in turn facilitates the recruitment of numerous key proteins of the repair machinery including among others p53-binding protein 1 (53BP1), mediator of DNA damage checkpoint protein 1 (MDC1), breast cancer 1 early onset (BRCA1) [66] resulting in a γH2AX signal up to 2 mega base pairs (Mbp) around the DSB [73].

1.4.2 DSB repair mechanisms

1.4.2.1 Non-homologous end joining

Conditions like cell cycle phase, chromatin status (eu- or heterochromatin) and the complexity of the DSB determine the repair pathway preferred [66], with NHEJ to be the predominant pathway for the repair of radiation-induced DSBs [69]. This mechanism starts with the binding of Ku70 and Ku80 proteins to DNA ends in a manner that allows the Ku70/Ku80 heterodimer to translocate along the DNA and recruit the DNA-dependent protein kinase catalytic subunit (DNA-PK_{cs}) complex [74]. DNA-PK_{cs} in turn is responsible for the regulation of the DNA ends processing to generate the 3'-OH and 5'-P ends required for ligation [75]. The assembly of the Ku heterodimer and DNA-PK_{cs} on DNA ends is followed by conformational changes, recruitment of Artemis for DSB end processing [76] and a complex termed DNA ligase IV/X-ray repair cross-complementing protein 4 (XRCC4) that facilitates the re-joining step [77].

1.4.2.2 Homologous recombination

The initial step of the HR comprises an ATM-dependent phosphorylation of C-terminal-binding protein 1 (CtBP)-interacting protein (CtiP) after binding of the MRN complex to the DSB. Activated CtiP resects the broken ends over a short distance which is continued by Bloom helicase (BLM) and exonuclease 1 (exo1) [78, 79]. The resulting single stranded DNA (ssDNA) is stabilised by the binding of replication protein A (RPA) [80]. Breast cancer type 2 susceptibility protein (BRCA2) exchanges RPA with RAD51 which results in the formation of a nucleoprotein filament [81]. This filament invades - guided by RAD54 - into the homologous sister chromatid resulting in ssDNA in the target chromatid (displacement loop (D-Loop)) [80]. The DNA synthesis starts at the 3'-end of the break by DNA-polymerase I, utilizing the sister chromatid as a template. During this process the single stranded area is enlarged (branch migration). Furthermore, the elongated 3'-end displaces from the homologous strand and binds to the resected second break end. HR is finished by filling up the single stranded areas and cutting of potential overlaps, resulting in two identical DNA double-strands [80, 82]. The final ligation is carried out by DNA-ligase I.

1.5 Oxidative stress response

Cells are permanently exposed to exogenous and endogenous noxae like irradiation, heat, nutrient deprivation and especially oxidative stress. The term ROS covers different kinds of chemically highly reactive molecules containing oxygen atoms, which play diverse roles in intracellular signal transduction, host defence, homeostasis and inflammation [83]. Important members of the ROS family are superoxide radical (O_2-•), hydrogen peroxide (H_2O_2) and the hydroxyl radical (OH•) [84], which are mainly formed as natural endogenous by-products of the mitochondrial electron transport chain, since approximately 1-2% of its electrons are leaked as O_2-• [85, 86].

Following environmental stress, the level of ROS increases dramatically resulting in a significant damage to cellular structures and induction of DSBs [83, 87]. Since ionising radiation mainly exerts its cytotoxic activity by the generation of ROS, antioxidant systems to maintain and control cellular redox balances are highly relevant for the radiation response. Moreover, ROS are involved in immunological defence mechanisms e.g. in activated macrophages by mounting an oxidative burst against invading pathogens and have a physiological role in cellular signalling that extends to every cell type of the immune system [53, 88].

Other important players in the production of ROS comprise xanthine oxidase (XO) and nicotinamide adenine dinucleotide phosphate (NADPH) oxidases (NOXs) [89, 90]. Activation of NOXs occurs in response to stimulation of insulin-, angiotensin-, fibroblast growth factor- and TNF-α receptors. Additional exogenous factors for ROS production are smoking (by activating NOX [91]) and auto-oxidizing xenobiotics [83]. The level of oxidative damage varies due to different conditions like hypoxia, obesity, hyper-glycaemia and high-cholesterol diet [84]. For instance, hypoxia was shown to result in a deregulation of the mitochondrial electron transport chain, followed by an increased production of ROS [92].

ROS are capable of damaging a broad range of target structures including lipids, DNA and proteins, resulting in modifications and potentially severe consequences for the cell [83]. The interaction of ROS with varied lipids has a widespread impact by the formation of isoprostanes or oxidation of arachidonyl-palmitoyl-phosphatidylcholine to produce an agonist for Toll-like receptor 4 (TLR4), resulting in an inflammatory stimulus [93]. Moreover, ROS has been shown to induce a broad variation of DNA damage. Radicals can react with DNA by addition of double bonds present in DNA bases and by abstraction of an H atom from the methyl group of thymine and of the C-H bonds in 2-deoxyribose

[85]. This generates products such as 8-oxoguanine (8-OH-dG), 5-hydroxymethyluracil (5-OH-Me-Ura) and 5-hydroxy-5-methylhydantoin (5-OH-MeHyd), which are linked to rheumatoid arthritis, diabetes mellitus type II and various types of cancer [94-97]. The most severe DNA damage, however, caused by ROS is the DSB [87, 98, 99]. Already one unrepaired DSB can be lethal or promote carcinogenesis [100, 101]

Finally, ROS on the one hand are capable of inhibiting serine/threonine phosphatases and caspases by a reversible oxidation of their cysteine residues. On the other hand, oxidation of cysteines that coordinate Zn2+ in Zn2+-finger proteins (including kinases) may result in an activation of e.g. protein kinase C [83]. Additionally, metalloproteases which maintain an inactive state by coordinating Zn2+ can be activated by oxidation of cysteines. Growing evidence further exists on a role of ROS as a second messenger during cell growth, differentiation, inflammation [102, 103] and regulation of redox sensitive transcription factors like AP-1 and NF-κB, which are linked to inflammation and have been shown to be modulated by LD-RT [104, 105].

A pivotal mechanism in the regulation of the cellular anti-oxidative stress/damage response and homeostasis is the activation of the transcription factor nuclear factor E2-related factor 2 (Nrf2), which tightly controls the expression of genes encoding antioxidant proteins and ROS detoxifying enzymes [106]. Under non-stressed conditions, Nrf2 is coupled to Kelch-like ECH-associated protein 1 (Keap1) that fosters its proteasomal degradation [107]. In more detail, Keap1 is a substrate adaptor for the ubiquitination of Nrf2 in a cullin-3 (Cul3)-dependent manner, which leads to the continuous proteasomal degradation of Nrf2 [107]. Following oxidative stress, the ubiquitin E3 ligase activity of the Keap1–Cul3 complex declines by oxidation of cysteines in Keap1 while Nrf2 is stabilised and enters the nucleus [108]. After translocation, Nrf2 heterodimerises with small V-maf musculoaponeurotic fibrosarcoma oncogene homolog (Maf) proteins and binds to the antioxidant response element (ARE) which regulates the expression of multiple antioxidant and cytoprotective enzymes [106], most prominent superoxide dismutase (SOD), catalase (CAT) and glutathione-peroxidase (GPx) [109]. Consequently, Nrf2 is considered as a key player in the cellular stress response [110].

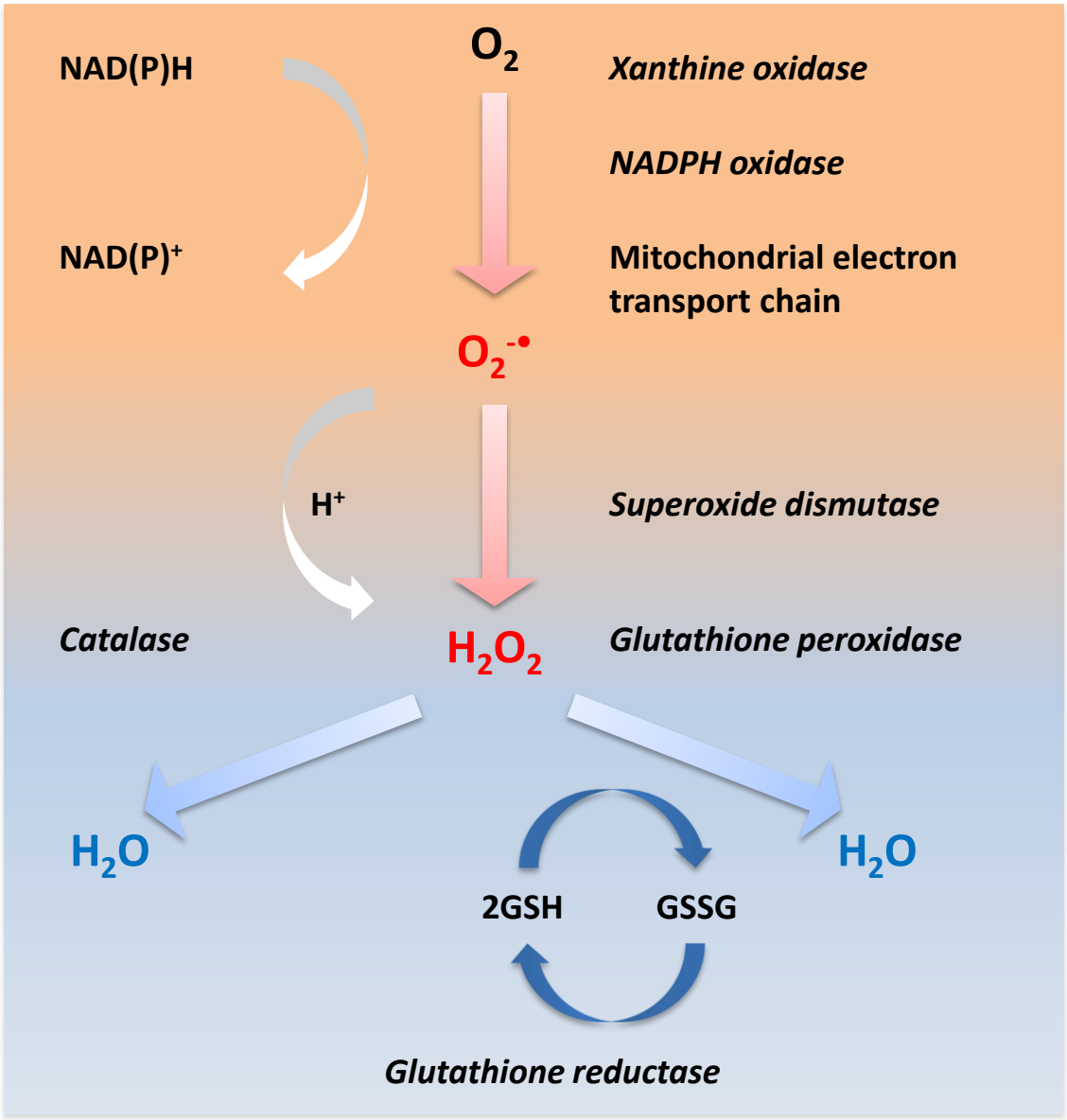

Figure 4. Major pathways of reactive oxygen species generation and detoxification

Molecular oxygen (O2) can be processed into superoxide (O2•-) by specialised enzymes such as the nicotinamide adenine dinucleotide phosphate (NADPH)- or xanthine oxidases or originate as a by-product of cellular metabolism, particularly the mitochondrial electron transport chain. Superoxide dismutase (SOD) converts the O2•- to hydrogen peroxide (H2O2), which is further processed to water or alcohols via catalase (CAT) or glutathione peroxidase (GPx), respectively. Glutathione reductase renews the consumed glutathione by catalysing the reduction of glutathione disulphide (GSSG) to the sulfhydryl form glutathione (GSH). Figure modified according to [111].

As an integral part of the ROS metabolism, SOD biochemically catalyses the dismutation of toxic O_2•- into hydrogen peroxide H_2O_2 [112], which in turn is detoxified to H_2O or alcohols in a glutathione-dependent reduction step by glutathione peroxidase (GPx) [113].

Glutathione is renewed by glutathione reductase (GR) which catalyses the reduction of glutathione disulphide (GSSG) to the sulfhydryl form glutathione (GSH) [114]. Another possibility of detoxification is the decomposition of hydrogen peroxide to water and oxygen via CAT [112] (Figure 4).

A misbalance of oxidants and antioxidants is linked to a plethora of human diseases like chronic obstructive pulmonary disease (COPD) [115], cancer [116] and ageing [117]. The disequilibrium can be caused by either excess levels of ROS or depletion in antioxidant defence pathways [118]. In several recent clinical studies, high levels of certain oxidative damage biomarkers seem to be a prognostic marker for a higher risk of disease [119-121]. On the contrary, suggestions for an inverse correlation of particular biomarkers (e.g. neuroprostanes) and prognosis were reported by Seet et al. [122].

1.6 Aim of the project

The purpose of the present thesis was to analyse molecular mechanisms implicated in the anti-inflammatory effects of low-dose radiation therapy. In line with that, a putative interrelationship between DNA damage repair and the involvement of ROS in a discontinuous dose-response relationship typically observed following low-dose irradiation was recently suggested. A mechanistic involvement of the DNA damage repair and cellular antioxidative response in the modulation of the anti-inflammatory effects and functional properties of ECs following low-dose anti-inflammatory irradiation, however, remains to be established. In the present study was aimed to analyse radiation effects in ECs with a particular focus on DNA damage repair, ROS production, expression and activity of the enzymes SOD, CAT, GPX and the redox-sensitive transcription factor Nrf2 and to correlate expression of these factors to functional properties like leukocyte adhesion to ECs.

2 Material and methods

2.1 Material

2.1.1 Appliances

Appliance	Model/Description	Company
Centrifuges	mini Spin Eppendorf 5810 UNIVERSAL 320R	Eppendorf, Hamburg Eppendorf, Hamburg Hettich, Tuttlingen
Developer	Optimax Typ TR	HS Laborgeräte, Wiesloch
Electrophoresis chamber,		Bio-Rad, München
ELISA reader	VIKTOR™ 1420 Multilabel Counter with Wallac 1420n Manager	Perkin Elmer, Waltham USA
Flow Cytometer	FACSCalibur with Cell Quest Pro software	Becton Dickinson, Heidelberg
Freezing container	Mr. Frosty™	Thermo Fisher Scientific, Dreieich
IKA® shaker	MTS 4	IKA Labortechnik, Staufen
Incubator	HERA cell 240+240i	Thermo Fisher Scientific, Dreieich
Laminar flow hood	HERA safe	Thermo Fisher Scientific, Dreieich
Linear accelerator	SL75/5	Elekta, Crawley. UK
Microscope (cell culture)	AxioVert A1	Zeiss, Jena
Microscope with software and camera system	AxioImager Z1 with Axio Vision Imager Software 4.6.2 and AxioCam MRm and AxioCam MRc	Zeiss, Jena
pH meter	pH Meter 765 Calimatic	Knick, Berlin
Photometer	Bio Photometer	Eppendorf, Hamburg
Real-time PCR	Step One Plus	Applied Biosystems,

		Darmstadt
Semi-dry transfer cell	Transblot SD	Bio-Rad, München
Shaker-incubator	ES-20	BioSan, Riga, Latvia
Water bath	Typ W/B 5	Gesellschaft für Labor-technik, Burgwedel

2.1.2 Consumables

Description	**Company**
100 mm cell culture dishes	Sarstedt, Nümbrecht
15 ml tubes	Greiner Bio-One, Frickenhausen
50 ml tubes	Greiner Bio-One, Frickenhausen
60 mm cell culture dishes	Sarstedt, Nümbrecht
96 Well micro-plates	Greiner Bio-One, Frickenhausen
Amersham™ Hyperfilm™ ECL High performance chemiluminescence film	GE Healthcare, Buckinghamshire, UK
Blotting paper GB003	VWR, Darmstadt
CELLSTAR® 12-well cell culture plates	Greiner Bio-One, Frickenhausen
CELLSTAR® 24-well cell culture plates	Greiner Bio-One, Frickenhausen
CELLSTAR® 6-well cell culture plates	Greiner Bio-One, Frickenhausen
CELLSTAR® Filter Top cell culture flasks	Greiner Bio-One, Frickenhausen
Counting Chamber Slides, Fast read 102™	Immune-Systems, Paignton, UK
Cover foil, Easy seal (80x140 mm)	Greiner Bio-One, Frickenhausen
Culture slides 8 Chambers	BD Falcon, Erembodegem, Belgium
FACS tubes, flow cytometry	Sarstedt, Nümbrecht
Fuji Medical X-Ray Film / Super RX	Fujifilm, Düsseldorf
Glass beakers	Schott, Mainz
Insulin syringes	B.Braun, Melsungen
Microscope Cover Glasses (18x18mm) and (24x60mm)	Marienfeld, Lauda-Königshofen
Microscopic Slides	Thermo Fisher Scientific, Dreieich
Pipette-tips with wide aperture	Starlab, Hamburg
Pipette-tips, TipOne®, Graduated, Blue/Yellow/White and Filter Tips	Starlab, Hamburg

Polystyrene Round-Bottom tubes (14 ml)	Beckton Dickinson, Heidelberg
QIAshredder shredder column	Qiagen, Hilden
Reaction tubes (0.5 ml)	Eppendorf, Hamburg
Reaction tubes (1.5 ml, 2 ml)	Sarstedt, Nümbrecht

2.1.3 Chemicals and media

Description	**Company**
2′ ,7′ -dichlorodihydrofluoresceindiacetate (H_2DCFDA)	MoBiTec, Göttingen
4′.6-Diamidin-2-phenylindol (DAPI)	Molecular Probes, Eugen
Adefo Citroline 2000 (Developer)	Adefo-Chemie, Dietzenbach
Adefofix (Fixer)	Adefo-Chemie, Dietzenbach
Albumin Fraction V (pH 7)	AppliChem, Darmstadt
Ammonium peroxodisulfate (APS)	Roth, Karlsruhe
Biocoll	Biochrome, Berlin
Bovine Serum Albumin (BSA)	AppliChem, Darmstadt
Bromophenol blue	AppliChem, Darmstadt
Cy3-Streptavidin	Jackson ImmunoResearch, West Grove, USA
Deoxynucleotides (dNTP) Mix	New England Biolabs, Frankfurt
Dichloroacetic acid (DCA)	AppliChem, Darmstadt
Dithiothreitol (DTT)	Sigma Aldrich, München
dNTPs	Thermo Scientific, Hudson, USA
Dulbecco´s Phosphate Buffered Saline (PBS)	PAA Laboratories, Pasching, Austria
Dulbecco's Modified Eagle Medium (DMEM)	Invitrogen, Darmstadt
Ethylenediaminetetraacetic acid (EDTA)	AppliChem, Darmstadt
FACSFlow	Becton Dickinson, Heidelberg
Foetal Calf Serum Gold (A15-151)	PAA Laboratories, Pasching, Austria
Halt™ Protease Inhibitor Single-Use Cocktail	Thermo Fisher Scientific, Dreieich
HANKS' Balanced Salt Solution	Sigma Aldrich, München

Human TNF-α, premium grade	Miltenyi Macs, Auburn, USA
Milk powder	Roth, Karlsruhe
M-MLV reverse transcriptase	Promega, Heidelberg
NHS-biotin	Sigma-Aldrich, München
Non Reducing Lane Marker, Sample Buffer	Thermo Fisher Scientific, Dreieich
Penicillin / Streptomycin (5 U ml^{-1})	Invitrogen, Darmstadt
Pierce® ECL, Western Blotting Substrate	Thermo Scientific, Karlsruhe
Ponceau S	AppliChem, Darmstadt
ProSieve® QuadColor™ Protein Marker	Lonza, Köln
qPCR Rox Mix	Thermo Scientific, Karlsruhe
Random hexamers	Thermo Scientific, Karlsruhe
Ribonuclease A	QIAGEN, Hilden
RNAse/DNase-free water	Invitrogen, Darmstadt
Rotiphoresis gel 30	Roth, Karlsruhe
SDS-Pellets	Roth, Karlsruhe
Sodium chloride (NaCl)	Sigma Aldrich, München
Sodium dodecylsulfate (SDS)	Roth, Karlsruhe
Sodium hydroxide (NaOH)	Sigma Aldrich, München
Tetramethylethylenediamin (TEMED)	Roth, Karlsruhe
Trichloroacetic acid (TCA)	AppliChem, Darmstadt
Tris hydroxymethyl aminomethane (Tris)	Roth, Karlsruhe
Triton X-100	AppliChem, Darmstadt
Trypsin/Ethylene diamine tetraacetic acid (EDTA, 0.25%)	Invitrogen, Darmstadt
Tween® 20	AppliChem, Darmstadt
Vectashield® Mounting Medium	Vector, Burlingame, USA

2.1.4 Buffers and solutions

2.1.4.1 Immunofluorescence

DAPI concentration	600 ng/ml in PBS
Fixing solution	3.7% Formaldehyde in PBS
Permeabilisation solution	0.25% Triton X-100 in PBS
Blocking/Antibody dilution solution	3% BSA in PBS

2.1.4.2 Western immunoblotting

RIPA-Buffer (10x)

150 mM	NaCl
50 mM	Tris, pH 8.0
1%	Triton X-100
0.5%	Dichloroacetic acid (DCA)
0.1%	SDS

1M Tris HCl (pH 8.8)

Adjust volume to 500 ml with distilled water

Adjust pH 8.8 with HCl

1M Tris HCl (pH 6.8)

Adjust volume to 500 ml with distilled water

Adjust pH 6.8 with HCl

Electrophoresis Buffer

25 mM	Tris
191 mM	Glycine
3.47 mM	SDS

Adjust volume to 1 l with distilled water

TBS (10x) (pH 7.5)

1.53 M	NaCl
100 mM	Tris

Adjust volume to 1 l with distilled water

Adjust pH 7.5 with HCl

TBS-T

100 ml	TBS (10x)
1 ml	Tween 20

Adjust volume to 1 l with distilled water

Milk powder block solution

5%	Milk powder in TBS-T

Ponceau-Solution

65.7 µM	Ponceau S
37.5 ml	Trichloroacetic acid (TCA)

Adjust volume to 250 ml with distilled water

Reducing Electrophoresis Buffer (6x)

50%	Glycerol
0.6 M	DTT
10.3%	SDS
0.35 M	Tris pH 6.8
0.012%	Bromophenol blue

Adjust volume to 10 ml with distilled water

Transfer Buffer

30 mM	Tris
160 mM	Glycine
20%	Methanol
0.05%	SDS

Adjust volume to 1 l with distilled water

Table 1. Pipetting scheme for discontinuous SDS-electrophoresis gels (8.3 cm x 7.3 cm x 1 mm)

	Separation gel 10%	**Collection gel 5%**
Distilled water	4.7 ml	5.5 ml
Rotiphoresis Gel 30	5.4 ml	836 µl
Tris HCl (pH 8.8)	6.0 ml	-
Tris HCl (pH 6.8)	-	626 µl
10% SDS	162 µl	50 µl
20% APS	54 µl	40 µl
TEMED	12 µl	5 µl

2.1.5 Antibodies

2.1.5.1 Primary antibodies

Table 2. Primary antibodies used for immunofluorescence, flow cytometry and western immunoblotting

Target	Molecular Weight [kDa]	Dilution	Host	Company	Catalogue Number
CAT	60	1:500	Rabbit	Cell Signaling	#12980
CENP-F	330	1:500	Rabbit	Santa Cruz	sc-22791
GPx1	22	1:1000	Rabbit	Cell Signaling	#3206
Nrf2	97	1:250	Rabbit	Cell Signaling	#12721
SOD1 (Cu/Zn)	18	1:1000	Mouse	Cell Signaling	#4266
β-Actin	42	1:10000	Mouse	Sigma Aldrich	A5441
γH2AX	17	1:1000	Mouse	Millipore	JBW301 05-636

2.1.5.2 Secondary antibodies

2.1.5.2.1 Immunofluorescence/flow cytometry

Table 3. Secondary antibodies used for immunofluorescence and flow cytometry

Target	Dilution	Host	Company	Label	Catalogue Number
Anti-rabbit	1:500	goat	Life technologies	Alexa Fluor^{R} 488	A11034
Anti-mouse	1:500	goat	Life technologies	Alexa Fluor^{R} 594	A11032

2.1.5.2.2 Western immunoblotting

Table 4. Secondary antibodies used for western immunoblotting

Coupled enzyme	Specificity	Host	Dilution	Company	Catalogue Number
Horse radish peroxidase	mouse	goat	1:1000	Santa Cruz	#sc-2055
Horse radish peroxidase	rabbit	goat	1:2000	Santa Cruz	#sc-2054

2.1.6 Primers and probes for real-time PCR

Table 5. Forward/reverse primers and probes used for real-time PCR

Target	Sequence 5' – 3'	Primer	Company	Reference	Additional information
SOD1	GGTCCTCACTTTAATCCTCTATCCAG	SOD1 forward	MWG	[123]	
SOD1	CCAACATGCCTCTCTTCATCC	SOD1 reverse	MWG	[123]	
SOD1	AACACGGTGGGCCAA	SOD1 probe	MWG	[123]	5'Fluorescein (FAM) 3' TAMRA
RPL37A	TGTGGTTCCTGCATGAAGACA	RPL37A forward	STRATIFYER	[124]	
RPL37A	GTGACAGCGGAAGTGGTATTGTAC	RPL37A reverse	STRATIFYER	[124]	
RPL37A	TGGCTGGCGGTGCCTGGA	RPL37A probe	STRATIFYER	[124]	5'Fluorescein (FAM); 3' TAMRA

Table 6. Inhibitors and Activators

Name	Target	Concentration	Company	Catalogue Number
KU0060648	DNA-PK	1 µM	Tocris	4840
KU60019	ATM	1 µM	Tocris	4176
N-Acetyl-L-cysteine (NAC)	Reactive Oxygen Species (ROS)	10 mM	Sigma Aldrich	A7250
AI-1	Keap1	100 µM	Calbiochem	492041

2.1.7 Commercial Kits

Table 7. Kits used for activity analysis

Target	Application	Company	Catalogue Number
Catalase	Enzymatic activity	Abcam	ab83464
Glutathione peroxidase	Enzymatic activity	Abcam	ab102530
Superoxide dismutase	Enzymatic activity	Sigma Aldrich	19160
Nrf2	DNA-binding activity	Cayman Chemicals	Cay600590-96

Table 8. Protein determination, RNA isolation and subcellular fractionation kits

Name	Company	Catalogue Number
Micro BCA™ Protein Assay Kit	Thermo Scientific	23235
NucleoSpin® RNA	Macherey-Nagel	740955
Nuclear Extraction Kit	Cayman Chemicals	Cay10009277-1

2.1.8 Cells

2.1.8.1 EA.hy926 and PBMC

The human endothelial cell (EC) line EA.hy926 was established by a fusion of human umbilical vein endothelial cells (HUVEC) and the adenocarcinoma epithelial cell line A549 [125] and was obtained from the American Type Culture Collection (ATCC). Peripheral blood mononuclear cells (PBMC) consisting of lymphocytes (T cells, B cells, and natural killer (NK) cells), monocytes and dendritic cells were enriched from EDTA blood of healthy donors by density gradient centrifugation (see 2.2.14) and were used in adhesion assays.

2.2 Methods

2.2.1 Cell culture and stimulation

EA.hy926 ECs were grown in Dulbecco's modified Eagle's medium (DMEM) supplemented with 10% foetal calf serum (FCS) 50 U/ml penicillin and 50 µg/ml streptomycin at 37°C in a humidified atmosphere containing 5% CO_2. Cells were passaged two times a week 1:10 by removing the media, washing with 5 ml PBS and adding of 3 ml trypsin-solution. After incubation at 37°C for 5 min, 7 ml DMEM was added and 9 ml of fresh DMEM was mixed with 1 ml of cell suspension and plated into T75 flasks.

For inflammatory stimulation, cells were commonly treated at 4 h before irradiation with the cytokine TNF-α at a concentration of 20 ng/ml. For adhesion assays, TNF-α was added 4 h before addition of PBMC according to previous published protocols [126].

2.2.2 Freezing and thawing of cells

For stepwise freezing, EA.hy926 ECs were trypsinised, centrifuged (150 x g, 4 min), resuspended at a concentration of 3 x 10^6 cells/ml in precooled cryomedium (DMEM + 20% FCS + 5% dimethyl sulfoxide (DMSO)), transferred into cryotubes and stored in a freezing container at -20°C to allow a gentle cooling by 1°C per hour. Next, tubes were transferred to a -80°C refrigerator for long term storage. Cells were thawed by transferring

into PBS followed by centrifugation (150 x g, 4 min) and resuspended in fresh and warm (37°C) medium and transferred into a T75 flask.

2.2.3 Cell lysis

For cell lysis, EA.hy926 ECs were washed once with PBS and scraped in radioimmunoprecipitation assay buffer (RIPA) at 24 h after irradiation. Lysates were transferred to a 1.5 ml reaction tube and incubated for 30 min on ice. After centrifugation at 14,000 x g for 15 min at 4°C, supernatant was transferred into a new 1.5 ml reaction tube and stored at -80°C.

2.2.4 Determination of protein concentration

The protein concentrations of lysates and nuclear extracts were determined by a bicinchoninic acid assay (BCA) kit. The assay is based on the reduction of Cu2+ to Cu1+ by proteins in an alkaline medium with the sensitive and selective colorimetric detection of the cuprous cation (Cu^{1+}) by BCA. First, copper chelates with proteins in an alkaline environment form a light blue complex. In a second step, BCA reacts with the reduced (cuprous) cations to form a purple-coloured reaction product The BCA/copper complex is water-soluble and can be detected at 562 nm with an ELISA reader. The intensity of the coloured reaction product is a direct function of protein concentration that can be determined by comparing its absorbance value to a BSA standard curve, in parallel performed in the range of 0 – 40 µg/ml protein.

2.2.5 SDS-PAGE/western immunoblotting

Sodium dodecyl sulphate polyacrylamide gel electrophoresis (SDS-Page) gels were prepared for electrophoresis according to the pipette schema provided in Table 1 and 20 - 30 µg (determined as described in 2.2.4) of total protein extract was loaded per lane. Prior to electrophoresis, samples were heated at 95°C for 10 min, centrifuged for 1 min at 14,000 x g at 4°C, transferred to the electrophoresis apparatus and separated by 25 mA per gel. Next, gels were placed on 7 x 9 cm filter papers, soaked in transferring-buffer and covered with the blotting membrane followed by two additional filter papers and transferred on a semi-dry blotting apparatus for protein transfer at 50 mA per gel for 150 –

210 min. To confirm correct protein transfer and equal loading, the membranes were next incubated in Ponceau S solution for 1 min and subsequently destained with distilled water. Next, membranes were blocked in 5% milk powder/TBS-T at room temperature for 30 min until primary antibodies, diluted in 5% BSA/TBS-T prior to application, were added and incubated at 4°C overnight. For detection of proteins, membranes were covered with horseradish peroxidase-conjugated goat anti-rabbit and goat anti-mouse secondary antibodies (diluted in 5% milk powder/TBS-T) for 60 min. Finally, membranes were incubated for 1 min with working solutions of an enhanced chemiluminescent (ECL) substrate placed in plastic sheet protectors and exposed to Hyperfilm ECL prior to film development.

2.2.6 SOD activity assay

To assess SOD activity, 1 × 106 of EA.hy926 ECs were plated in T25 cell culture flasks 24 h before irradiation. At indicated time points, medium was removed and cells were incubated with 200 µl of working solution buffer and 20 µl of enzyme working solution for 20 min. The assay utilises a water-soluble tetrazolium salt which is converted to a water-soluble formazan dye after reduction by a superoxide anion. The rate of the reduction through O_2 is linearly related to the activity of xanthine oxidase (XO) and is inhibited by SOD. The reduction can be visualised by absorption at 440 nm and is used as an indirect quantification of SOD activity.

Given that the focus was set on the irradiation effects on non-stimulated and TNF-α stimulated cells, SOD activity levels were given as relative values in arbitrary units relative to the activity of non-irradiated controls (set to 100%).

2.2.7 Catalase activity assay

For analysing CAT activity, 1 × 106 of EA.hy926 ECs were plated in T25 cell culture flasks 24 h before irradiation. At indicated time points, cells were washed with PBS and 150 µl of ice cold assay buffer were added to the cells. For homogenisation, cells were pushed ten times through a 30 gauge syringe. After centrifugation with 10,000 x g for 15 min at 4°C, 80 µl of the supernatant were transferred to a 96-well plate. 50 µl of developer mix was added and incubated for 10 min at room temperature. The assay is based on the reaction of unconverted H_2O_2 with OxiRed™ probe to produce a product which can be measured

spectrophotometrically. Absorbance was determined at a wavelength of 570 nm using an ELISA reader. Relative activity levels were calculated as described in 2.2.6.

2.2.8 Glutathione peroxidase activity assay

To assess GPx activity, 1 × 106 of EA.hy926 ECs were plated into T25 cell culture flasks 24 h before irradiation. At indicated time points after X-ray exposure, cells were washed with PBS, suspended in 150 µl of ice cold assay buffer and homogenised by pushing ten times through a 30 gauge syringe. After centrifugation with 10,000 x g for 15 min at 4°C, 50 µl of the supernatant were transferred to a 96-well plate. 50 µl of reaction mix was added and incubated for 10 min at room temperature. In the assay, GPx reduces cumene hydroperoxide while glutathione (GSH) is oxidised to glutathione disulphide (GSSG). The GSSG is reduced to GSH along with a consumption of nicotinamide adenine dinucleotide phosphate (NADPH) as the decrease of NADPH is proportional to GPx activity. Changes in NAPDH content were determined spectrophotometrically with an absorbance at a wavelength of 340 nm using an ELISA reader. Relative activity levels were calculated as described in 2.2.6.

2.2.9 Subcellular fractionation

For separation of cytoplasmic and nuclear fractions, EA.hy926 ECs were washed with PBS and scraped with 1 ml of ice-cold PBS. The scraped cells were transferred to pre-chilled 1.5 ml reaction tubes and centrifuged at 150 x g at 4°C for 5 min. Supernatants were discarded and the pellet was resuspended in 500 µl ice-cold hypotonic buffer with phosphatase/protease inhibitors and incubated on ice for 15 minutes. Next, 25 µl of nonidet P-40 was added and the tubes were centrifuged at 14,000 x g at 4°C for 45 sec. The cytoplasmic fraction was transferred to 1.5 ml reaction tubes. The pellet was resuspended in 100 µl nuclear extraction buffer containing DTT, protease/phosphatase inhibitors and was incubated at 4°C for 90 min with shaking. Following incubation, the reaction tubes were centrifuged at 14,000 x g for 15 min. The supernatant containing the nuclear fraction was collected into new 1.5 ml reaction tubes. Protein concentrations were determined by BCA assay as described in 2.2.4.

2.2.10 Nrf2 DNA-binding activity assay

For the measurement of DNA-binding activity, equal amounts of proteins (30 µg) in nuclear extracts (see 2.2.9) were incubated over night at 4°C with a specific consensus double-stranded DNA sequence containing the Nrf2 response element, immobilised onto the wells of a 96-well plate. After incubation, wells were emptied and washed 5 times with 200 µl 1x wash buffer. Primary antibody, detecting specifically bound activated Nrf2, was added and incubated for 1 h at RT. After subsequent washing 5 times with 1x wash buffer, secondary HRP-coupled antibodies was added and again incubated for 1 h at RT. Following subsequent washing, 100 µl of developing solution was added. The reaction was stopped by adding 100 µl of stop solution. Quantification of DNA-binding activity was performed by sensitive colorimetric readout at 450 nm with an ELISA reader. Relative DNA-binding activity levels were calculated as described in 2.2.6.

2.2.11 mRNA isolation

For isolation of mRNA, cells were washed with PBS, trypsinised and centrifuged 5 min at 180 x g. Pellets were resuspended and lysed in 350 µl RA1-buffer supplemented with 3.5 µl of β-mercaptoethanol. The lysate was transferred to shredder columns and centrifuged for 1 min at 15,000 x g and 4°C. The flow through was loaded on NucleoSpin®Filter and centrifuged at 11,000 x g for 1 min into a 2 ml collection tube. After adding of 350 µl 70% Ethanol, the mixture was transferred on a NucleSpin® RNA II column and centrifuged at 11,000 x g for 30 s. 350 µl membrane desalting buffer was added on the column, centrifuged at 11,000 x g for 1 min and rDNase was added, followed by 15 min incubation. The column was washed with 200 µl RA2 buffer and 600 µl RA3 buffer each followed by centrifugation at 11,000 x g for 30 s. Washing was performed in 250 µl RA3 buffer followed by centrifugation at 11,000 g for 2 min. Finally, the RNA was eluted with 100 µl RNase free H_2O and centrifugation at 11,000 x g for 1 min. For each sample, total RNA content was assessed by absorbance at 260 nm and purity by A_{260nm}/A_{280nm} ratios.

2.2.12 cDNA synthesis

By the usage of reverse transcriptase, random hexamers and dNTPs, RNA was reverse transcribed to cDNA. First, 700 ng RNA and 350 ng random hexamers were denatured in a PCR device for 15 min at 70°C. This step was followed by addition of a master mix containing reverse transcriptase (200 U) and dNTPs (500 µM). Synthesis was performed as follows: 10 min 25 °C; 30 min 37°C; 30 min 42 °C.

2.2.13 Real-time PCR

For quantitative real-time PCR (qPCR), 2.5 µl cDNA was mixed with 12.5 µl of qPCR Rox Mix and 10 µM each forward/reverse primers and probes for SOD1 or RPL37A. Each qPCR was conducted in at least duplicates with the following setup: 15 min 95°C followed by 40 cycles each 15 s at 95°C and 1 min at 60°C. Relative quantification was performed by using the comparative Ct (ΔΔCt) method. This involves comparing the Ct values of irradiated with mock-treated samples. The Ct values corresponded to the number of cycles at which the fluorescence emission monitored in the real-time PCR reaction reaches a certain threshold. Additionally, the Ct values were normalised to an endogenous housekeeping gene using 60S ribosomal protein L37 (RPL37A) as internal reference. Relative mRNA expression levels were calculated as described in 2.2.6.

2.2.14 Isolation and biotinylation of PBMC

For the preparation of peripheral blood mononuclear cells (PBMC), EDTA blood of healthy donors was used. After dilution with HANKS' balanced salt solution (1:1), 35 ml of the suspenison was carefully layered onto 15 ml of a Biocoll solution in a 50 ml tube. Following centrifugation at 1000 x g for 20 min without breaks, the layer containing the PBMC was carefully removed and cells were transferred into a new 50 ml tube and washed with HANKS' solution twice by centrifugation at 180 x g for 8 min (Figure 5). Finally, cells were resuspended in RPMI medium + 10% FCS. All steps were performed at room temperature. PBMCs were biotinylated with a biotin-N-hydroxysuccinimid ester (NHS-biotin). For this purpose, 10 µl of NHS-biotin (10 mg/ml in dimethylformamid (DMF)) per 1 ml of PBMC in RPMI supplemented with 10% FCS were incubated for 15 min on ice. After centrifugation with 150 x g for 8 min, cells were suspended with 500 µl

1 M ammonium chloride and PBS was added subsequently. Cells were washed with 4°C PBS following a centrifugation with 150 x g for 8 min and resuspended in RPMI + 10% FCS and quantified using counting chamber slides.

2.2.15 Adhesion Assay

For adhesion assays (Figure 5), EA.hy926 ECs were plated into 12-well plates, grown to confluence and irradiated with doses ranging from 0 to 3 Gy in the presence of either DMSO or AI-1 (100 µM) or ROS scavenger NAC (10 mM). At 20 h after irradiation, cells were stimulated with TNF-α (20 ng/ml).

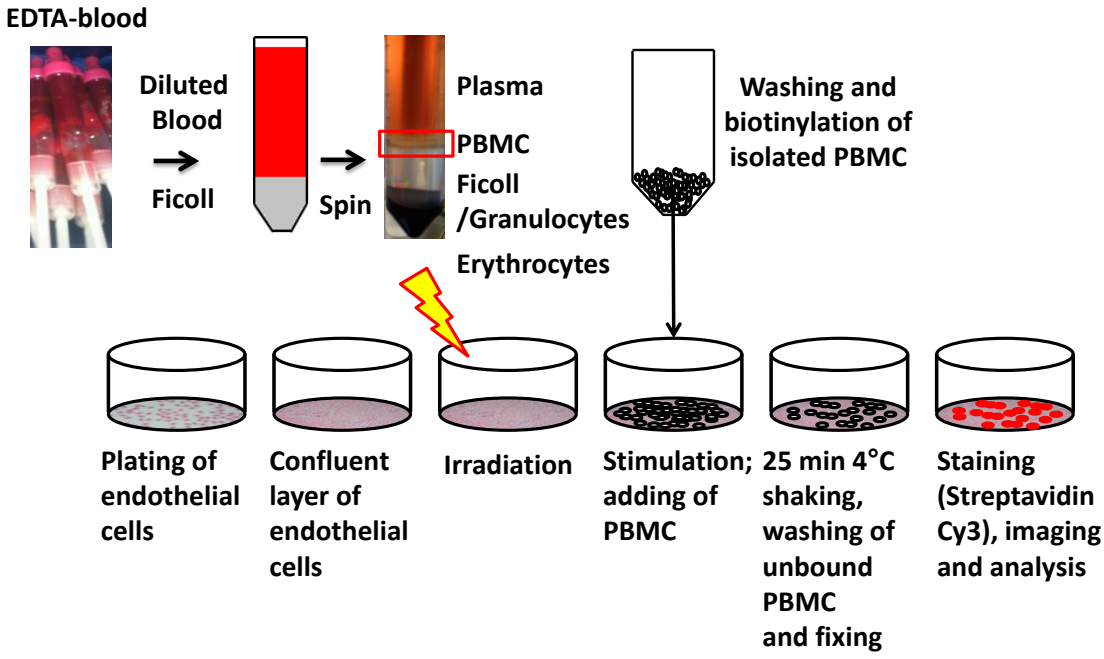

Figure 5. Scheme of adhesion assay

Upper row: PBMCs were isolated from EDTA blood of healthy donors, washed and subsequently biotinylated. Lower row: EA.hy926 ECs were grown to confluence, irradiated and stimulated. Biotinylated PBMCs were added, adhered for 30 min at 4 °C with dynamic shaking conditions and unbound PBMCs were removed by washing with PBS. After fixation, adhered PBMCs were visualised by Streptavidin-Cy3 conjugates and adhesion events (number of bound PBMC) were quantitated.

At 24 h after irradiation, biotinylated PBMCs at a concentration of 4 x 10^5 cells/ml were added to the EC and incubated for another 30 min at 4°C with gentle shaking (dynamic conditions). Next, unbound PBMCs were removed by washing with PBS and adherent PBMC were fixed with precooled (-20°C) Methanol and subsequently labelled with a streptavidin-Cy3 conjugate. Finally, adhesion events were quantitated by a fluorescence microscopy at a 250-fold magnification. The counts of a minimum of ten selected fields were averaged as one data point. The value of mock-irradiated samples was taken as a fixed intercept (100%) for the respective series of experiments.

2.2.16 Immunofluorescence staining

EA.hy926 ECs were grown on glass coverslips in 6-well plates for 48 h, treated with TNF-α, NAC, HR and NHEJ inhibitors or were mock-treated and irradiated. Inhibitors (Table 6) were added 1 h and NAC 4 h before irradiation. At different time points (1 h, 4 h and 24 h) after irradiation, cells were fixed with 3.7% formaldehyde for 15 min prior to washing twice with PBS. After permeabilisation (5 min 0.25% Triton-X 100 in PBS) and two times washing with PBS, cells were blocked in 3% BSA in PBS for at least 60 min. Primary antibodies (see 2.1.5.1) were incubated for 1 h followed by three washing steps with PBS and incubation with appropriate secondary antibodies (see 2.1.5.2.1) for 1 h in the dark. As the signal of phospho-histone H2AX may differ in a cell-cycle dependent manner with a doubled amount of DNA in the G2 phase leading to a higher number of γH2AX foci [127], cells were stained for Centromere protein-F (CENP-F), which is only detectable in S/G2-phase cells. Subsequently, the coverslips were washed, nuclei were counterstained with DAPI solution and coverslips were mounted with Vectashield. Images were acquired using an AxioImager Z1 microscope, equipped with an Axiocam camera and Axiovision 4.6 software. For quantification, at least 40 nuclei in the G1 and 40 nuclei in the G2 phase were analysed and combined to one data point. CENP-F positive cells were excluded by their pan-nuclear γH2AX-signal.

2.2.17 Flow cytometry

2.2.17.1 Analysis of cellular protein level

Intracellular protein levels were determined by flow cytometry using specific primary antibodies targeting antioxidative proteins. At indicated times, cells were trypsinised on ice and washed with PBS. Cells were fixed with 3.7% paraformaldehyde for 15 min, permeabilised by 96% ice cold ethanol for 30 min on ice and treated with blocking buffer (1% BSA in PBS) for 30 min. Primary antibodies at a dilution of 1:100 in blocking buffer were added for 60 min. Following washing with 0.5% BSA in PBS, appropriate secondary antibodies were added at a dilution of 1:100 in blocking buffer with incubation in the dark for 30 min at RT. Following final washes, cells were resuspended in PBS for FACS analysis using a cytometer and Cellquest Pro software. Relative expression levels were calculated as described in 2.2.6.

2.2.17.2 Detection of reactive oxygen species

Intracellular ROS levels were determined by flow cytometry using the cell membrane permeable dye 2′, 7′-dichlorodihydrofluoresceindiacetate (H_2DCFDA), which is further processed in the cell by cleavage of the acetate groups by intracellular esterases and oxidation. Consequently the non-fluorescent H_2DCFDA is converted to the fluorescent 2', 7'-dichlorofluorescein (DCF) which can be measured by flow cytometry.

Prior to harvesting, cells were incubated for 90 minutes with H_2DCFDA at a concentration of 2 µM in serum-free medium. At indicated times, cells were trypsinised on ice, washed once with PBS and analyses were performed using a cytometer and Cellquest Pro software. The mean fluorescence of mock-treated cells was subtracted to eliminate unspecific background intensity for every sample. Relative ROS levels were calculated as described in 2.2.6.

2.2.18 Irradiation

Irradiation was performed at a linear accelerator (SL75/5, Elekta) with 6 MeV/100 cm focus-surface distance and a dose rate of 4 Gy/min. In parallel, mock-treated controls were kept at ambient temperature in the accelerator control room. Dosimetry was regularly performed by medical physicists of the Department of Radiotherapy and Oncology.

2.3 Data analysis

Experimental data are presented as mean ± standard error of the mean (SEM) from at least three or more independent experiments. To test statistical significance, a two-sided unpaired Student's t-test was performed using Excel® software. Results were considered statistically significant if a p-value of less than 0.05 was reached, more significant if $p < 0.01$ and highly significant if $p < 0.001$, respectively. Relative values were calculated as previously described in 2.2.6.

3 Results

3.1 Time and dose kinetics of γH2AX foci after low-dose radiation

For decades, an anti-inflammatory and analgesic effect of LD-RT has been well established in the treatment of a multiplicity of benign diseases and chronic degenerative disorders [11]. Although the knowledge of the underlying cellular and molecular mechanisms is still at an early stage, a modulation of EC activity has already been proven to comprise a key element in the therapeutic effects of LD-RT.

To analyse the effects of low-dose X-ray exposure on DNA damage induction and repair, immunofluorescence analysis of phosphorylation of the histone variant H2AX on serine 139 (γH2AX foci) as a marker for the presence of DNA-DSBs was applied [127].

For this purpose, EA.hy926 ECs were plated onto glass coverslips, grown to 95% confluence and were stimulated with TNF-α (20 ng/ml) or mock treated at 4 h before irradiation with single doses of 0.3, 0.5, 0.7 or 1 Gy. Histone γH2AX foci levels were investigated at 1 h, 4 h and 24 h (residual foci) after irradiation. As γH2AX foci levels may differ in a cell-cycle dependent manner with a doubled amount of DNA in the G2 phase [127], both, cells in the G1 and G2 phase as differentiated by the intensity of the centromere protein F (CENP-F) signal (Figure 6 A) were taken into consideration to improve accuracy of foci measurement.

Irrespective of stimulation with TNF-α, at early time points (1 h, 4 h) a linear dose-response relationship of γH2AX foci was evident. Data from at least three independent experiments are depicted in Figure 6 B/C. By contrast, at 24 h after irradiation the number of residual γH2AX foci was significantly ($p < 0.05$) elevated after a 0.5 Gy exposure as compared to irradiation with doses of 0.3 Gy and 0.7 Gy (Figure 6 D). Notably, these characteristics could be observed in both, G1 and G2 cells (with expected elevated numbers of γH2AX foci in G2) indicating that the discontinuity in foci numbers at 24 h was not related to cell cycle distribution (Figure 6 E/F; Supplementary Figure 1).

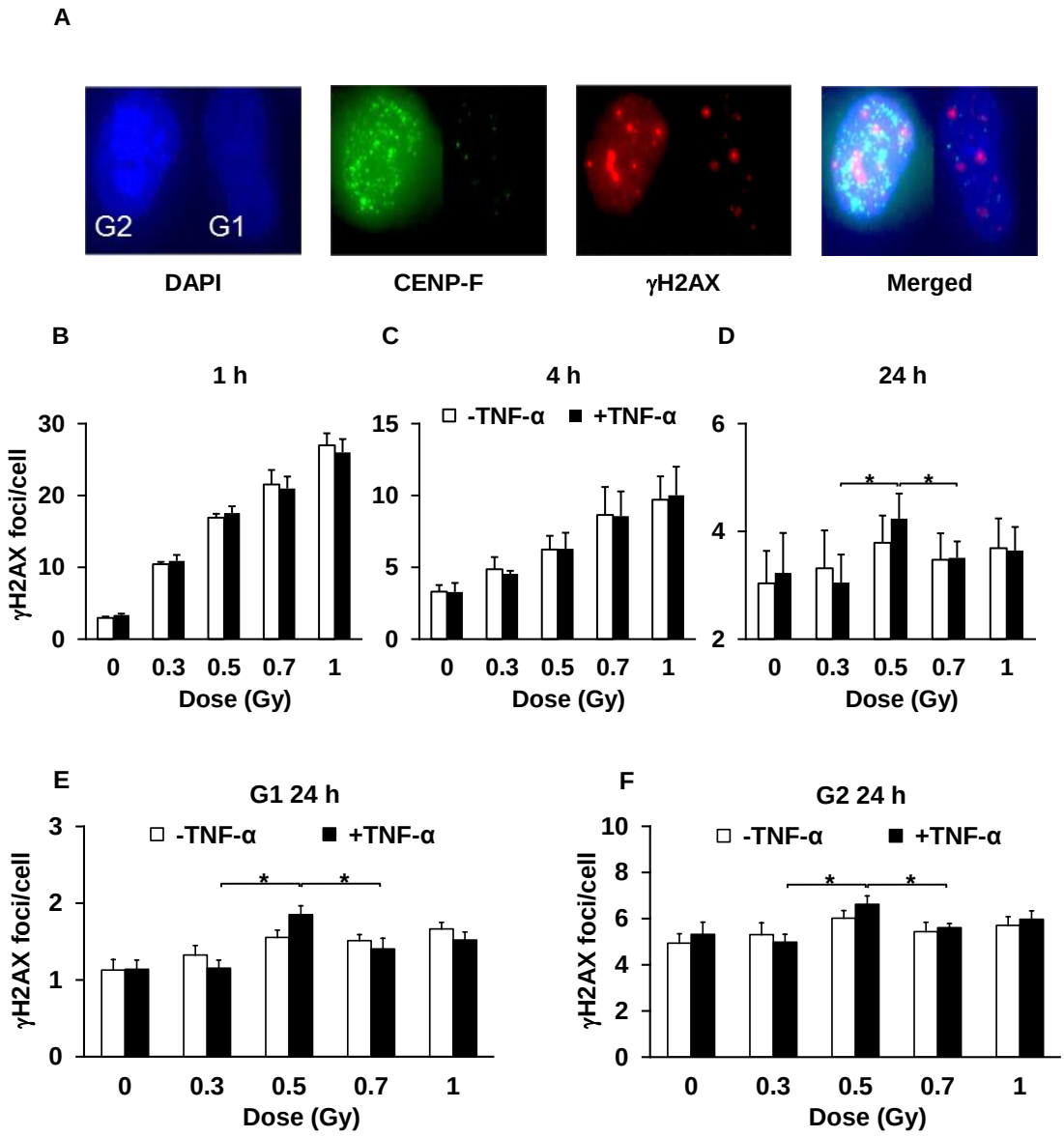

Figure 6. Dose and time kinetics of γH2AX foci in EA.hy926 EC following low-dose X-irradiation

EA.hy926 EC were plated onto coverslips and stimulated with TNF-α (20 ng/ml) (black bars) at 4 h before irradiation with the doses indicated. Mock-treated cells (white bars) served as a control. At 1 h (B), 4 h (C) and 24 h (D) post irradiation, cells were fixed, stained for γH2AX, DAPI and CENP-F (A) and data of a total of 80 nuclei (40 G1 phase (CENP-F negative) and 40 G2 phase (CENP-F positive)) were combined for a single data point. Exemplary results for γH2AX foci 24 h after irradiation of G1 phase cells (E) and G2 phase cells (F). Data represent means ± SEM from at least three independent experiments. Asterisks indicate significant differences (* $p < 0.05$) vs. 0.3 Gy and 0.7 Gy irradiated ECs.

In summary, these data indicate that the induction of DSBs and DNA damage repair in EA.hy926 ECs at early time points follows a linear dose-response relationship, at later time points, by contrast, a discontinuity with locally elevated levels of γH2AX foci at 0.5 Gy were observed. The molecular mechanisms and factors involved in these characteristics, however, remain elusive and may originate from a dysregulation of DNA damage repair. Thus, next the impact of the most prominent DSB repair pathways HR and NHEJ on residual γH2AX foci levels following low-dose irradiation was analysed.

3.2 γH2AX foci after low-dose radiation and inhibition of DNA damage repair

For this purpose, small molecule inhibitors targeting ATM [128] and DNA-PK [129], proteins essential in HR and NHEJ were applied. ATM promotes the initial resection of DSBs by activation of the nuclease CtiP via phosphorylation [130]. This resection is required for processing of the DSB by other nucleases and is an important initial step in HR. Consequently, the number of DSBs repaired by HR is expected to be decreased after ATM inhibition by KU60019 (ATMi) [131]. DNA-PK and its catalytic subunit DNA-PK_{cs} are responsible for the opening of the DNA ends to additional proteins involved in NHEJ. Furthermore, the enzyme is essential for processing of the DSB to generate the 3'-OH and 5'-P ends required for ligation [75, 132]. Since NHEJ is reported as the predominant repair pathway dealing with approximately 80% of X-ray-induced DSBs with rapid kinetics [101], an inhibition of DNA-PK by KU0060648 (DNA-PKi) is expected to result in a pronounced repair defect.

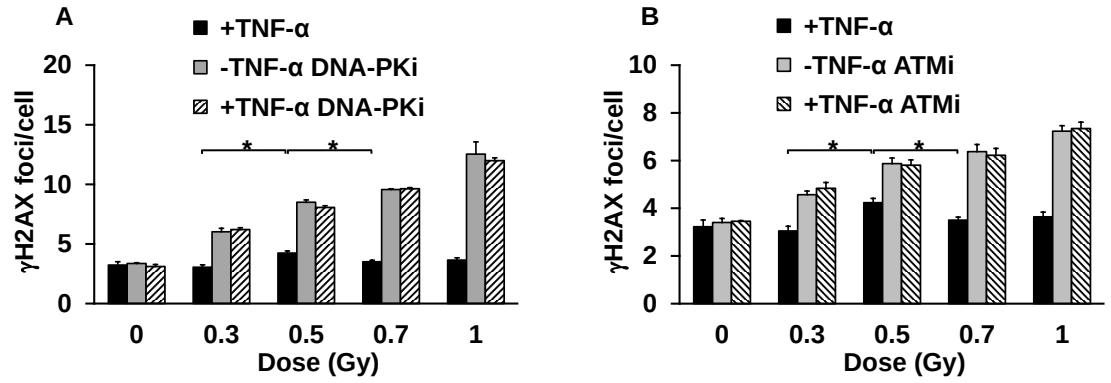

Figure 7. γH2AX foci levels in EA.hy926 EC following low-dose X-irradiation in the presence of inhibitors for NHEJ and HR

EA.hy926 EC were plated onto coverslips and stimulated with TNF-α (20 ng/ml) at 4 h before irradiation with the doses indicated. Cells were treated with inhibitors for (A) DNA-PK (DNA-PKi) or (B) ATM (ATMi) 1 h before irradiation. Mock-inhibitor treated cells served as a control. At 24 h post irradiation, cells were fixed, stained for γH2AX, DAPI and CENP-F and data of a total of 80 nuclei (40 G1 phase (CENP-F negative) and 40 G2 phase (CENP-F positive)) were combined for a single data point. Data represent means ± SEM from at least three independent experiments. Asterisks indicate significant differences (* $p < 0.05$) vs. 0.3 Gy and 0.7 Gy irradiated ECs.

Both inhibition of ATM and DNA-PK did not affect background levels of γH2AX foci in mock-irradiated and non-stimulated or TNF-α stimulated ECs, respectively. Irradiation with doses ranging from 0.3 to 1 Gy resulted in a linear dose-response-relationship of γH2AX foci levels in line with an abolishment of the discontinuous dose-response characteristics as reported before. This effect was equal in ATMi and in DNA-PKi treated cells independent of TNF-α stimulation (Figure 7).

Given that the number of γH2AX foci 24 h after IR is only slightly but significantly increased after an exposure to 0.5 Gy, it may be possible that the effect of inhibition of the repair pathways on the biphasic induction of γH2AX foci is not detectable due to an overlay with the elevated number of γH2AX foci after inhibition of DNA damage repair. Consequently, these results do not clearly indicate an involvement of either HR or NHEJ in the biphasic appearance of residual γH2AX foci following low-dose exposure. For this reason, other factors were analysed to further explore underlying molecular mechanisms implicated in the discontinuous appearance of γH2AX foci following LD-RT. For this purpose, the next focus was set on ROS as a potential element since ROS are reported to induce DSBs [133].

3.3 Levels of reactive oxygen species after low-dose radiation

Following environmental stress, including ionising radiation, ROS levels increase dramatically resulting in a significant damage of cellular structures and induction of DNA damage [98]. Moreover, previous studies indicated a biphasic regulation of the oxidative burst in activated macrophages revealing changes in the production of ROS after exposure to LD-RT in another cellular system [53].

To investigate a putative role of ROS production in the non-linear levels of γH2AX foci, EA.hy926 EC were stimulated with TNF-α 4 h before irradiation or mock-treatment and ROS levels were analysed by measurement of the fluorescent dye 2',7'-dichloro-fluorescein (DCF) using a flow cytometer.

For controls, forward and side scatter analyses were performed, indicating that neither irradiation, stimulation with TNF-α nor application of DCF markedly alters cellular morphology (Figure 8 A). Furthermore the relative percentage (to total cells measured) of cells used for analysis was only marginally affected by LD-RT. The fluorescence of non-DCF-stained cells, served as a blank value. As depicted in Figure 8 B, application of DCF increased the intensity of the fluorescence signal, which was further elevated by irradiation with a dose of 0.5 Gy indicating elevated levels of intracellular ROS.

As displayed in Figure 8 C, a biphasic appearance of DCF fluorescence with a local maximum at a dose of 0.5 Gy became evident at 24 h after irradiation irrespective of inflammatory stimulation of the EC by TNF-α. At doses of 0.7 Gy a decreased expression of ROS was observed followed by an increase at a dose of 1 Gy.

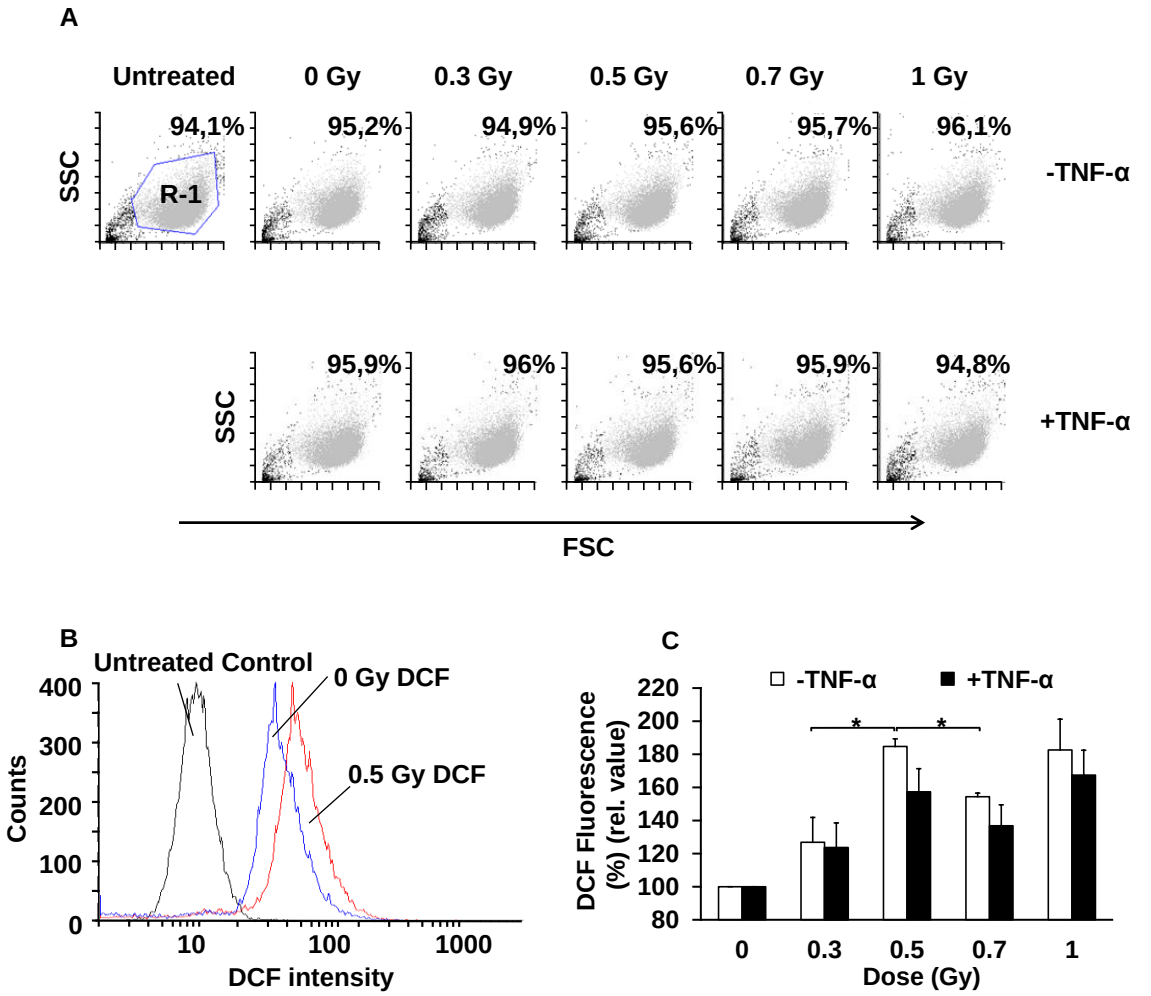

Figure 8. ROS levels in EA.hy926 ECs following low-dose X-irradiation

(A) Representative flow cytometer dot plots showing forward scatter (FSC) versus side scatter (SSC) for each treatment regimen. R-1 indicates the population of cells used for the analysis of 2′, 7′-dichlorodihydrofluoresceindiacetate (DCF) fluorescence. The numbers indicate the percentage of cells used for analysis - relative to total cells measured. (B) Representative histograms showing an increase of DCF fluorescence as a marker of ROS production in TNF-α stimulated, non-irradiated (blue line) and irradiated (0.5 Gy, red line) cells. Non-DCF treated cells (black line) served as a control and were subtracted for each quantification. (C) Quantification of relative DCF-fluorescence in EA.hy926 ECs at 24 h after irradiation with the doses indicated. Relative values were calculated relative to non-irradiated cells of the appropriate kind of stimulation. Data represent means ± SEM from at least three independent experiments. Asterisks indicate significant differences (* $p < 0.05$) vs. 0.3 Gy and 0.7 Gy irradiated ECs.

In conclusion, here an increase of total ROS to 80% in non-stimulated and 60% in TNF-α stimulated cells as compared to mock-irradiated cells, overlapping with elevated levels of γH2AX foci levels in terms of dose (0.5 Gy) and timing (24 h) is indicated. Thus, next an

apparently functional interrelationship between ROS production and γH2AX induction following LD-RT was analysed.

3.4 γH2AX foci after low-dose radiation and scavenging of reactive oxygen species by N-acetyl-cysteine

To further investigate a functional impact of ROS induction and a discontinuous level of γH2AX foci at 24 h after LD-RT, EA.hy926 EC were irradiated in the presence of the ROS scavenger NAC. NAC is an aminothiol and synthetic precursor of intracellular cysteine and glutathione and comprises an antioxidant and ROS scavenger used in scientific research [134, 135]. In pilot experiments (Figure 9 A) NAC treatment (10 mM) was proven to significantly diminish total ROS levels to 20 % of non-treated controls in stimulated and non-stimulated EA.hy926 cells, irradiated with a dose of 0.5 Gy.

As shown in Figure 9 B, the non-linear appearance of γH2AX foci was completely abolished upon treatment with NAC, indicating a correlation between ROS production and the biphasic characteristics of γH2AX foci levels.

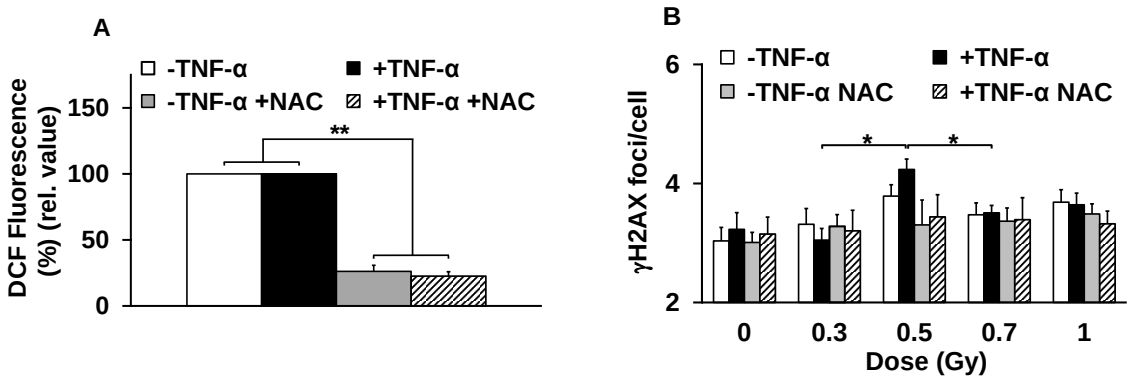

Figure 9. γH2AX foci levels in EA.hy926 EC following low-dose X-irradiation in the presence of the ROS scavenger NAC

EA.hy926 ECs were stimulated with TNF-α (20 ng/ml) or mock-treated and were irradiated in the presence of NAC (10 mM, applied 4 h before irradiation). At 24 h after irradiation relative DCF-fluorescence (A) and γH2AX foci levels (B) were analysed. Relative values were calculated as compared to mock-irradiated cells of the appropriate stimulation. Cells without NAC treatment served as a comparison (black bars). Data represent means ± SEM from at least three independent experiments. Asterisks indicate significant differences (* $p < 0.05$; ** $p < 0.01$) vs. 0.3 Gy and 0.7 Gy irradiated ECs or NAC vs. mock treated ECs.

As ROS production is mediated and regulated by a variety of enzymes implicated in the cellular anti-oxidant defence, next, experiments on the expression and activity of selected factors like SOD, CAT and GPx were conducted to explore molecular mechanisms implicated in the discontinuous induction of ROS and subsequent modulation of γH2AX foci levels.

3.4.1 Analysis of the antioxidative defence mechanisms after low-dose radiation

3.4.1.1 Expression and activity of ROS detoxifying enzymes after low-dose radiation

First, the impact of the enzyme SOD which is reported to be involved in detoxification of ROS by the conversion of the superoxide radical (O_2•-) to H_2O_2 and O_2 [136] was examined. SOD exists in three isoforms in mammals (cytoplasmic Cu/ZnSOD (SOD1), mitochondrial MnSOD (SOD2), extracellular Cu/ZnSOD (SOD3)), however, SOD1 is reported to be mainly responsible for total SOD activity [136]. Consequently, SOD1 expression was investigated on the level of protein in western immunoblotting, while enzymatic activity was quantitated for total SOD by a colorimetric assay.

As illustrated in Figure 10 A and Figure 10 C, total SOD1 protein expression and SOD activity displayed a discontinuous dose response dependency with a relative minimum at 0.5 Gy as proven by western immunoblotting and colorimetric assays. By densitometric analysis, the relative amount of protein reduction was quantified (Figure 10 B). Exposure of EA.hy926 EC to 0.5 Gy and less pronounced to 0.7 Gy resulted in a reduction of approximately 50% and 30% of SOD1 expression in ECs, as compared to mock-irradiated controls (Figure 10 B). The expression of SOD1 at 24 h after a dose of 0.5 Gy was lower as compared to mock-irradiated controls, while the activity was equal to controls. However, the SOD activity in cells irradiated with a dose of 0.5 Gy was significantly decreased as compared to cells treated with a dose of 0.3 Gy and 0.7 Gy.

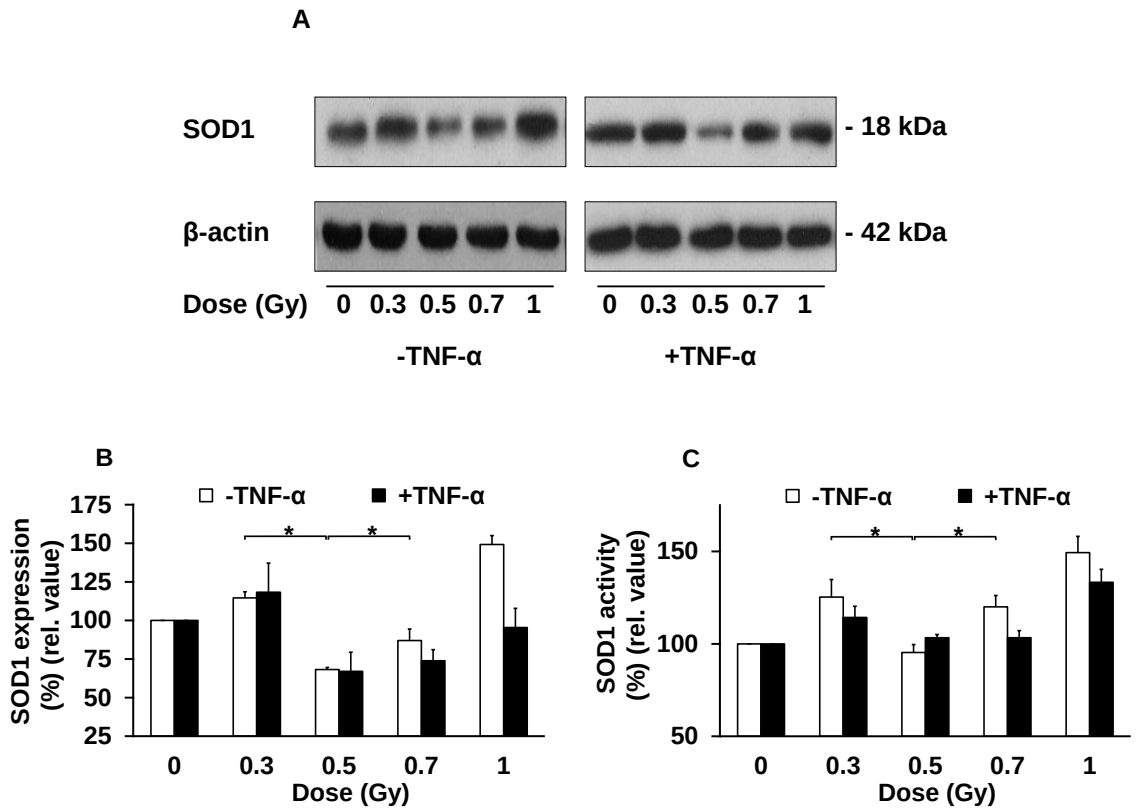

Figure 10. SOD1 protein expression and SOD activity in EA.hy926 ECs following low-dose X-irradiation

(A) Western immunoblots from total cellular proteins at 24 h after irradiation using antibodies against SOD1 and β-actin for loading control. Data are displayed as one representative from three independent experiments. (B) Reduction of SOD1 protein expression normalised to β-actin control as determined by densitometric analysis using the ImageJ software package and data from (A). (C) Relative SOD activity as analysed at 24 h after irradiation by using a colorimetric activity assay. Relative values were calculated to mock-irradiated cells with the appropriate stimulation. Data represent means ± SEM from at least three independent experiments. Asterisks indicate significant differences (* $p < 0.05$) vs. 0.3 Gy and 0.7 Gy irradiated ECs.

In summary, expression of SOD1 and its enzymatic activity is modulated by LD-RT, displaying a local minimum after a 0.5 Gy exposure in line with a maximum of ROS induction shown in Figure 8 C. Notably, changes in protein expression were more pronounced than the levels of activity. A putative explanation for this observation might be, that SOD1 is reported as the major component of SOD activity, but SOD2 and SOD3 are also involved in the conversion of superoxide (O_2•-) to H_2O_2 and O_2.

H_2O_2 derived from SOD enzymatic activity is further processed by GPx or CAT, resulting in H_2O, alcohols and O_2 [112, 113]. To further unravel additional antioxidant factors implicated in the non-linear induction/regulation of ROS, an additionally focus was set on CAT and GPx expression and activity. Moreover, to further improve the sensitivity of protein detection as compared to western immunoblotting, levels of GPx1 protein, the most abundant of eight known GPx isoforms [137, 138] and expression of CAT were analysed in following experiments by flow cytometry (Figure 11 A).

First, feasibility of the intracellular staining procedure and quantification of protein expression by a flow cytometer were evaluated (Figure 11 A). A clear increase of fluorescence intensity became evident when antibody treated samples were compared to mock-treated cells. Irradiation of the cells further resulted in a distinct enhancement of fluorescence levels, equivalent to increased amounts of the intracellular proteins.

At 4 h before irradiation with doses ranging from 0.3 to 1 Gy, EA.hy926 ECs were stimulated with TNF-α (20 ng/ml) and relative CAT and GPx protein expression as determined by flow cytometry (20,000 cells/events) and colorimetric activity assays at 24 h after irradiation were analysed.

Again, irrespective of stimulation with TNF-α, a non-linear dose-response relationship of both CAT (Figure 11 B) and GPx1 protein levels (Figure 11 C), with increased values at 0.3 Gy, a minimum at 0.5 Gy and a further increase following exposure to doses of 0.7 and 1 Gy was observed. In line with that observation, activity assays performed in parallel further confirmed a discontinuous appearance of enzymatic activity of CAT and GPx with decreased values (compared to doses of 0.3 or 0.7 Gy) following irradiation with a dose of 0.5 Gy (Figure 11 D/E).

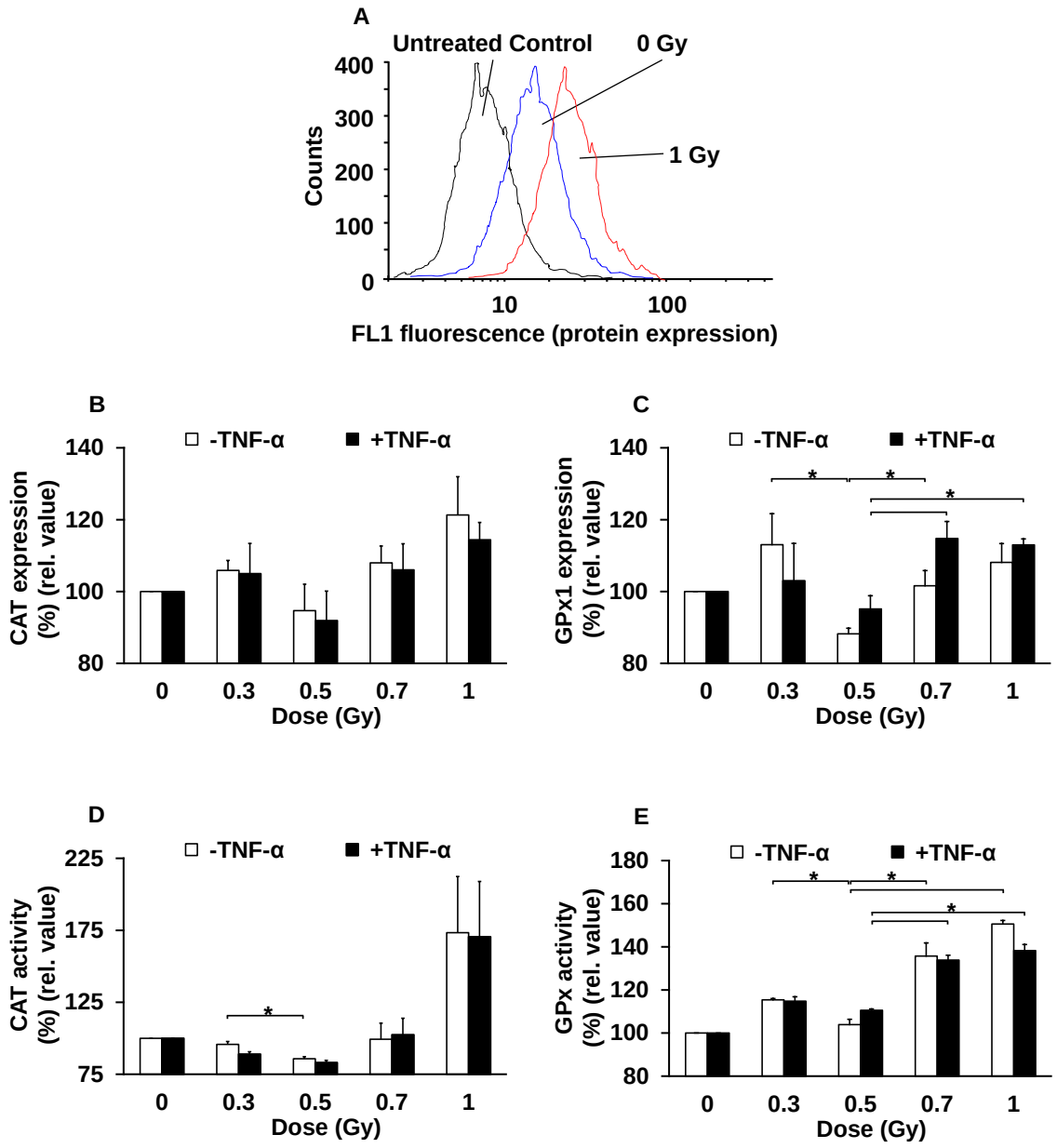

Figure 11. CAT/GPx1 protein expression and CAT/GPx activity in EA.hy926 cells following low-dose X-irradiation

(A) Representative histograms showing FL1 fluorescence (protein expression) for control (dotted line; no antibody); non-irradiated cells (full line) and cells irradiated with 1 Gy (dashed line). Mock-treated cells served as a control and their fluorescence values were subtracted in every quantification. Reduction of CAT (B) and GPx1 (C) protein expression as determined by a flow cytometer. Relative CAT (D) and GPx (E) activity analysed at 24 h after irradiation by using colorimetric activity assays. Relative values were calculated to mock-irradiated cells. Data represent means ± SEM from at least three independent experiments. Asterisks indicate significant differences (* $p < 0.05$).

To sum up, these data indicate a discontinuous regulation of a variety of enzymes implicated in the cellular antioxidative defence with highly comparable dose kinetics and a common reduction most prominent following a 0.5 Gy exposure.

3.4.1.2 mRNA expression of SOD1 after low-dose radiation

Mammalian protein expression is regulated by a variety of mechanisms, like the level of transcription, post-transcriptional silencing, post-translational modifications and protein stability [139-141]. Notably, LD-RT is reported to modulate protein expression with (TGF-β_1) [38] or without (iNOS) [142] influencing mRNA levels. Next, to investigate whether or not LD-RT affects mRNA levels of the proteins reported before, exemplary quantification of SOD1 mRNA was performed by qPCR. As this factor displayed the most notably regulation in protein expression after LD-RT, the levels of mRNA of SOD1 were evaluated 24 h after irradiation.

Figure 12 depicts a non-linear level of SOD1 mRNA following irradiation with doses > 1 Gy, confirming a regulation of SOD1 on the mRNA level after LD-RT. Exposure of EA.hy926 EC to doses of 0.3 up to 1 Gy resulted in decreased SOD1 mRNA levels at a dose of 0.5 Gy as compared to 0.3 Gy and 0.7 Gy irradiated cells, similar to the levels obtained in mock-irradiated control cells.

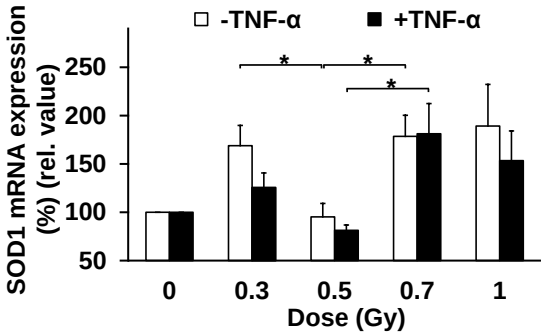

Figure 12. SOD1 mRNA expression levels in EA.hy926 cells following low-dose X-irradiation

Relative mRNA levels of SOD1 (ΔΔCT method) 24 h after low-dose radiation as analysed by qPCR with RPL37A as an internal control. Relative values were calculated relative to mock-irradiated controls. Data represent means ± SEM from at least three independent experiments. Asterisks indicate significant differences (* $p < 0.05$) vs. 0.3 Gy and 0.7 Gy irradiated ECs.

These results indicate a modulation of antioxidative factors by low-dose irradiation on the level of transcription implicating further overall regulatory mechanisms to be involved. As a consequence, the putative role of the redox-sensitive transcription factor Nrf2 was analysed.

3.4.2 Modulation of Nrf2 expression and DNA-binding activity

To further elucidate common underlying molecular mechanisms, the expression and DNA-binding activity of the transcription factor Nrf2 was evaluated by flow cytometry and colorimetric assays, respectively. Nrf2 is reported to be involved in the oxidative stress response by inducing the expression of detoxifying enzymes under the control of an ARE-promoter [106, 109]. As a consequence, Nrf2 is considered as a key player in the cellular stress response [110] that might be involved in the regulation of enzymes by LD-RT reported in previous experiments.

As presented in Figure 13 A, Nrf2 protein expression displayed a discontinuous dose-response dependency with a slight decreased expression following irradiation with a dose of 0.3 Gy, a relative decrease at a 0.5 Gy exposure of approximately 90% (non-stimulated cells) and 80% (TNF-α stimulated cells) of non-irradiated cells, and a minor increased expression after doses of 0.7 Gy or 1 Gy, respectively. In agreement with these data, Nrf2 DNA-binding activity was analysed in nuclear extracts by colorimetric ELISA utilizing a specific double-stranded DNA sequence containing the Nrf2 response element. Again, a discontinuous dose-response relationship was observed revealing a minimum value caused by an irradiation with a dose of 0.5 Gy (Figure 13 B).

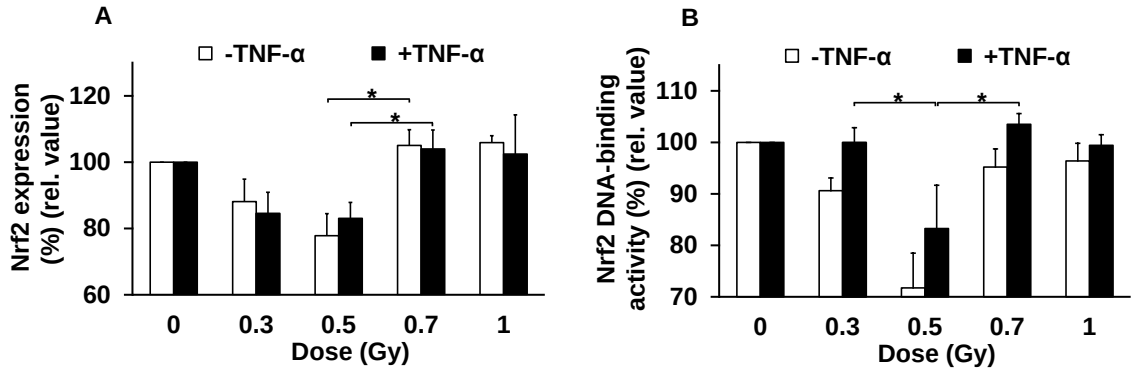

Figure 13. Nrf2 protein expression and DNA-binding activity in EA.hy926 cells following low-dose X-irradiation

(A) Relative changes in Nrf2 protein expression determined by flow cytometry at 24 h after irradiation. (B) Relative Nrf2 DNA-binding activity in nuclear extracts as analysed by a colorimetric assay, using a specific double-stranded DNA sequence containing the Nrf2 response element. Relative values were calculated as compared to mock-irradiated cells. Data represent means ± SEM from of at least three independent experiments. Asterisks indicate significant differences (* $p < 0.05$) vs. 0.3 Gy and 0.7 Gy irradiated ECs.

Interestingly, the reduction of Nrf2 expression following LD-RT exposure is more pronounced in TNF-α stimulated EAhy926 cells although the DNA-binding activity was extenuated more distinct in non TNF-α stimulated cells, proposing an effect of TNF-α on the level of Nrf2 DNA-binding activity.

In summary, a discontinuous expression and enzymatic activity of the enzymes SOD, CAT and GPx concomitant with a lowered expression and DNA-binding activity of their common redox-sensitive transcription factor Nrf2 most pronounced 24 h following an irradiation with a dose of 0.5 Gy were reported.

3.5 Functional analysis

3.5.1 Adhesion after scavenging of reactive oxygen species by N-acetyl-cysteine and low-dose radiation

Finally, to investigate whether low-dose X-irradiation modulated induction of ROS and Nrf2 activity is associated with altered functional properties of EA.hy926 ECs, leukocyte (PBMC) adhesion was analysed in the presence of the ROS scavenger NAC or the Nrf2 activator AI-1. The adhesion process is a major initial step in the inflammatory cascade, guided by modulatory cytokines/chemokines and surface molecules like integrins and selectins [142] and is reported to comprise a key modulatory element in the anti-inflammatory efficacy of LD-RT.

Figure 14 A exemplarily indicates PBMCs adhered to ECs and visualised by a Cy3-Streptavidin complex that binds to a biotin protein coupled to the membranes of the PBMCs.
As illustrated in Figure 14 B and in accordance with previous published data [39, 143], PBMC/EA.hy926 EC adhesion was significantly suppressed by more than 50%, 24 h after irradiation with a single dose of 0.5 Gy. On the contrary, ROS scavenging by NAC resulted in a pronounced increase of adhesion events and thus implicates a partial, but significant diminution of the anti-adhesive effect of low-dose X-ray exposure.

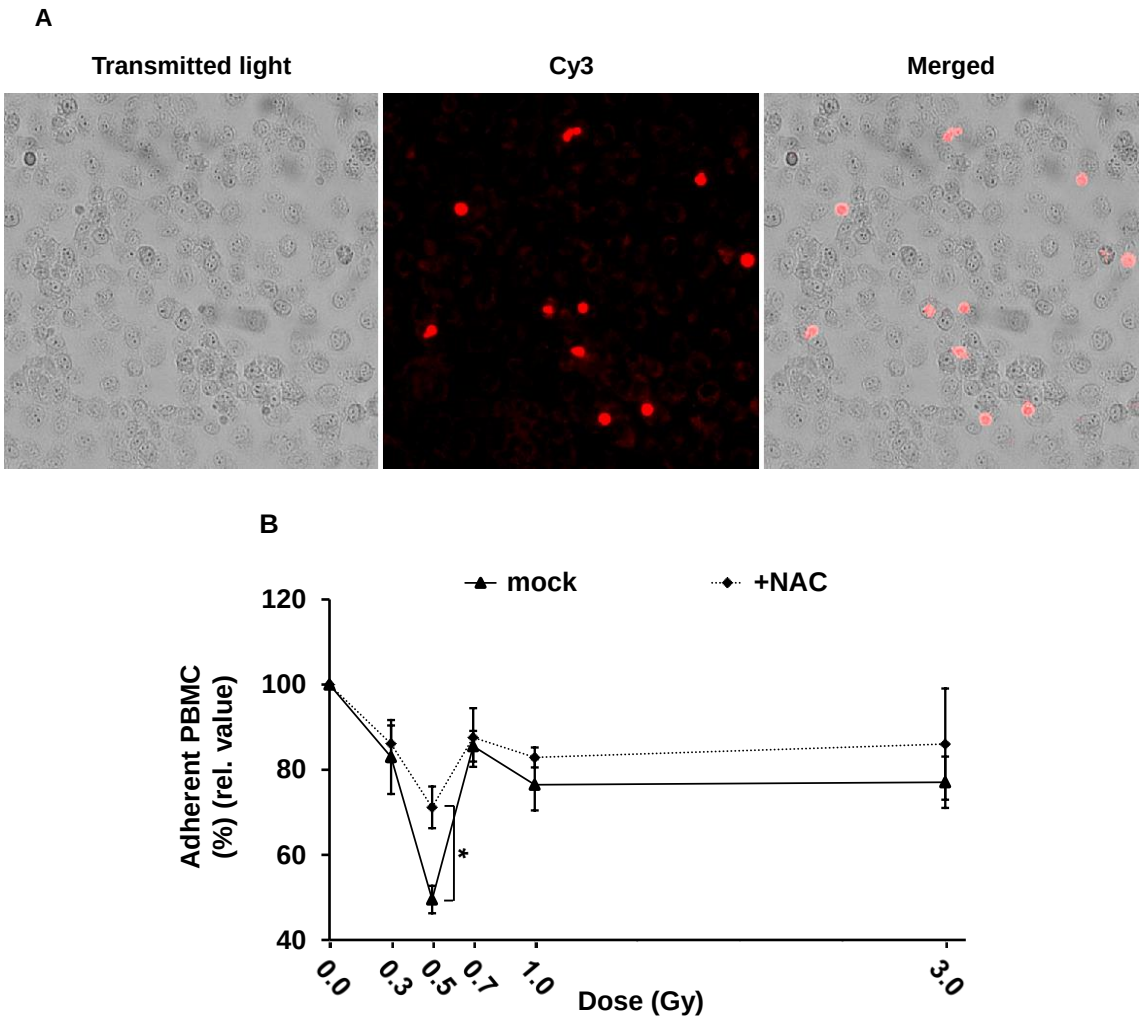

Figure 14. Adhesion of PBMC to TNF-α stimulated EA.hy926 ECs following low-dose X-irradiation in the presence or absence of NAC

(A) Representative pictures of ECs (transmitted light) and adhered PBMC (Cy3; in red) to ECs. (B) The percentage of adherent PBMCs to endothelial cells after irradiation with the doses indicated in the presence (dashed line) or absence (full line) of NAC (10 mM) relative to the values of non-irradiated stimulated controls (TNF-α (20 ng/ml) given 4 h before adding of PBMCs). PBMCs were incubated for 30 min at 4°C with gentle shaking, adherent cells were fixed, visualised and adhesion events were quantitated by fluorescence microscopy. Data represent means ± SEM from at least three independent experiments. Asterisks indicate significant differences (* $p < 0.05$) as compared to non-treated cells.

3.5.2 Adhesion after indirect activation of Nrf2 and low-dose radiation

According to preceding experiments, Nrf2 reveals a non-linear protein expression and DNA-binding activity that coincides with a discontinuous induction of ROS that in turn functionally mediates the adhesion process. Accordingly, in this work, it was analysed whether activation of the Nrf2 by a small molecule activator also results in a modification of the adhesion process.

As a permanent degradation of Nrf2 is mediated by binding to Keap1, a small molecule inhibitor (AI-1) of this interaction was applied to stabilise the Nrf2 protein. AI-1 covalently modifies cysteine 151 residue (Cys151)-dependent binding of Keap1 to Nrf2, serving as an anchor for adaptor for Cul3-ubiquitin E3 ligase complex [144]. Consequently, binding of Keap1 to Nrf2 is disrupted, enabling Nrf2 nuclear translocation and an increased transcription of target genes.

Control experiments ensuring the activity of the compound AI-1 in EA.hy926 EC revealed a significantly decreased ROS production, both in 0.5 Gy-irradiated cells and mock-treated cells, respectively (representative results for 0.5 Gy are depicted in Figure 15 A). Moreover, a stabilization of the Nrf2 protein by AI-1 was clearly visible in western immunoblotting by increased protein expression upon Al-1 treatment (Figure 15 B). Incubation with the Nrf2 activator AI-1 resulted in a significantly less pronounced reduction of PBMC/EC adhesion especially following irradiation with doses of 0.5 and 0.7 Gy (Figure 15 C), similar to the effects observed by ROS scavenging with NAC as reported before. This effect was less distinct at lower (0.3 Gy) and higher (1 Gy and 3 Gy) doses of irradiation.

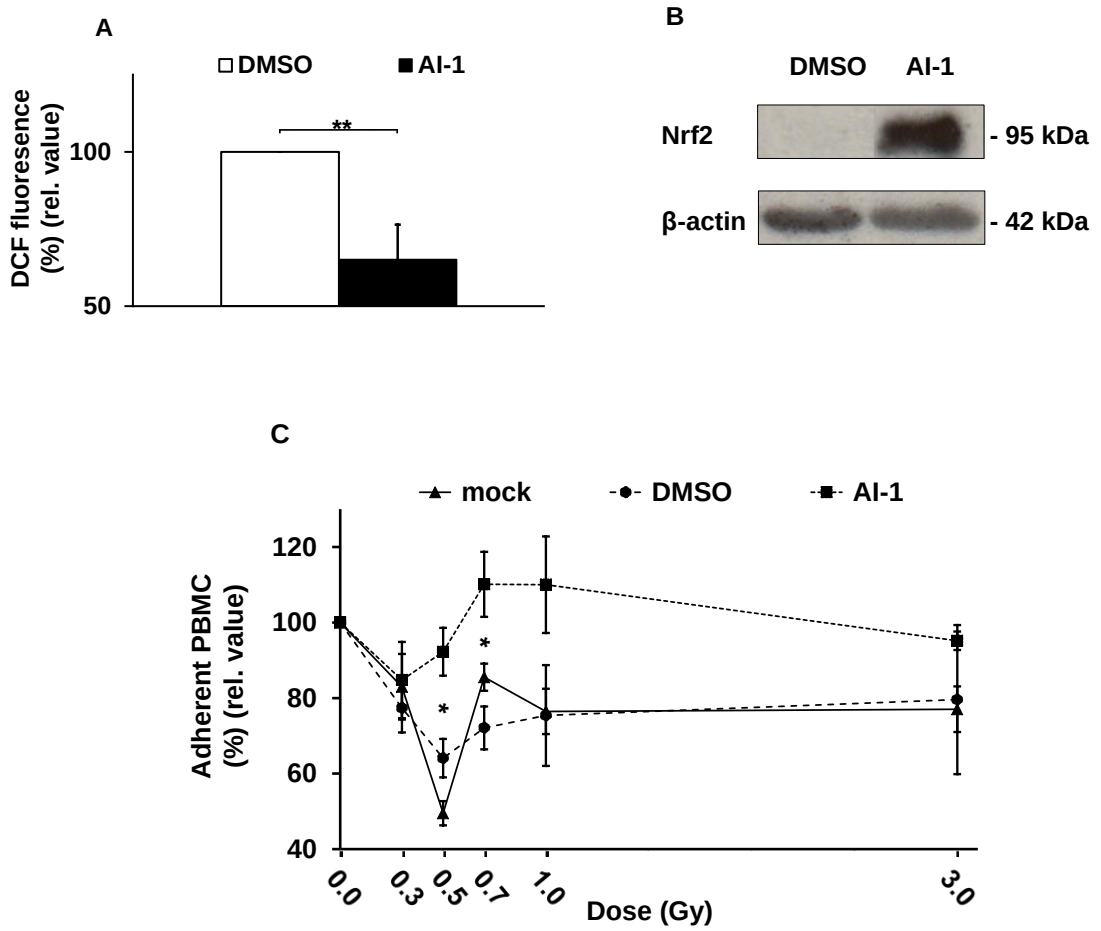

Figure 15. Adhesion of PBMC to TNF-α stimulated EA.hy926 ECs following low-dose X-irradiation in the presence of AI-1 or DMSO

(A) Quantification of relative DCF-fluorescence in EA.hy926 ECs at 24 h after irradiation with a dose of 0.5 Gy in the presence of AI-1 or solvent DMSO. (B) Western immunoblots from total cellular proteins at 24 h after irradiation using antibodies against Nrf2 and β-actin for loading control. Data are displayed as one representative from three independent experiments. (C) The percentage of PBMCs adherent to ECs after irradiation with the doses indicated in the presence of DMSO (dashed line) or AI-1 (100 µM) (fine dashed line). Relative values were calculated in comparison to mock-irradiated, stimulated cells. Cells without treatment (full line) are shown as a reference. PBMCs were incubated for 30 min at 4°C with gentle shaking, adherent cells were fixed, visualised and adhesion events were quantitated by fluorescence microscopy. Data represent means ± SEM from at least three independent experiments. Asterisks indicate significant differences (* $p < 0.05$) as compared to DMSO-treated cells.

In conclusion, both, treatment with NAC or an indirect impairment of ROS by activating the antioxidative system with AI-1 resulted in a diminution of the distinct reduction of PBMC/EC adhesion by LD-RT, typically observed following irradiation with a dose of

0.5 Gy. These experiments thus clearly indicate that the reduction of PBMC adhesion to stimulated EAhy926 ECs is at least in part mediated by Nrf2 activation and ROS levels.

4 Discussion

Based on growing evidences for non-(DNA) targeted effects, the classical paradigm in radiation biology, that deposition of energy to the nucleus and resulting DNA damage solely is responsible for the biological consequences of radiation exposure has been challenged. Among these novel evidences, bystander or out of field (abscopal) mechanisms and adaptive responses have received significant attention in the last decades [145, 146]. These novel concepts further take into consideration an intercellular communication [147] and a close interrelationship of irradiated cells with the surrounding tissue and components of the immune system. Furthermore, a hallmark of these effects is a common appearance at low doses and a non-linear dose-response relationship [56] shared with the anti-inflammatory effects of low-dose X-irradiation therapy (LD-RT) investigated in the present work. Exploring underlying cellular mechanisms, a variety of recent investigations further indicated the involvement of a multitude of cellular immune compounds and pathways in these characteristics, including a modulation of PBMC adhesion to ECs and a modulation of cytokine and transcription factor expression in ECs, leukocytes and macrophages (reviewed in [142, 148]).

Although considerable progress has been achieved in the understanding of immune modulatory effects of ionising radiation, the underlying molecular mechanisms are presently not fully resolved and a deeper insight in the interplay and modulation of the various cellular processes by irradiation has yet to be achieved. In line with that, high-dose exposure with single doses exceeding 2 Gy displays a pronounced pro-inflammatory effect [3], whereas irradiation with single doses below 1 Gy experimentally and clinically reveals anti-inflammatory properties [6, 142, 149]. The fact that different doses affect the immune system in diametrically opposed ways may implicate the involvement of complex mechanisms of DNA damage response and immune modulation differentially operating at different dose levels. However, the impact of DNA damage response, ROS production and the antioxidative defence system to give rise or contribute to these effects in EC remains unsolved.

In that context, ECs may comprise ideal targets for modulatory properties of low-dose radiation exposure due to their crucial role in the regulation of the local inflammatory process. This is due to their ability to recruit leukocytes to the site of local inflammation and by expressing a variety of cytokines/chemokines essential for the inflammatory cascades [150]. In the present study the focus was set on the endothelial cell line EA.hy926 which has been established by fusion of primary human umbilical vein

endothelial cells (HUVEC) and the adenocarcinoma epithelial cell line A549 [125]. As it cannot be excluded that the cancerous fusion partner A549 may influence some properties of EA.hy926 cells, exemplary experiments on SOD expression and activity HUVECs were performed indicating a similar dose-response relationship [151]. Comparability between these cells is further supported by studies indicating similarities between EA.hy926 ECs and HUVECs in terms of adhesion properties and surface marker expression if stimulated with the cytokine TNF-α [152]. Additionally, experiments performed in primary human microvascular ECs (HMVEC) for GPx expression and activity indicating a similar dose response relationship as depicted in Figure 11 [153]. Thus, EA.hy926 cells may comprise a valuable system to investigate the role of DNA damage response, ROS induction and cellular antioxidative defence mechanisms following low-dose irradiation.

A putative interrelationship between DNA damage repair and a discontinuous dose-response relationship following low-dose irradiation was recently suggested [154]. By assessing the number of serine 139 phosphorylated histone H2AX (γH2AX) foci, a marker of radiation-induced DSBs [73], a biphasic behaviour of γH2AX foci levels with a low-dose hypersensitivity in whole blood and less pronounced for isolated T-lymphocytes after X-irradiation was reported in line with a delayed repair with 40% of initial γH2AX foci, persisting 24 hours post-irradiation [154]. A mechanistic involvement of DNA damage repair mechanisms in the modulation of these non-linear dose-response effects remains to be established. However, one may assume that the discontinuous levels of residual γH2AX foci in the present thesis are related to the phenomenon of low-dose hyper-radiosensitivity (HRS) and induced radioresistance (IRR), which have been reported for cellular survival at doses below 0.3 Gy and in the dose range of 0.3 Gy to 0.6 Gy, respectively [155]. The current understanding of these processes is that the region of HRS (< 0.3 Gy) represents an area of increased apoptotic cell death in cells that failed to undergo an ATM-dependent G2 phase cell cycle arrest and thus proceed through mitosis with damaged DNA. On the contrary, a transition to IRR originates from a change in the balance of G2 checkpoint induction, allowing time for repair of DNA damage and increase cell survival. Moreover, Xue et al. demonstrated by inhibition or activation of ATM, that HRS/IRR is ATM-dependent, as there were no HRS/IRR observable in either ATM stimulator or inhibitor treated cells [156]. In this regard, accumulating evidences exist on a reduced NHEJ repair response associated with HRS and persistent RAD51 foci, an essential component of the ATM-dependent HR pathway at late time points after low-dose exposure [157]. This may indicate that a deregulation of both repair pathways may

contribute to the non-linear numbers of DSBs, although in the present investigation, ambiguous data were obtained after inhibition of ATM by KU60019. Moreover, future investigations should further address a putative involvement of accumulation of DSBs at stalled replication forks [158] to contribute to the levels of residual γH2AX following a low-dose exposure especially in S phase cells.

Although as yet not proven in an experimental setup the “Local Effect Model” (LEM) suggested by Friedrich et al. [159] might serve as a theoretical hypothesis to unravel the question of the appearance of discontinuous dose-response relationships. This model is based on the assumption that DNA is organised in giant loops [160, 161], consisting of about two Mbp length [162, 163]. It further proposes that DSBs can occur in an isolated manner (1 DSB per giant loop) or in a clustered form (≥ 2 DSBs per giant loop) (Figure 16 A). Although not experimentally accessible at present, one may speculate that the ratio of isolated to clustered DSBs is changing in a dose of range of 0 – 1 Gy with 0.5 Gy as a threshold dose, potentially leading to a shift in cellular reactions in response to an increased relative amount of clustered DSBs (Figure 16 B). Although this hypothesis still remains highly speculative, it might give a valuable explanation for the non-linear dose effects reported in this work as well as in numerous publications on the immune modulatory efficacy of low-dose irradiation (reviewed in [36]).

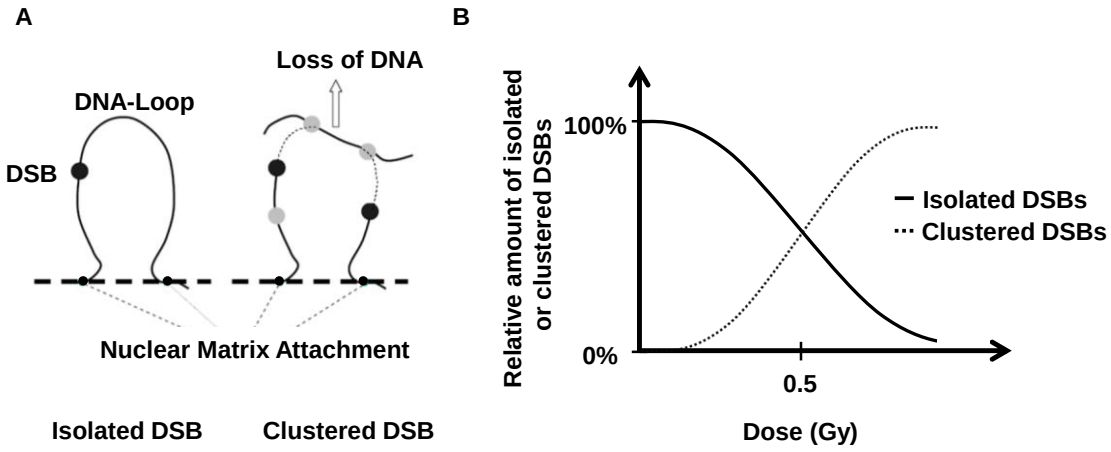

Figure 16. Scheme of isolated or clustered DSB (Local Effect Model) and proposed model for the origination of a non-linear dose-response

(A) An induction of one DSB in a single DNA loop leads to an isolated DSB, whereas two or more DSBs in a single DNA loop result in clustered DSBs with potential loss of large DNA pieces. (B) Proposed relative amounts of isolated DSBs (full line) in comparison to clustered DSBs (dashed line) suggesting a cross-over of both populations at a threshold dose of 0.5 Gy. (Figure 16 (A) was modified according to [159].)

Following environmental stress, levels of ROS increase dramatically resulting in a significant damage to cellular structures and induction of DSBs [98, 133]. Since ionising radiation exerts its cytotoxic activity in particular by the generation of ROS, antioxidant systems to maintain and control cellular redox balances are relevant for cellular survival and radiation response. Besides, ROS are essential for various biological functions, including cell survival, cell growth, proliferation, differentiation, and immune responses e.g. in activated macrophages by mounting an oxidative burst against invading pathogens. Additionally, ROS have a physiological role in cellular signalling that extends to every cell type of the immune system [53, 88, 164].

Although recent data imply an involvement of a variety of molecular mechanisms in the anti-inflammatory characteristics of EC following low-dose irradiation [36], the impact of ROS production to give rise or contribute to these effects in EC remains elusive. Here for the first time a discontinuous induction of ROS in Ea.hy926 ECs following a low-dose X-ray exposure with a most pronounced effect at a dose of 0.5 Gy (Figure 8) is reported. Notably, a discontinuous regulation of ROS production following X-irradiation in a comparable dose range between 0.3 and 0.6 Gy is also reported in stimulated murine RAW 264.7 macrophages mounting an oxidative burst [53]. However, as compared to elevated levels at a dose of 0.5 Gy in the present investigation, a significant reduction of

ROS production was observed in these cells. This may indicate that the variety of regulatory effects observed after low-dose X-ray exposure may reflect different functional consequences that are specific for a given cell type (ECs vs. macrophages) or cellular (micro-) environment. Interestingly, Kang et al. recently demonstrated that ROS induction after treatment of osteosarcoma and mammary epithelial cells with the radiation mimetic neocarzinostatin is, at least in part, mediated by histone H2AX overexpression or DNA damage-triggered γH2AX accumulation. Moreover, γH2AX foci induction by ROS was abrogated by treatment with the ROS scavenger NAC, knockdown of the NADP(H) oxidase Nox1 and by a dominant negative Ras-related C3 botulinum toxin substrate 1 (Rac1) mutant (Rac1N17) indicating an involvement of the Nox1 and Rac1 GTPase pathway [165]. These findings thus point to a more complex and reciprocal regulation of γH2AX and ROS production that may further contribute to a discontinuous appearance of γH2AX foci in EA.hy926 ECs after low-dose X-irradiation in the dose range < 1 Gy.

Cellular ROS production is tightly regulated by coordinated activities of pro-oxidant and anti-oxidant defence systems. To further elucidate mechanisms that may contribute to non-linear levels of γH2AX foci and ROS, the activity of the enzyme SOD that dismutates O2•- into H_2O_2 with the latter to be degraded into H_2O and O_2 by CAT and GPx activity was analysed [112]. In the present study, a diminished activity of these enzymes in EA.hy926 ECs most pronounced at 24 h after irradiation with a dose of 0.5 Gy was observed (Figure 10, Figure 11).
Data on the expression of SOD following low-dose irradiation, however, are controversial in literature at present. Similar to the findings presented in this work, they include a reduction in SOD activity in spleens of healthy BALB/C mice following total body irradiation with a dose of 0.4 Gy [166]. By contrast, they further comprise reports on increased mRNA expression following irradiation with a dose of 0.2 Gy or 0.5 Gy in splenic tissue of BALB/c or C57BL/6NJcl mice suffering from hepatopathy or cold brain injury [167, 168]. These results pinpoint to a cell type- and environment-related regulation of anti-oxidative defence mechanisms that should be addressed in continuative investigations on the role of SOD in low-dose irradiation responses in different cellular systems.

Based on the findings on SOD expression the analyses were expanded to CAT and GPx, additional factors in the antioxidative defence system to toxic H_2O_2 by reducing it to H_2O in a glutathione-dependent reaction (GPx). Again, a discontinuous dose-response relationship of CAT and GPx expression and activity with a local minimum following

irradiation with a dose of 0.5 Gy (Figure 11) was observed. As for SOD activity, data on the expression of CAT and GPx in literature are ambiguous. In accordance to the results in the present thesis, Peltola et al. for instance, reported on a downregulation (18%) of CAT activity at 24 h after irradiation with a dose of 0.5 Gy and 26 % after irradiation with 3 Gy in mouse liver tissue. This downregulation, however, was not detectable in the testis [169] indicating a tissue or cell type-specific regulation of CAT activity upon irradiation treatment. On the contrary, Beck and colleagues indicated an upregulation of factors implicated on oxidative stress response in EA.hy926 ECs following a 0.5, 2 and 5 Gy exposure [170]. Importantly, the latter data were derived from cells irradiated with high LET nickel ions indicating that the quality of radiation may substantially impact the expression of anti-oxidative factors in ECs.

The major cellular system to defend against the deleterious consequences of ROS induction and to restore a cellular redox homeostasis involves a multitude of genes regulated on the level of transcription by the presence of an ARE element in their promoter regions [171]. This motive is activated primarily by binding of the transcription factor Nrf2 that commonly regulates the transcription of a variety of antioxidant factors and ROS detoxifying enzymes [171]. In the present investigation, for the first, a time a non-linear expression and DNA-binding activity of Nrf2 (Figure 13) that was related to a diminished expression of SOD1, CAT and GPx1 (Figure 10, Figure 11) was observed. In accordance to these findings, a plausible involvement of Nrf2 in response to low-dose radiation exposure has already been demonstrated in a variety of cellular systems. For instance, an elevated expression and nuclear translocation of Nrf2 at 24 h following γ-irradiation with doses higher than 0.1 Gy has been observed in RAW264.7 macrophages [172]. More recent data further confirmed the induction of Nrf2 and enhanced expression of SOD and heme oxygenase (HO)-1 in human skin fibroblast HS27 cells following X-irradiation with a dose of 0.5 Gy [173]. By contrast, Nrf2 activation was not detectable at 24 h after irradiation with doses of 1-2 Gy in human monocytic THP1 cells [174] or was delayed for 5 days following a 2-8 Gy exposure in human breast cancer cells [175]. This further suggests a differential and cell type-specific induction and regulation of antioxidative mechanisms after irradiation with an early onset in cells of the immune system, e.g. ECs and macrophages as compared to malignant cells.

Notably, the reduction of Nrf2 DNA-binding activity at 0.5 Gy (Figure 13 B) is more pronounced as compared to the reduction in total Nrf2 protein expression (Figure 13 A), indicating additional levels of regulation. Indeed, Nrf2, in association with small V-maf

avian musculoaponeurotic fibrosarcoma oncogene homolog (Maf) transcription factor or members of the Jun protein family, forms an heterodimeric transcriptional complex to bind and regulate ARE-driven target genes [176, 177]. Thus, it is tempting to speculate that a modulation of those cofactors may further contribute to the decreased Nrf2 DNA-binding activity.

When assaying functional consequences of ROS induction and Nrf2 expression in EA.hy926 ECs, here it is reported that both approaches (pre-treatment with the ROS scavenger NAC or the Nrf2 activator AI-1), are leading to an abolishment of the diminution of PBMC adhesion to ECs following a 0.5 Gy exposure [38, 39]. The adhesion assay used in this investigation is an established model for the modulation of the inflammatory response and it is also discussed as a marker for radiation exposure [178]. Hallmann et al. [179, 180] and Morigi et al. [181] demonstrated, that two different assay conditions of adhesion of PBMC onto activated ECs are influenced by different cell adhesion molecules. Whereas cell adhesion in the dynamic assay/shear stress at 4°C is predominantly mediated by selectin, integrins account for most of the cell adhesion in a static assay (37°C, with no agitation). The dynamic experimental conditions used in this work (shear stress, 4°C) were adapted to measure selectin-mediated adhesion as preceding investigations revealed a reduced expression of the surface marker E-selectin on activated EA.hy926 to contribute to the modulation of the adhesion process following LD-RT [39].

The attenuation of the hampered PBMC adhesion by treatment with the ROS scavenger NAC or by an indirect activation via stabilization of Nrf2 (Figure 14 B, Figure 15 C) further pinpoints to the importance of ROS as a modulator of inflammatory pathways following low-dose irradiation. In line with that, H_2O_2 has been reported to stimulate neutrophil and eosinophil granulocyte adhesion in an autocrine or paracrine manner by upregulation of β2 integrin [182]. Moreover, the authors speculate on ROS to comprise an effector for changes in morphological or functional properties of ECs, including permeability and the expression of adhesion molecules. Indeed, growing evidence has emerged that ROS are involved in cellular adhesion to surfaces [183] as well as in monocyte binding to ECs [184]. In line with that, the inhibitory properties of anti-inflammatory drugs like Tanshinone IIA or simvastatin on TNF-α induced monocyte EC adhesion has been linked to suppression of isoprenoid-dependent generation of ROS [185], transcription factor Nuclear factor κB (NF-κB)-dependent adhesion molecule intercellular adhesion molecule-1 (ICAM-1) and vascular cell adhesion molecule-1 (VCAM-1) expression [186, 187]. More recent data further indicate an involvement of the phosphatidylinositol 3-kinase

(PI3K)/AKT/Nrf2 signalling pathway in suppressing ROS/NF-κB-mediated ICAM-1 and E-selectin expression in EA.hy926 ECs [188]. Although experimentally not addressed in the present investigation, it is tempting to assume that a modulation of NF-κB activity and adhesion molecule expression contributes to the regulation of the adhesion process following ROS scavenging by NAC or activation of Nrf2 by AI-1 in EA.hy926 ECs. This hypothesis in addition is supported by previous data on a non-linear induction of NF-κB DNA-binding and transcriptional activity and an altered surface expression of E-selectin to contribute to a reduced mononuclear cell adhesion in EA.hy926 ECs following 0.5 Gy irradiation [39, 42, 58]. Applying of DNA-binding and transcriptional activity assays after LD-RT was recently reported to result in a biphasic transcriptional activity of NF-κB in stimulated EA.hy926 ECs at 24 h after irradiation with locally elevated values following an exposure of 0.5 Gy [58]. Moreover, NF-κB activation has been shown to be regulated by ROS via both the classical (canonical) and the alternative pathways including atypical inhibitor κBα (IκBα) phosphorylation independently of IκB kinase (IKK) [189]. Although experimentally not proven at present, it is tempting to speculate that elevated levels of ROS at a dose of 0.5 Gy may contribute to an increased NF-κB activity and as a consequence, to an increased secretion of the cytokine TGF-β_1 [38, 42]. By using neutralising antibodies to TGF-β_1, it was shown that TGF-β_1 comprises a key component mediating the anti-adhesive efficacy of LD-RT [38, 42]. This assumption is further supported by a recent report indicating that ROS may comprise a regulator of adhesion molecules very late antigen-4 (VLA-4) and VCAM-1 mediated monocyte/macrophage adhesion to EC following irradiation with a dose of 0.5 Gy [190].

Finally, there is growing evidence on a tight crosstalk between the Nrf2 and NF-κB pathway with both antagonistic and synergistic effects [191]. Whereas activation of Nrf2 antioxidative signalling attenuates NF-κB mediated inflammatory responses in a colorectal cancer model [192], NF-κB signalling inhibits the Nrf2 pathway by a direct interaction of subunit p65 and Keap1 or a histone deacetylase 3 or CREB binding protein mediated transcriptional repression [193]. Thus, a more complex interrelationship of both NF-κB and Nrf2 and regulation of corresponding targeted genes may contribute to a fine tuning of the adhesion process and the inflammation process in general, in EA.hy926 ECs following LD-RT.

From a clinical point of view, the present experimental data highly support the preclinical observation that irradiation with single doses between 0.3 Gy and 1 Gy seem to be most effective for inducing anti-inflammatory responses. In line with that, a variety of recent

clinical investigations have indicated an isoeffective clinical response in patients with benign calcaneodynia, benign painful shoulder or painful elbow syndromes, when treated with a single fraction of 0.5 or 1 Gy while keeping the fractionation scheme [12, 64, 194]. These clinical results are the basis for dose reduction of LD-RT in the future clinical practice, which may contribute to a lowered carcinogenic radiation risk, while maintaining the beneficial effects associated with irradiation.

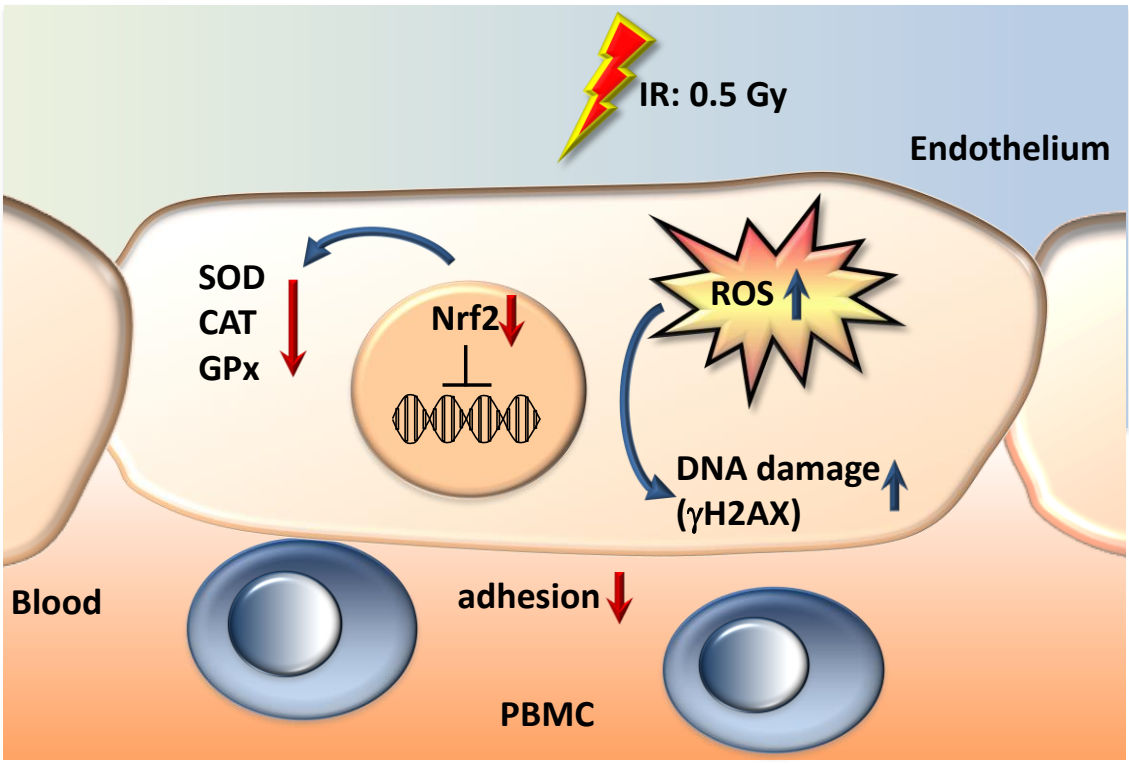

Figure 17. Advanced model on factors involved in the anti-inflammatory effect of low-dose irradiation therapy

Exposure of endothelial cells (ECs) to a dose of 0.5 Gy results in a modulation of antioxidative factors like superoxide dismutase (SOD), catalase (CAT), glutathione peroxidase (GPx) and transcription factor nuclear factor E2-related factor 2 (Nrf2) expression/activity resulting in increased reactive oxygen species (ROS) levels that functionally contributes to a hampered peripheral blood mononuclear cell (PBMC)/EC adhesion and increased levels of phospho-histone H2AX foci (γH2AX). These effects may contribute to the anti-inflammatory impact of low-dose radiation therapy (LD-RT). IR: ionising radiation.

In conclusion, data obtained during this dissertation revealed a discontinuous regulation of residual γH2AX foci levels most prominent following irradiation with a dose of 0.5 Gy and a modulation of physiologic properties of ECs like leukocyte adhesion. A modulation of these processes include transcriptional mechanisms like Nrf2 mediated regulation of ROS

detoxifying enzymes (pictured in Figure 17) and putatively seems to be interconnected with the DNA damage response. Nevertheless, the exact impact of DNA repair mechanisms are not fully resolved at present. It is to assume that the discontinuous dose-response curve and biphasic kinetics most likely originate from an overlay of various individual processes which are initiated at different thresholds, display different time kinetics, and operate in a staggered manner

Although considerable progress has been achieved during the last two decades in the understanding of the molecular mechanisms being prominent after a low-dose exposure, still a multitude of unresolved questions exists, fostering further investigations. As inflammatory diseases are characterised by complex (patho-) physiological networks, ongoing research should focus on additional immunological mechanisms and cellular components and a differential regulation of ROS and their associated factors in other cellular systems and in appropriate preclinical animal models. Additionally, the kind, type and dosage of the stimulation may be varied in order to get more insight in the complex regulation of the anti-inflammatory effects of LD-RT. Moreover, getting closer to the daily clinical situation, effects of a fractionated radiation scheme and other radiation qualities (e.g. heavy ions) require further investigations.

In the long run, these efforts will give extended insight in the radiobiology of low-dose radiation exposure and may help further to improve clinical radiation therapy of non-malignant diseases.

5 References

[1] Stenbek O. Om behandling of kronsik ledgangs-rheumatism med Röntgenstralar. Sv Läk Förh 1898;1:117.

[2] Sokolow N. Röntgenstrahlen gegen Gelenkrheumatismus. Wien Med 1898 Wochenschr. 570.

[3] Williams J, Chen Y, Rubin P, Finkelstein J, Okunieff P. The biological basis of a comprehensive grading system for the adverse effects of cancer treatment. Seminars in radiation oncology 2003;13:182-8.

[4] Betz N, Ott OJ, Adamietz B, Sauer R, Fietkau R, Keilholz L. Radiotherapy in early-stage Dupuytren's contracture. Long-term results after 13 years. Strahlentherapie und Onkologie : Organ der Deutschen Rontgengesellschaft [et al] 2010;186:82-90.

[5] Heyd R, Seegenschmiedt MH, Rades D, Winkler C, Eich HT, Bruns F, et al. Radiotherapy for symptomatic vertebral hemangiomas: results of a multicenter study and literature review. International journal of radiation oncology, biology, physics 2010;77:217-25.

[6] Seegenschmiedt MH, Micke O, Willich N. Radiation therapy for nonmalignant diseases in Germany. Current concepts and future perspectives. Strahlenther Onkol 2004;180:718-30.

[7] Trombetta M, Werts ED, Parda D. The role of radiotherapy in the treatment of hidradenitis suppurativa: case report and review of the literature. Dermatology online journal 2010;16:16.

[8] Seegenschmiedt MH, Keilholz L. Epicondylopathia humeri (EPH) and peritendinitis humeroscapularis (PHS): evaluation of radiation therapy long-term results and literature review. Radiotherapy and oncology : journal of the European Society for Therapeutic Radiology and Oncology 1998;47:17-28.

[9] Seegenschmiedt MH, Olschewski T, Guntrum F. [Optimization of radiotherapy in Dupuytren's disease. Initial results of a controlled trial]. Strahlentherapie und Onkologie : Organ der Deutschen Rontgengesellschaft [et al] 2001;177:74-81.

[10] von Pannewitz G. Die Röntgentherapie der Arthritis deformans. Ergebnisse der medizinischen Strahlenforschung 1933;6:62-126.

[11] Seegenschmiedt MH, Makoski, H. B., Trott, K. R., and Brady, L. W. E. . Radiotherapy for Non-Malignant Disorders. Berlin: Springer Verlag; 2008.

[12] Ott OJ, Jeremias C, Gaipl US, Frey B, Schmidt M, Fietkau R. Radiotherapy for benign calcaneodynia: long-term results of the Erlangen Dose Optimization (EDO) trial.

Strahlentherapie und Onkologie : Organ der Deutschen Rontgengesellschaft [et al] 2014;190:671-5.

[13] Ott OJ, Jeremias C, Gaipl US, Frey B, Schmidt M, Fietkau R. Radiotherapy for achillodynia : results of a single-center prospective randomized dose-optimization trial. Strahlentherapie und Onkologie : Organ der Deutschen Rontgengesellschaft [et al] 2013;189:142-6.

[14] Brown WM, Doll R. Mortality from cancer and other causes after radiotherapy for ankylosing spondylitis. British medical journal 1965;2:1327-32.

[15] Cannon B, Randolph JG, Murray JE. Malignant irradiation for benign conditions. The New England journal of medicine 1959;260:197-202.

[16] Rainsford KD. Anti-inflammatory drugs in the 21st century. Sub-cellular biochemistry 2007;42:3-27.

[17] Medzhitov R. Inflammation 2010: new adventures of an old flame. Cell 2010;140:771-6.

[18] Rather LJ. Disturbance of function (functio laesa): the legendary fifth cardinal sign of inflammation, added by Galen to the four cardinal signs of Celsus. Bulletin of the New York Academy of Medicine 1971;47:303-22.

[19] Murphy K. Janeway's Immunobiology. Abingdon: Taylor & Francis Ltd.; (2011).

[20] Osta B, Benedetti G, Miossec P. Classical and Paradoxical Effects of TNF-alpha on Bone Homeostasis. Frontiers in immunology 2014;5:48.

[21] Mosmann TR. Properties and functions of interleukin-10. Advances in immunology 1994;56:1-26.

[22] Deshmane SL, Kremlev S, Amini S, Sawaya BE. Monocyte chemoattractant protein-1 (MCP-1): an overview. Journal of interferon & cytokine research : the official journal of the International Society for Interferon and Cytokine Research 2009;29:313-26.

[23] Zhang H, Park Y, Wu J, Chen X, Lee S, Yang J, et al. Role of TNF-alpha in vascular dysfunction. Clinical science 2009;116:219-30.

[24] Kim H, Hwang JS, Woo CH, Kim EY, Kim TH, Cho KJ, et al. TNF-alpha-induced up-regulation of intercellular adhesion molecule-1 is regulated by a Rac-ROS-dependent cascade in human airway epithelial cells. Experimental & molecular medicine 2008;40:167-75.

[25] Lee CW, Lin WN, Lin CC, Luo SF, Wang JS, Pouyssegur J, et al. Transcriptional regulation of VCAM-1 expression by tumor necrosis factor-alpha in human tracheal smooth muscle cells: involvement of MAPKs, NF-kappaB, p300, and histone acetylation. Journal of cellular physiology 2006;207:174-86.

[26] Danese S, Semeraro S, Marini M, Roberto I, Armuzzi A, Papa A, et al. Adhesion molecules in inflammatory bowel disease: therapeutic implications for gut inflammation. Digestive and liver disease : official journal of the Italian Society of Gastroenterology and the Italian Association for the Study of the Liver 2005;37:811-8.

[27] Ley K, Zarbock A. Hold on to your endothelium: postarrest steps of the leukocyte adhesion cascade. Immunity 2006;25:185-7.

[28] Lawrence MB, Springer TA. Leukocytes roll on a selectin at physiologic flow rates: distinction from and prerequisite for adhesion through integrins. Cell 1991;65:859-73.

[29] Hemler ME. VLA proteins in the integrin family: structures, functions, and their role on leukocytes. Annual review of immunology 1990;8:365-400.

[30] Springer TA. Traffic signals for lymphocyte recirculation and leukocyte emigration: the multistep paradigm. Cell 1994;76:301-14.

[31] Taniguchi K, Karin M. IL-6 and related cytokines as the critical lynchpins between inflammation and cancer. Seminars in immunology 2014;26:54-74.

[32] Coffelt SB, de Visser KE. Cancer: Inflammation lights the way to metastasis. Nature 2014;507:48-9.

[33] Diegelmann RF, Evans MC. Wound healing: an overview of acute, fibrotic and delayed healing. Frontiers in bioscience : a journal and virtual library 2004;9:283-9.

[34] Serhan CN, Savill J. Resolution of inflammation: the beginning programs the end. Nature immunology 2005;6:1191-7.

[35] Rodel F, Keilholz L, Herrmann M, Sauer R, Hildebrandt G. Radiobiological mechanisms in inflammatory diseases of low-dose radiation therapy. International journal of radiation biology 2007;83:357-66.

[36] Rodel F, Frey B, Manda K, Hildebrandt G, Hehlgans S, Keilholz L, et al. Immunomodulatory properties and molecular effects in inflammatory diseases of low-dose x-irradiation. Frontiers in oncology 2012;2:120.

[37] Kern PM, Keilholz L, Forster C, Hallmann R, Herrmann M, Seegenschmiedt MH. Low-dose radiotherapy selectively reduces adhesion of peripheral blood mononuclear cells to endothelium in vitro. Radiotherapy and oncology : journal of the European Society for Therapeutic Radiology and Oncology 2000;54:273-82.

[38] Roedel F, Kley N, Beuscher HU, Hildebrandt G, Keilholz L, Kern P, et al. Anti-inflammatory effect of low-dose X-irradiation and the involvement of a TGF-beta1-induced down-regulation of leukocyte/endothelial cell adhesion. International journal of radiation biology 2002;78:711-9.

[39] Hildebrandt G, Maggiorella L, Rodel F, Rodel V, Willis D, Trott KR. Mononuclear cell adhesion and cell adhesion molecule liberation after X-irradiation of activated endothelial cells in vitro. International journal of radiation biology 2002;78:315-25.

[40] Arenas M, Gil F, Gironella M, Hernandez V, Jorcano S, Biete A, et al. Anti-inflammatory effects of low-dose radiotherapy in an experimental model of systemic inflammation in mice. Int J Radiat Oncol Biol Phys 2006;66:560-7.

[41] Rodel F, Keilholz L, Herrmann M, Weiss C, Frey B, Voll R, et al. Activator protein 1 shows a biphasic induction and transcriptional activity after low dose X-irradiation in EA.hy.926 endothelial cells. Autoimmunity 2009;42:343-5.

[42] Rodel F, Frey B, Capalbo G, Gaipl U, Keilholz L, Voll R, et al. Discontinuous induction of X-linked inhibitor of apoptosis in EA.hy.926 endothelial cells is linked to NF-kappaB activation and mediates the anti-inflammatory properties of low-dose ionising-radiation. Radiother Oncol 2010;97:346-51.

[43] Hengartner MO. The biochemistry of apoptosis. Nature 2000;407:770-6.

[44] Kern P, Keilholz L, Forster C, Seegenschmiedt MH, Sauer R, Herrmann M. In vitro apoptosis in peripheral blood mononuclear cells induced by low-dose radiotherapy displays a discontinuous dose-dependence. International journal of radiation biology 1999;75:995-1003.

[45] Gaipl US, Meister S, Lodermann B, Rodel F, Fietkau R, Herrmann M, et al. Activation-induced cell death and total Akt content of granulocytes show a biphasic course after low-dose radiation. Autoimmunity 2009;42:340-2.

[46] Rodel F, Hofmann D, Auer J, Keilholz L, Rollinghoff M, Sauer R, et al. The anti-inflammatory effect of low-dose radiation therapy involves a diminished CCL20 chemokine expression and granulocyte/endothelial cell adhesion. Strahlenther Onkol 2008;184:41-7.

[47] Valledor AF, Comalada M, Santamaria-Babi LF, Lloberas J, Celada A. Macrophage proinflammatory activation and deactivation: a question of balance. Advances in immunology 2010;108:1-20.

[48] Adams DO. Molecular interactions in macrophage activation. Immunol Today 1989;10:33-5.

[49] Fujiwara N, Kobayashi K. Macrophages in inflammation. Curr Drug Targets Inflamm Allergy 2005;4:281-6.

[50] Nathan C. Nitric oxide as a secretory product of mammalian cells. Faseb J 1992;6:3051-64.

[51] Holthusen H. Involvement of the NO/cyclic GMP pathway in bradykinin-evoked pain from veins in humans. Pain 1997;69:87-92.

[52] Hildebrandt G, Seed MP, Freemantle CN, Alam CA, Colville-Nash PR, Trott KR. Mechanisms of the anti-inflammatory activity of low-dose radiation therapy. International journal of radiation biology 1998;74:367-78.

[53] Schaue D, Marples B, Trott KR. The effects of low-dose X-irradiation on the oxidative burst in stimulated macrophages. Int J Radiat Biol 2002;78:567-76.

[54] Lodermann B, Wunderlich R, Frey S, Schorn C, Stangl S, Rodel F, et al. Low dose ionising radiation leads to a NF-kappaB dependent decreased secretion of active IL-1beta by activated macrophages with a discontinuous dose-dependency. Int J Radiat Biol 2012;88:727-34.

[55] Wunderlich R, Ernst A, Rodel F, Fietkau R, Ott O, Lauber K, et al. Low and moderate dose of ionising radiation up to 2 Gy modulates transmigration and chemotaxis of activated macrophages, provokes an anti-inflammatory cytokine milieu, but does not impact on viability and phagocytic function. Clinical and experimental immunology 2014.

[56] Hildebrandt G. Non-cancer diseases and non-targeted effects. Mutat Res 2010;687:73-7.

[57] Mothersill C, Seymour C. Radiation-induced non-targeted effects of low doses-what, why and how? Health Phys 2011;100:302.

[58] Rodel F, Hantschel M, Hildebrandt G, Schultze-Mosgau S, Rodel C, Herrmann M, et al. Dose-dependent biphasic induction and transcriptional activity of nuclear factor kappa B (NF-kappaB) in EA.hy.926 endothelial cells after low-dose X-irradiation. Int J Radiat Biol 2004;80:115-23.

[59] von Pannewitz G. Die Röntgentherapie der Arthritis deformans. Ergebnisse der medizinischen Strahlenforschung 1933;6:62-126.

[60] Frey B, Gaipl US, Sarter K, Zaiss MM, Stillkrieg W, Rodel F, et al. Whole body low dose irradiation improves the course of beginning polyarthritis in human TNF-transgenic mice. Autoimmunity 2009;42:346-8.

[61] Keffer J, Probert L, Cazlaris H, Georgopoulos S, Kaslaris E, Kioussis D, et al. Transgenic mice expressing human tumour necrosis factor: a predictive genetic model of arthritis. The EMBO journal 1991;10:4025-31.

[62] Schaue D, Jahns J, Hildebrandt G, Trott KR. Radiation treatment of acute inflammation in mice. International journal of radiation biology 2005;81:657-67.

[63] Ott OJ, Hertel S, Gaipl US, Frey B, Schmidt M, Fietkau R. The Erlangen Dose Optimization Trial for radiotherapy of benign painful shoulder syndrome : Long-term results. Strahlentherapie und Onkologie : Organ der Deutschen Rontgengesellschaft [et al] 2014;190:394-8.

[64] Ott OJ, Hertel S, Gaipl US, Frey B, Schmidt M, Fietkau R. The Erlangen Dose Optimization trial for low-dose radiotherapy of benign painful elbow syndrome. Long-term results. Strahlenther Onkol 2014;190:293-7.

[65] Sallmyr A, Fan J, Rassool FV. Genomic instability in myeloid malignancies: increased reactive oxygen species (ROS), DNA double strand breaks (DSBs) and error-prone repair. Cancer letters 2008;270:1-9.

[66] Thompson LH. Recognition, signaling, and repair of DNA double-strand breaks produced by ionizing radiation in mammalian cells: the molecular choreography. Mutation research 2012;751:158-246.

[67] Yao Y, Dai W. Genomic Instability and Cancer. Journal of carcinogenesis & mutagenesis 2014;5.

[68] Hall EJG, A.J. L. Radiobiology for the Radiologist: Lippincott Williams & Wilkins.; 2006.

[69] Rothkamm K, Kruger I, Thompson LH, Lobrich M. Pathways of DNA double-strand break repair during the mammalian cell cycle. Molecular and cellular biology 2003;23:5706-15.

[70] Khanna KK, Jackson SP. DNA double-strand breaks: signaling, repair and the cancer connection. Nature genetics 2001;27:247-54.

[71] Richard DJ, Cubeddu L, Urquhart AJ, Bain A, Bolderson E, Menon D, et al. hSSB1 interacts directly with the MRN complex stimulating its recruitment to DNA double-strand breaks and its endo-nuclease activity. Nucleic acids research 2011;39:3643-51.

[72] You ZS, Bailis JM, Johnson SA, Dilworth SM, Hunter T. Rapid activation of ATM on DNA flanking double-strand breaks. Nature cell biology 2007;9:311-U193.

[73] Rogakou EP, Pilch DR, Orr AH, Ivanova VS, Bonner WM. DNA double-stranded breaks induce histone H2AX phosphorylation on serine 139. The Journal of biological chemistry 1998;273:5858-68.

[74] Lieber MR. The mechanism of double-strand DNA break repair by the nonhomologous DNA end-joining pathway. Annual review of biochemistry 2010;79:181-211.

[75] Meek K, Douglas P, Cui X, Ding Q, Lees-Miller SP. trans Autophosphorylation at DNA-dependent protein kinase's two major autophosphorylation site clusters facilitates end processing but not end joining. Mol Cell Biol 2007;27:3881-90.

[76] Beucher A, Birraux J, Tchouandong L, Barton O, Shibata A, Conrad S, et al. ATM and Artemis promote homologous recombination of radiation-induced DNA double-strand breaks in G2. The EMBO journal 2009;28:3413-27.

[77] Ahnesorg P, Smith P, Jackson SP. XLF interacts with the XRCC4-DNA ligase IV complex to promote DNA nonhomologous end-joining. Cell 2006;124:301-13.

[78] Gravel S, Chapman JR, Magill C, Jackson SP. DNA helicases Sgs1 and BLM promote DNA double-strand break resection. Genes & development 2008;22:2767-72.

[79] Garcia V, Phelps SE, Gray S, Neale MJ. Bidirectional resection of DNA double-strand breaks by Mre11 and Exo1. Nature 2011;479:241-4.

[80] San Filippo J, Sung P, Klein H. Mechanism of eukaryotic homologous recombination. Annual review of biochemistry 2008;77:229-57.

[81] Yuan SS, Lee SY, Chen G, Song M, Tomlinson GE, Lee EY. BRCA2 is required for ionizing radiation-induced assembly of Rad51 complex in vivo. Cancer research 1999;59:3547-51.

[82] Le Breton C, Dupaigne P, Robert T, Le Cam E, Gangloff S, Fabre F, et al. Srs2 removes deadly recombination intermediates independently of its interaction with SUMO-modified PCNA. Nucleic Acids Res 2008;36:4964-74.

[83] Nathan C, Ding A. SnapShot: Reactive Oxygen Intermediates (ROI). Cell 2010;140:951- e2.

[84] Halliwell B. Free radicals and antioxidants: updating a personal view. Nutrition reviews 2012;70:257-65.

[85] Cooke MS, Evans MD, Dizdaroglu M, Lunec J. Oxidative DNA damage: mechanisms, mutation, and disease. FASEB journal : official publication of the Federation of American Societies for Experimental Biology 2003;17:1195-214.

[86] West AP, Shadel GS, Ghosh S. Mitochondria in innate immune responses. Nature reviews Immunology 2011;11:389-402.

[87] Richards SA, Muter J, Ritchie P, Lattanzi G, Hutchison CJ. The accumulation of un-repairable DNA damage in laminopathy progeria fibroblasts is caused by ROS generation and is prevented by treatment with N-acetyl cysteine. Human molecular genetics 2011;20:3997-4004.

[88] Cachat J, Deffert C, Hugues S, Krause KH. Phagocyte NADPH oxidase and specific immunity. Clinical science 2015;128:635-48.

[89] Lambeth JD. NOX enzymes and the biology of reactive oxygen. Nature reviews Immunology 2004;4:181-9.

[90] Goncharov NV, Avdonin PV, Nadeev AD, Zharkikh IL, Jenkins RO. Reactive Oxygen Species in Pathogenesis of Atherosclerosis. Current pharmaceutical design 2014.

[91] Kim M, Han CH, Lee MY. NADPH oxidase and the cardiovascular toxicity associated with smoking. Toxicological research 2014;30:149-57.

[92] Hielscher A, Gerecht S. Hypoxia and free radicals: Role in tumor progression and the use of engineering-based platforms to address these relationships. Free radical biology & medicine 2014.

[93] Evans AR, Junger H, Southall MD, Nicol GD, Sorkin LS, Broome JT, et al. Isoprostanes, novel eicosanoids that produce nociception and sensitize rat sensory neurons. The Journal of pharmacology and experimental therapeutics 2000;293:912-20.

[94] Rehman A, Nourooz-Zadeh J, Moller W, Tritschler H, Pereira P, Halliwell B. Increased oxidative damage to all DNA bases in patients with type II diabetes mellitus. FEBS letters 1999;448:120-2.

[95] Bashir S, Harris G, Denman MA, Blake DR, Winyard PG. Oxidative DNA damage and cellular sensitivity to oxidative stress in human autoimmune diseases. Annals of the rheumatic diseases 1993;52:659-66.

[96] Matsui A, Ikeda T, Enomoto K, Hosoda K, Nakashima H, Omae K, et al. Increased formation of oxidative DNA damage, 8-hydroxy-2'-deoxyguanosine, in human breast cancer tissue and its relationship to GSTP1 and COMT genotypes. Cancer letters 2000;151:87-95.

[97] Oliva MR, Ripoll F, Muniz P, Iradi A, Trullenque R, Valls V, et al. Genetic alterations and oxidative metabolism in sporadic colorectal tumors from a Spanish community. Molecular carcinogenesis 1997;18:232-43.

[98] Roos WP, Kaina B. DNA damage-induced cell death: from specific DNA lesions to the DNA damage response and apoptosis. Cancer letters 2013;332:237-48.

[99] Jackson SP, Bartek J. The DNA-damage response in human biology and disease. Nature 2009;461:1071-8.

[100] Frankenberg-Schwager M, Frankenberg D. DNA double-strand breaks: their repair and relationship to cell killing in yeast. International journal of radiation biology 1990;58:569-75.

[101] Kakarougkas A, Jeggo PA. DNA DSB repair pathway choice: an orchestrated handover mechanism. The British journal of radiology 2014;87:20130685.

[102] Sauer H, Wartenberg M, Hescheler J. Reactive oxygen species as intracellular messengers during cell growth and differentiation. Cellular physiology and biochemistry : international journal of experimental cellular physiology, biochemistry, and pharmacology 2001;11:173-86.

[103] Bryan N, Ahswin H, Smart N, Bayon Y, Wohlert S, Hunt JA. Reactive oxygen species (ROS)--a family of fate deciding molecules pivotal in constructive inflammation and wound healing. European cells & materials 2012;24:249-65.

[104] Schonthaler HB, Guinea-Viniegra J, Wagner EF. Targeting inflammation by modulating the Jun/AP-1 pathway. Annals of the rheumatic diseases 2011;70 Suppl 1:i109-12.

[105] Nathan C, Cunningham-Bussel A. Beyond oxidative stress: an immunologist's guide to reactive oxygen species. Nature reviews Immunology 2013;13:349-61.

[106] Niture SK, Khatri R, Jaiswal AK. Regulation of Nrf2-an update. Free radical biology & medicine 2014;66:36-44.

[107] Kobayashi A, Kang MI, Okawa H, Ohtsuji M, Zenke Y, Chiba T, et al. Oxidative stress sensor Keap1 functions as an adaptor for Cul3-based E3 ligase to regulate proteasomal degradation of Nrf2. Molecular and cellular biology 2004;24:7130-9.

[108] Suzuki T, Motohashi H, Yamamoto M. Toward clinical application of the Keap1-Nrf2 pathway. Trends in pharmacological sciences 2013;34:340-6.

[109] Zhu H, Itoh K, Yamamoto M, Zweier JL, Li Y. Role of Nrf2 signaling in regulation of antioxidants and phase 2 enzymes in cardiac fibroblasts: protection against reactive oxygen and nitrogen species-induced cell injury. FEBS letters 2005;579:3029-36.

[110] Braun S, Hanselmann C, Gassmann MG, auf dem Keller U, Born-Berclaz C, Chan K, et al. Nrf2 transcription factor, a novel target of keratinocyte growth factor action which regulates gene expression and inflammation in the healing skin wound. Molecular and cellular biology 2002;22:5492-505.

[111] Aitken RJ, Roman SD. Antioxidant systems and oxidative stress in the testes. Advances in experimental medicine and biology 2008;636:154-71.

[112] Rhee SG, Yang KS, Kang SW, Woo HA, Chang TS. Controlled elimination of intracellular H(2)O(2): regulation of peroxiredoxin, catalase, and glutathione peroxidase via post-translational modification. Antioxidants & redox signaling 2005;7:619-26.

[113] Kim YJ, Jang MG, Noh HY, Lee HJ, Sukweenadhi J, Kim JH, et al. Molecular characterization of two glutathione peroxidase genes of Panax ginseng and their expression analysis against environmental stresses. Gene 2014;535:33-41.

[114] Ray A, Chatterjee S, Mukherjee S, Bhattacharya S. Arsenic trioxide induced indirect and direct inhibition of glutathione reductase leads to apoptosis in rat hepatocytes. Biometals : an international journal on the role of metal ions in biology, biochemistry, and medicine 2014;27:483-94.

[115] Boutten A, Goven D, Artaud-Macari E, Boczkowski J, Bonay M. NRF2 targeting: a promising therapeutic strategy in chronic obstructive pulmonary disease. Trends in molecular medicine 2011;17:363-71.

[116] Yu JH, Kim H. Oxidative stress and cytokines in the pathogenesis of pancreatic cancer. Journal of cancer prevention 2014;19:97-102.

[117] Finkel T, Holbrook NJ. Oxidants, oxidative stress and the biology of ageing. Nature 2000;408:239-47.

[118] Scandalios JG. Oxidative stress responses--what have genome-scale studies taught us? Genome biology 2002;3:REVIEWS1019.

[119] Basu S. Bioactive eicosanoids: role of prostaglandin F(2alpha) and F(2)-isoprostanes in inflammation and oxidative stress related pathology. Molecules and cells 2010;30:383-91.

[120] Giustarini D, Dalle-Donne I, Tsikas D, Rossi R. Oxidative stress and human diseases: Origin, link, measurement, mechanisms, and biomarkers. Critical reviews in clinical laboratory sciences 2009;46:241-81.

[121] Davies SS, Roberts LJ, 2nd. F2-isoprostanes as an indicator and risk factor for coronary heart disease. Free radical biology & medicine 2011;50:559-66.

[122] Seet RC, Lee CY, Chan BP, Sharma VK, Teoh HL, Venketasubramanian N, et al. Oxidative damage in ischemic stroke revealed using multiple biomarkers. Stroke; a journal of cerebral circulation 2011;42:2326-9.

[123] Gagliardi S, Cova E, Davin A, Guareschi S, Abel K, Alvisi E, et al. SOD1 mRNA expression in sporadic amyotrophic lateral sclerosis. Neurobiology of disease 2010;39:198-203.

[124] Psyrri A, Kalogeras KT, Kronenwett R, Wirtz RM, Batistatou A, Bournakis E, et al. Prognostic significance of UBE2C mRNA expression in high-risk early breast cancer. A Hellenic Cooperative Oncology Group (HeCOG) Study. Annals of oncology : official journal of the European Society for Medical Oncology / ESMO 2012;23:1422-7.

[125] Edgell CJ, McDonald CC, Graham JB. Permanent cell line expressing human factor VIII-related antigen established by hybridization. Proceedings of the National Academy of Sciences of the United States of America 1983;80:3734-7.

[126] Rödel F, Frey B, Capalbo G, Gaipl U, Keilholz L, Voll R, et al. Discontinuous induction of X-linked inhibitor of apoptosis in EA.hy.926 endothelial cells is linked to NF-kappaB activation and mediates the anti-inflammatory properties of low-dose ionising-radiation. Radiotherapy and oncology : journal of the European Society for Therapeutic Radiology and Oncology 2010;97:346-51.

[127] Lobrich M, Shibata A, Beucher A, Fisher A, Ensminger M, Goodarzi AA, et al. gammaH2AX foci analysis for monitoring DNA double-strand break repair: strengths, limitations and optimization. Cell cycle 2010;9:662-9.

[128] Wang H, Shi LZ, Wong CC, Han X, Hwang PY, Truong LN, et al. The interaction of CtIP and Nbs1 connects CDK and ATM to regulate HR-mediated double-strand break repair. PLoS genetics 2013;9:e1003277.

[129] Kanungo J. DNA-dependent protein kinase and DNA repair: relevance to Alzheimer's disease. Alzheimer's research & therapy 2013;5:13.

[130] Sartori AA, Lukas C, Coates J, Mistrik M, Fu S, Bartek J, et al. Human CtIP promotes DNA end resection. Nature 2007;450:509-14.

[131] Golding SE, Rosenberg E, Valerie N, Hussaini I, Frigerio M, Cockcroft XF, et al. Improved ATM kinase inhibitor KU-60019 radiosensitizes glioma cells, compromises insulin, AKT and ERK prosurvival signaling, and inhibits migration and invasion. Molecular cancer therapeutics 2009;8:2894-902.

[132] Cui X, Yu Y, Gupta S, Cho YM, Lees-Miller SP, Meek K. Autophosphorylation of DNA-dependent protein kinase regulates DNA end processing and may also alter double-strand break repair pathway choice. Mol Cell Biol 2005;25:10842-52.

[133] Friedberg EC. DNA damage and repair. Nature 2003;421:436-40.

[134] Zafarullah M, Li WQ, Sylvester J, Ahmad M. Molecular mechanisms of N-acetylcysteine actions. Cellular and molecular life sciences : CMLS 2003;60:6-20.

[135] Sun SY. N-acetylcysteine, reactive oxygen species and beyond. Cancer biology & therapy 2010;9:109-10.

[136] Fukai T, Ushio-Fukai M. Superoxide dismutases: role in redox signaling, vascular function, and diseases. Antioxidants & redox signaling 2011;15:1583-606.

[137] Hamanishi T, Furuta H, Kato H, Doi A, Tamai M, Shimomura H, et al. Functional variants in the glutathione peroxidase-1 (GPx-1) gene are associated with increased intima-media thickness of carotid arteries and risk of macrovascular diseases in japanese type 2 diabetic patients. Diabetes 2004;53:2455-60.

[138] Brigelius-Flohe R, Maiorino M. Glutathione peroxidases. Biochimica et biophysica acta 2013;1830:3289-303.

[139] Pressman S, Bei Y, Carthew R. Posttranscriptional gene silencing. Cell 2007;130:570.

[140] Thomas MP, Lieberman J. Live or let die: posttranscriptional gene regulation in cell stress and cell death. Immunological reviews 2013;253:237-52.

[141] Landry CR, Freschi L, Zarin T, Moses AM. Turnover of protein phosphorylation evolving under stabilizing selection. Frontiers in genetics 2014;5:245.

[142] Rodel F, Frey B, Gaipl U, Keilholz L, Fournier C, Manda K, et al. Modulation of inflammatory immune reactions by low-dose ionizing radiation: molecular mechanisms and clinical application. Curr Med Chem 2012;19:1741-50.

[143] Rodel F, Schaller U, Schultze-Mosgau S, Beuscher HU, Keilholz L, Herrmann M, et al. The induction of TGF-beta(1) and NF-kappaB parallels a biphasic time course of leukocyte/endothelial cell adhesion following low-dose X-irradiation. Strahlentherapie und Onkologie : Organ der Deutschen Rontgengesellschaft [et al] 2004;180:194-200.

[144] Hur W, Sun Z, Jiang T, Mason DE, Peters EC, Zhang DD, et al. A small-molecule inducer of the antioxidant response element. Chemistry & biology 2010;17:537-47.

[145] Prise KM, O'Sullivan JM. Radiation-induced bystander signalling in cancer therapy. Nat Rev Cancer 2009;9:351-60.

[146] Rodel F, Frey B, Multhoff G, Gaipl U. Contribution of the immune system to bystander and non-targeted effects of ionizing radiation. Cancer letters 2015;356:105-13.

[147] Barcellos-Hoff MH. How do tissues respond to damage at the cellular level? The role of cytokines in irradiated tissues. Radiat Res 1998;150:S109-20.

[148] Arenas M, Sabater S, Hernandez V, Rovirosa A, Lara PC, Biete A, et al. Anti-inflammatory effects of low-dose radiotherapy. Indications, dose, and radiobiological mechanisms involved. Strahlentherapie und Onkologie : Organ der Deutschen Rontgengesellschaft [et al] 2012;188:975-81.

[149] Ott OJ, Hertel S, Gaipl US, Frey B, Schmidt M, Fietkau R. Benign painful shoulder syndrome: initial results of a single-center prospective randomized radiotherapy dose-optimization trial. Strahlenther Onkol 2012;188:1108-13.

[150] Speyer CL, Ward PA. Role of endothelial chemokines and their receptors during inflammation. Journal of investigative surgery : the official journal of the Academy of Surgical Research 2011;24:18-27.

[151] Large M, Reichert S, Hehlgans S, Fournier C, Rodel C, Rodel F. A non-linear detection of phospho-histone H2AX in EA.hy926 endothelial cells following low-dose X-irradiation is modulated by reactive oxygen species. Radiation oncology 2014;9:80.

[152] Thornhill MH, Li J, Haskard DO. Leucocyte endothelial cell adhesion: a study comparing human umbilical vein endothelial cells and the endothelial cell line EA-hy-926. Scandinavian journal of immunology 1993;38:279-86.

[153] Large M, Hehlgans S, Reichert S, Gaipl US, Fournier C, Rodel C, et al. Study of the anti-inflammatory effects of low-dose radiation : The contribution of biphasic regulation of the antioxidative system in endothelial cells. Strahlentherapie und Onkologie : Organ der Deutschen Rontgengesellschaft [et al] 2015.

[154] Beels L, Werbrouck J, Thierens H. Dose response and repair kinetics of gamma-H2AX foci induced by in vitro irradiation of whole blood and T-lymphocytes with X- and gamma-radiation. International journal of radiation biology 2010;86:760-8.

[155] Joiner MC, Marples B, Lambin P, Short SC, Turesson I. Low-dose hypersensitivity: current status and possible mechanisms. International journal of radiation oncology, biology, physics 2001;49:379-89.

[156] Xue L, Yu D, Furusawa Y, Cao J, Okayasu R, Fan S. ATM-dependent hyper-radiosensitivity in mammalian cells irradiated by heavy ions. International journal of radiation oncology, biology, physics 2009;75:235-43.

[157] Martin LM, Marples B, Lynch TH, Hollywood D, Marignol L. Exposure to low dose ionising radiation: Molecular and clinical consequences. Cancer letters 2013;338:209-18.

[158] Unno J, Takagi M, Piao J, Sugimoto M, Honda F, Maeda D, et al. Artemis-dependent DNA double-strand break formation at stalled replication forks. Cancer science 2013;104:703-10.

[159] Friedrich T, Scholz U, Elsasser T, Durante M, Scholz M. Calculation of the biological effects of ion beams based on the microscopic spatial damage distribution pattern. International journal of radiation biology 2012;88:103-7.

[160] Johnston PJ, MacPhail SH, Banath JP, Olive PL. Higher-order chromatin structure-dependent repair of DNA double-strand breaks: factors affecting elution of DNA from nucleoids. Radiation research 1998;149:533-42.

[161] Ostashevsky J. A polymer model for the structural organization of chromatin loops and minibands in interphase chromosomes. Molecular biology of the cell 1998;9:3031-40.

[162] Yokota H, van den Engh G, Hearst JE, Sachs RK, Trask BJ. Evidence for the organization of chromatin in megabase pair-sized loops arranged along a random walk path in the human G0/G1 interphase nucleus. The Journal of cell biology 1995;130:1239-49.

[163] Solovjeva L, Svetlova M, Stein G, Chagin V, Rozanov Y, Zannis-Hadjopoulos M, et al. Conformation of replicated segments of chromosome fibres in human S-phase nucleus. Chromosome research : an international journal on the molecular, supramolecular and evolutionary aspects of chromosome biology 1998;6:595-602.

[164] Yang Y, Bazhin AV, Werner J, Karakhanova S. Reactive oxygen species in the immune system. International reviews of immunology 2013;32:249-70.

[165] Kang MA, So EY, Simons AL, Spitz DR, Ouchi T. DNA damage induces reactive oxygen species generation through the H2AX-Nox1/Rac1 pathway. Cell death & disease 2012;3:e249.

[166] Kojima S, Matsuki O, Nomura T, Kubodera A, Honda Y, Honda S, et al. Induction of mRNAs for glutathione synthesis-related proteins in mouse liver by low doses of gamma-rays. Biochim Biophys Acta 1998;1381:312-8.

[167] Yamaoka K, Kojima S, Takahashi M, Nomura T, Iriyama K. Change of glutathione peroxidase synthesis along with that of superoxide dismutase synthesis in mice spleens after low-dose X-ray irradiation. Biochimica et biophysica acta 1998;1381:265-70.

[168] Kataoka T. Study of antioxidative effects and anti-inflammatory effects in mice due to low-dose X-irradiation or radon inhalation. Journal of radiation research 2013;54:587-96.

[169] Peltola V, Parvinen M, Huhtaniemi I, Kulmala J, Ahotupa M. Comparison of effects of 0.5 and 3.0 Gy X-irradiation on lipid peroxidation and antioxidant enzyme function in rat testis and liver. Journal of andrology 1993;14:267-74.

[170] Beck M, Rombouts C, Moreels M, Aerts A, Quintens R, Tabury K, et al. Modulation of gene expression in endothelial cells in response to high LET nickel ion irradiation. International journal of molecular medicine 2014;34:1124-32.

[171] Nguyen T, Nioi P, Pickett CB. The Nrf2-antioxidant response element signaling pathway and its activation by oxidative stress. The Journal of biological chemistry 2009;284:13291-5.

[172] Tsukimoto M, Tamaishi N, Homma T, Kojima S. Low-dose gamma-ray irradiation induces translocation of Nrf2 into nuclear in mouse macrophage RAW264.7 cells. Journal of radiation research 2010;51:349-53.

[173] Lee EK, Kim JA, Park SJ, Kim JK, Heo K, Yang KM, et al. Low-dose radiation activates Nrf1/2 through reactive species and the Ca(2+)/ERK1/2 signaling pathway in human skin fibroblast cells. BMB reports 2013;46:258-63.

[174] Yoshino H, Kiminarita T, Matsushita Y, Kashiwakura I. Response of the Nrf2 protection system in human monocytic cells after ionising irradiation. Radiat Prot Dosimetry 2012;152:104-8.

[175] McDonald JT, Kim K, Norris AJ, Vlashi E, Phillips TM, Lagadec C, et al. Ionizing radiation activates the Nrf2 antioxidant response. Cancer research 2010;70:8886-95.

[176] Motohashi H, Katsuoka F, Engel JD, Yamamoto M. Small Maf proteins serve as transcriptional cofactors for keratinocyte differentiation in the Keap1-Nrf2 regulatory pathway. Proc Natl Acad Sci U S A 2004;101:6379-84.

[177] Jeyapaul J, Jaiswal AK. Nrf2 and c-Jun regulation of antioxidant response element (ARE)-mediated expression and induction of gamma-glutamylcysteine synthetase heavy subunit gene. Biochem Pharmacol 2000;59:1433-9.

[178] Li MJ, Cui FM, Cheng Y, Sun D, Zhou PK, Min R. Changes in the adhesion and migration ability of peripheral blood cells: potential biomarkers indicating exposure dose. Health physics 2014;107:242-7.

[179] Hallmann R, Jutila MA, Smith CW, Anderson DC, Kishimoto TK, Butcher EC. The peripheral lymph node homing receptor, LECAM-1, is involved in CD18-independent adhesion of human neutrophils to endothelium. Biochemical and biophysical research communications 1991;174:236-43.

[180] Hallmann R. Complex regulation of granulocyte adhesion to cytokine-activated endothelium. Behring Institute Mitteilungen 1993:138-43.

[181] Morigi M, Zoja C, Figliuzzi M, Foppolo M, Micheletti G, Bontempelli M, et al. Fluid shear stress modulates surface expression of adhesion molecules by endothelial cells. Blood 1995;85:1696-703.

[182] Nagata M. Inflammatory cells and oxygen radicals. Current drug targets Inflammation and allergy 2005;4:503-4.

[183] Chiarugi P, Pani G, Giannoni E, Taddei L, Colavitti R, Raugei G, et al. Reactive oxygen species as essential mediators of cell adhesion: the oxidative inhibition of a FAK tyrosine phosphatase is required for cell adhesion. The Journal of cell biology 2003;161:933-44.

[184] Renier G, Mamputu JC, Desfaits AC, Serri O. Monocyte adhesion in diabetic angiopathy: effects of free-radical scavenging. Journal of diabetes and its complications 2003;17:20-9.

[185] Park SY, Lee JS, Ko YJ, Kim AR, Choi MK, Kwak MK, et al. Inhibitory effect of simvastatin on the TNF-alpha- and angiotensin II-induced monocyte adhesion to endothelial cells is mediated through the suppression of geranylgeranyl isoprenoid-dependent ROS generation. Arch Pharm Res 2008;31:195-204.

[186] Chappell DC, Varner SE, Nerem RM, Medford RM, Alexander RW. Oscillatory shear stress stimulates adhesion molecule expression in cultured human endothelium. Circulation research 1998;82:532-9.

[187] Tang C, Xue HL, Bai CL, Fu R. Regulation of adhesion molecules expression in TNF-alpha-stimulated brain microvascular endothelial cells by tanshinone IIA: involvement of NF-kappaB and ROS generation. Phytother Res 2011;25:376-80.

[188] Huang CS, Lin AH, Yang TC, Liu KL, Chen HW, Lii CK. Shikonin inhibits oxidized LDL-induced monocyte adhesion by suppressing NFkappaB activation via up-regulation of PI3K/Akt/Nrf2-dependent antioxidation in EA.hy926 endothelial cells. Biochem Pharmacol 2015;93:352-61.

[189] Gloire G, Legrand-Poels S, Piette J. NF-kappaB activation by reactive oxygen species: fifteen years later. Biochemical pharmacology 2006;72:1493-505.

[190] Yuan Y, Lee SH, Wu S. The role of ROS in ionizing radiation-induced VLA-4 mediated adhesion of RAW264.7 cells to VCAM-1 under flow conditions. Radiation research 2013;179:62-8.

[191] Buelna-Chontal M, Zazueta C. Redox activation of Nrf2 & NF-kappaB: a double end sword? Cell Signal 2013;25:2548-57.

[192] Li W, Khor TO, Xu C, Shen G, Jeong WS, Yu S, et al. Activation of Nrf2-antioxidant signaling attenuates NFkappaB-inflammatory response and elicits apoptosis. Biochem Pharmacol 2008;76:1485-9.

[193] Liu GH, Qu J, Shen X. NF-kappaB/p65 antagonizes Nrf2-ARE pathway by depriving CBP from Nrf2 and facilitating recruitment of HDAC3 to MafK. Biochim Biophys Acta 2008;1783:713-27.

[194] Ott OJ, Hertel S, Gaipl US, Frey B, Schmidt M, Fietkau R. The Erlangen Dose Optimization Trial for radiotherapy of benign painful shoulder syndrome. Long-term results. Strahlenther Onkol 2014;190:394-8.

6 Appendix

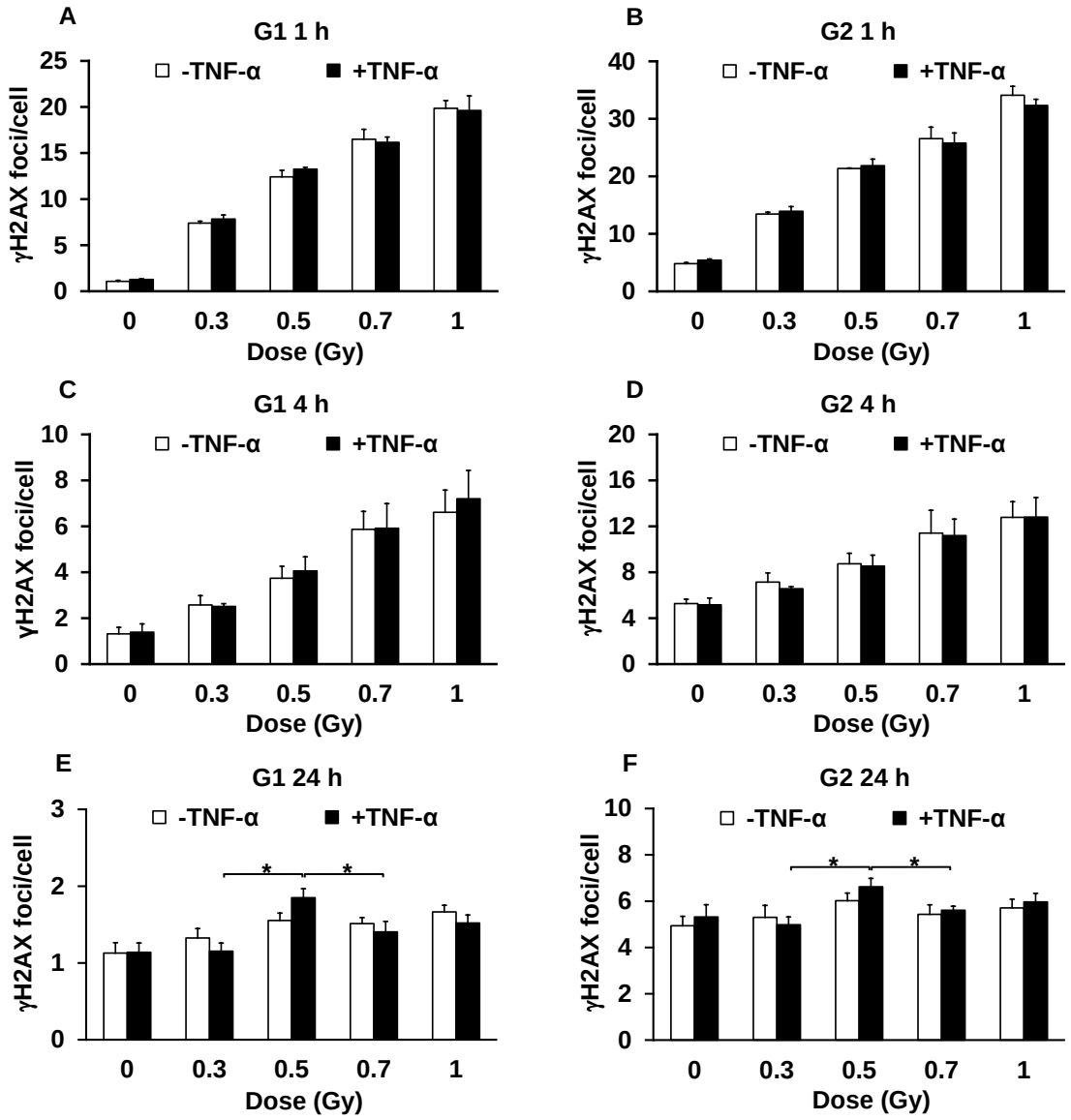

Supplementary Figure 1. Dose and time kinetics of γH2AX foci levels in EA.hy926 EC following low-dose X-irradiation divided into G1 and G2 phase

EA.hy926 EC were plated onto coverslips and stimulated with TNF-α (20 ng/ml) (black bars) at 4 h before irradiation with the doses indicated. Mock-treated cells served as a control. At 1 h (A/B) and 4 h (C/D) post irradiation, cells were fixed, stained for γH2AX, DAPI and CENP-F and data of a total of 40 nuclei ((G1 phase (A/C/E) and G2 phase (B/D/F)) were evaluated. Data represent means ± SEM from at least three independent experiments. *$p < 0.05$.

Own work

Experiments, data analysis and writing of the present thesis with exception of the following items, were all done by myself.

The activity assays in Figure 10 and Figure 11 were done by Dr. Sebastian Reichert (Department of Radiotherapy and Oncology, University of Frankfurt am Main, Germany).

Acknowledgements

First I want to thank Prof. Dr. Claus Rödel for giving me the opportunity to write my thesis in his department and use the facilities.
Additionally I want to thank the technicians for helping with the irradiation procedure and the medical physics department for taking care of the daily dosimetry of the LINACs.

I want to thank Prof. Dr. Franz Rödel for the supervision and help with my dissertation, his inspiring and motivating words and for creating the friendly atmosphere in the lab. It has been an instructive time.

I am grateful to Prof. Dr. Markus Löbrich for supervising my work and for presenting me the opportunity to participate in the graduate school GRK1657.

I am thankful to my second supervisor Prof. Dr. Bodo Laube for the uncomplicated collaboration and sorry again for the missing bag.

A huge dedication to all former and present members in the lab of molecular radiobiology: Dr. Judith Bergs, Dr. Sebastian Reichert, Dr. Henrik Sperling, PD Dr. Stephanie Hehlgans, Julius Oppermann, Fabian Weipert and Dr. Chrysi Petraki. Thanks for the funny, inspiring and friendly atmosphere in the lab.
Forever Radio X ;)

I want to greet the scholars and fellows of the GRK 1657, thanks for the nice retreats and seminars. I wish good luck to us all. And don't forget about the horses!

A special thanks to my family and friends for the moral and constructive support throughout the time of my thesis and my studies.

Words cannot express the thankfulness for my wife…

Curriculum Vitae

Name:	Martin Large
Day of birth:	14.03.1985
Place of birth:	Heidelberg, Germany
Nationality:	German
Family status:	Married

Education and Employment

Jan 2012 – Feb 2015	PhD student (GRK 1657 fellow) at the Faculty of Biology at Technical University of Darmstadt, Germany Subject: Cellular and molecular aspects of the anti-inflammatory effects of low-dose radiation Supervised by: Prof. M. Löbrich and Prof. B. Laube Principal investigator: Prof. F. Rödel Project accomplished at the Molecular Radiation Biology Laboratory at the Dept. of Radiotherapy and Oncology, University Hospital Frankfurt am Main, Germany
Oct 2006 – Dec 2011	Studies at the Faculty of Biology at Technical University of Darmstadt, Germany. Degree: Diploma (1.0)
Sep 2004 – Sep 2006	Alternative civilian service and subsequent employment at the county hospital of Weinheim, Germany
Sep 1995 – Juli 2004	School education at Kurpfalz Gymnasium Schriesheim, Germany. Degree: Abitur (2.0)

Publications

Large M, Reichert S, Hehlgans S, Fournier C, Rödel C, Rödel F (2014).
A non-linear detection of phospho-histone H2AX in EA.hy926 endothelial cells following low-dose X-irradiation is modulated by reactive oxygen species.
Published in: Radiation Oncology, 9(1), 80.

Large M, Hehlgans S, Reichert S, Gaipl US, Fournier C, Rödel C, Weiss C, Rödel F (2015). Study of the anti-inflammatory effects of low-dose radiation: The contribution of biphasic regulation of the antioxidative system in endothelial cells.

Published in Strahlenther Onkol. Epub ahead of print.

Conferences attended

Low-dose Research towards Multidisciplinary - DoReMi Integration 2nd Periodic Meeting, Paris, Frankreich
Large M, Reichert S, Hehlgans S, Rödel C, Rödel F.
Discontinuous DNA Damage Response in Endothelial Cells after Low-dose Irradiation (Talk)

19. Jährliche Konferenz der Deutschen Gesellschaft für Radioonkologie (DEGRO), Berlin
Large M, Reichert S, Hehlgans S, Rödel C, Rödel F.
Discontinuous DNA Damage Response in Endothelial Cells after Low-dose Irradiation (Poster)

13. Jahrestagung der GBS, Darmstadt
Large M, Reichert S, Hehlgans S, Rödel C, Rödel F.
Discontinuous DNA Damage Response in Endothelial Cells after Low-dose Irradiation (Poster)

Low-dose Research towards Multidisciplinary - DoReMi Integration 3rd Periodic Meeting, München
Large M, Reichert S, Hehlgans S, Rödel C, Rödel F.
A non-linear detection of phospho-histone H2AX in EA.hy926 endothelial cells following low-dose X-irradiation is modulated by ROS (Talk)

List of Abbreviations

Abbreviation	Full name
γH2AX	histone H2A, member X
µg	microgram
µl	microliter
µm	micrometre
µM	micromolar
53BP1	p53-binding protein 1
5-OH-MeHyd	5-hydroxy-5-methylhydantoin
5-OH-Me-Ura	5-hydroxymethyluracil
8-OH-dG	8-oxoguanine
AP-1	Activator protein 1
ARE	Antioxidant response element
ATM	Ataxia telangiectasia mutated
BLM	Bloom helicase
BRAF	proto-oncogene B-Raf
BRCA1	Breast cancer 1
BRCA2	Breast cancer type 2 susceptibility protein
BSA	Bovine serum albumin
TAMRA	Carboxytetramethylrhodamine
CAT	Catalase
CDK1	Cyclin-dependent kinase 1
CENP-F	Centromere protein-F
CIN	Chromosomal instability
CK2	Casein kinase 2

CO_2	Carbon dioxide
COPD	Chronic obstructive pulmonary disease
CPS	Comprehensive pain score
CtiP	CtBP-interacting protein
Cul3	Cullin-3
DAPI	4',6-diamidino-2-phenylindole
DMEM	Dulbecco's Modified Eagle Medium
DNA	Deoxyribonucleic acid
DNA DSBs	DNA Double-strand breaks
DNA-PK_{cs}	DNA-dependent protein kinase, catalytic subunit
DSB	DNA double-strand break
EC	Endothelial cell
ECL	Enhanced chemiluminescence
EDTA	Ethylenediaminetetraacetic acid
Exo1	Exonuclease 1
FACS	Fluorescence-activated cell sorting
G2	Gap 2 phase (of the cell cycle)
GPx	Glutathione-peroxidase
GR	Glutathione reductase
GSH	Glutathione
GSSG	Glutathione disulphide
GTP-binding protein	Guanosine nucleotide-binding protein
H_2DCFDA	2′ ,7′ -dichlorodihydrofluoresceindiacetate
H_2O_2	Hydrogen peroxide
HO-1	Heme oxygenase 1
HR	Homologous recombination

HRP	Horseradish peroxidase
HRS	Hyper-radiosensitivity
hSSB1	Human single stranded binding protein-1
ICAM-1	Intercellular adhesion molecule 1
ICAM-2	Intercellular adhesion molecule 2
IF	Immunofluorescence
IgG	Immunoglobulin G
IKK	IκB kinase
IL	Interleukin
iNOS	Inducible nitric oxide synthases
IR	Ionizing radiation
IRR	Induced radioresistance
IκBα	Inhibitor κBα
Keap1	Kelch-like ECH-associated protein
LD-RT	Low-dose radiation therapy
MAPK	Mitogen-activated protein kinase
MCP1	Monocyte chemoattractant protein-1
MDC1	Mediator of DNA damage checkpoint protein 1
MMR	Mismatch repair
MRE11	Meiotic recombination 11 homolog
mRNA	Messenger RNA
MRN-complex	Mre11, Rad50 and Nbs1 complex
NADPH	Nicotinamide adenine dinucleotide phosphate
NF-κB	nuclear factor kappa-light-chain-enhancer of activated B cells

NHEJ	Non-homologous end joining
NK	Natural killer
NOX	NADPH oxidase
Nrf2	Nuclear factor erythroid 2-related factor 2
O_2^{-}•	Superoxide
OH•	Hydroxyl radical
$ONOO^-$	Peroxynitrite
PA	Polyarthritis
PBMC	Peripheral blood mononuclear cells
PBS	Phosphate buffered saline
PCR	Polymerase chain reaction
PIKK	Phosphatidylinositol 3-kinase-related kinases
PMA	Phorbol myristate acetate
PMN	Polymorph nuclear cells
qPCR	Real-time/quantitative polymerase chain reaction
Ras-related C3 botulinum toxin substrate 1	Rac1
RIPA	Radioimmunoprecipitation assay buffer
ROS	Reactive oxygen species
RPA	Replication protein A
RT	Room temperature
SDS	Sodium dodecylsulfate
SEM	Standard error of the mean
SOD	Superoxide dismutase
ssDNA	Single stranded DNA

TAE buffer	Tris-Acetate-EDTA buffer
TBS buffer	Tris-buffered saline
TGF-β	Transforming growth factor beta
TNF-α	Tumour necrosis factor alpha
TRIS	Tris hydroxymethyl aminomethane
VCAM-1	Vascular cell adhesion molecule
VLA-4	Very late antigen-4
XIAP	X-chromosome linked inhibitor of apoptosis protein
XO	Xanthine oxidase
XRCC4	X-ray repair cross-complementing protein 4